University of South-Eastern Norway

Faculty of Technology, Natural Sciences and Maritime Sciences

Master's Thesis

Study programme:4317

Spring/Autumn 2024

Mahesh Bhandari

GIS-Based Multi-Criteria Modelling for Fluvial Flood Susceptibility Analysis in South-eastern Norway

University of South-Eastern Norway
Faculty of Technology, Natural Sciences and Maritime Sciences
Department of Natural Sciences and Environmental Health
PO Box 235
NO-3603 Kongsberg, Norway

http://www.usn.no

This thesis is worth 60 study points.

Acknowledgements

It has been a journey filled with obstacles, development, and invaluable assistance from multiple individuals and institutions to complete this master's thesis. I wish to extend my sincere appreciation to all individuals who have made valuable contributions towards the successful completion of this research undertaking.

Prior to anything else, I would like to express my sincere gratitude to my thesis advisor, Dieu Tein Bui, whose counsel, knowledge, and steadfast encouragement have been indispensable during this scholarly endeavour. Your guidance and support not only enhanced the quality of my research but also motivated me to surpass my own limitations.

The faculty members of USN, whose scholarly perspectives and constructive criticism had a profound impact on the development and improvement of this thesis, have my deepest gratitude. Your unwavering commitment to achieving high standards in both academia and research has consistently inspired me.

I would like to express my gratitude to my life partner, Roshni Neupane for her support, motivation and innumerable suggestions that have enhanced my scholarly journey and infused it with amicable moments.

Although a comprehensive list of all the contributors to this thesis would be impractical, I would like to assure you that all encouragement and support have been greatly valued and acknowledged.

Mahesh Bhandari

Abstract

Natural disasters have become an important global problem. Every year, catastrophic events such as floods, earthquakes, landslides, tornadoes, tsunamis, and volcanic eruptions cause extensive damage to property and infrastructure, and most tragically there is significant loss of human life. Floods, one of the most common types of natural disasters, are increasingly frequent and severe worldwide, leading to increasing financial losses. In Norway, floods occur every year and continuously cause noticeable impacts. Therefore, investing in flood research to develop comprehensive flood management strategies is essential.

The aim of this master's thesis is to study and identify potential flood zones in the Bø-Seljord basin of Telemark County, Norway, suing Multi-Criteria Modelling and Geographic Information Systems (GIS). To achieve this, a total of ten flood indicators were prepared using multi-sourced geospatial data. These indicators include elevation, slope, distance from rivers, drainage density, Topographic Wetness Index (TWI), Stream Power Index (SPI), Normalized Difference Vegetation Index (NDVI), Normalized Difference Snow Index (NDSI), land use and land cover, and geology. A multicollinearity analysis was then conducted for these indicators. The indicators were then analysed and assigned weights using Multi-Criteria Decision Analysis (MCDA). This process led to the generation of a fluvial flood susceptibility map. Finally, historical flood records were utilized to evaluate the accuracy of the map.

The results show that 16.5%, 9.7%, and 4.68% of the study area are classified as moderately, highly, and very highly susceptible to flooding, respectively. Overall, most of the study area, accounting for more than 65%, is found to be non-susceptible to flooding. The model's ROC-AUC value indicates of 0.957 indicates high predictive accuracy. Furthermore, the susceptibility map underwent sensitivity analysis, which also yielded favourable results.

The flood susceptibility map generated from this research may offer significant utility for local authorities, providing essential insights and information to improve decision-making processes and support the implementation of effective risk management strategies.

Keywords: GIS, MCDA, AHP, Flooding, Flood Susceptibility, ROC-AUC, and Natural Disaster

Sammendrag

Naturkatastrofer har blitt et viktig globalt problem. Hvert år katastrofale hendelser som flom, jordskjelv, jordskred, tornadoer, tsunamier og vulkanutbrudd omfattende skade på eiendom og infrastruktur, og mest tragisk er betydelig tap av menneskeliv. Flom, en av de vanligste typene naturkatastrofer, blir stadig hyppigere og mer alvorlige over hele verden, noe som fører til økende økonomiske tap. I Norge oppstår det flom hvert år, og det har kontinuerlig merkbare virkninger. Derfor er det viktig å investere in flomforskning for å utvikle omfattende flomhåndteringsstrategier

Målet med denne masteroppgaven er å studere og identifisere potensielle flomsoner i Bø-Seljord-bassenget i Telemark fylke, Norge, ved bruk av Multi-Criteria Modelling og Geografiske Informasjonssystemer (GIS). For å oppnå dette ble til sammen ti flomindikatorer utarbeidet ved bruk av geospatiale data fra flere kilder. Disse indikatorene inkluderer høyde, helning, avstand fra elver, dreneringstetthet, topografisk våthetsindeks (TWI), strømmekraftindeks (SPI), Normalisert Differanse Vegetasjons indeks (NDVI), Normalisert Differanse Snø indeks (NDSI), arealbruk og dekke, og geologi. En multikollineartets analyse ble deretter utført for disse indikatorene. Indikatorene ble deretter analysert og tildelt vekter ved bruk av Multi-Criteria Decision Analysis (MCDA). Denne prosessen førte til generering av et fluvialt flomktsomhetskart. Til slutt ble historiske flomregistre brukt for å evaluere kartets nøyaktighet.

Resultatene viser at 16.5%, 9.7% og 4.68% av studieområdet er klassifisert som moderat, høyt og svært høyt utsatt for flom. Totalt sett er det funnet at mesteparten av studieområdet, mer enn 65%, ikke et utsatt for flom. Modellens ROC-AUC-verdi på 0.957 indikerer høy prediktiv nøyaktighet. Videre gjennomgikk flomaktsomhetskartet en sensitivitetsanalyse, som også ga gunstige resultater.

Flomaktsomhetskartet som ble generert fra denne forskningen kan tilby betydelig for lokale myndigheter ved å gi essensiell innsikt og informasjon for å forbedre beslutningsprosesser og støtte implementeringen av effektive risikohåndteringsstrategier.

Nøkkelord: GIS, MCDA, AHP, Flom, Flomaktsomhet, ROC-AUC, Naturkatastrofe

Table of contents

List of Figures

List of Tables

Abbreviations

FSM: Flood susceptibility map

MCDA: Multi-Criteria Decision Analysis

MCDM: Multi-Criteria Decision Making

TWI: Topographic Wetness Index

SPI: Stream Power Index

LULC: Land-Use and Land Cover

RS: Remote Sensing

GIS: Geological Information System

AHP: Analytical Hierarchy Process

NDVI: Normalised Difference Vegetation Index

NDSI: Normalised Difference Snow Index

DEM: Digital Elevation Model

CI: Consistency Index

CR: Consistency Ratio

NVE: Norwegian Water Resources and Energy Directorate

SI: Sensitivity Index

ROC: Receiver Operating Characteristic

AUC: Area Under the ROC curve

LR: Logistic Regression

WLC: Weighted Linear Combination

FIM: Flood Inventory Map

ANP: Analytic Network Process

SVM: Support Vector Machine

ANN: Artificial Neural Network

1 Introduction

1.1 Background

Floods continue to be one of the most devastating weather-related disasters worldwide, causing a significant number of deaths each year and having a profound impact on socio-economic progress and environmental equilibrium (Melgar-García et al., 2023). Despite extensive measures taken to mitigate flooding, the resulting impact on human lives and property remains significant. Floods constitute for 34% of all natural disasters worldwide in terms of frequency and 40% in terms of economic losses (Zhu et al., 2023). The world lost an average of nearly USD 651 million due to riverine floods every year on average over the last ten years (UNDPR 2020). Projections suggest that flood-related problems will worsen as a result of increasing global warming and climate change, which are anticipated to lead to more frequent occurrences of intense rainfall events worldwide (Mishra & Kumar, 2020). According to (Rentschler et al., 2022), approximately 1.81 billion people, which is equivalent to around 23% of the world's population, are directly affected by floods that occur once every 100 years. Moreover, forecasts indicate that by 2050, around 68% of the population will live in urban regions (Rentschler et al., 2022). Therefore, it is essential to give priority to investing in research and innovation to improve flood forecasting techniques and establish efficient flood management strategies.

In Europe, floods have a significant impact, with damages increasingly driven by the expansion of human settlements and economic activities in flood-prone areas. This expansion has led to increased exposure and reduced natural storage capacities (Merz et al., 2012). Current estimates indicate that in the European Union and United Kingdom (collectively known as EU+ UK), river floods annually inflict damages totalling approximately 76 billion (ranging from 5.6 to 11.2 billion) and expose roughly 166,000 individuals (with a range of €124,000 to €276,000) to flood waters each year (Dottori et al., 2023). If the current climate mitigation and adaptation efforts are not altered, it is projected that the temperature will increase by 3º C by the year 2100, resulting in the annual flood damages in Europe expected to increase by 44 billion (with a range of 30 to 61 billion) by the end of the century. Simultaneously, an estimated €370,000 to €675,000 Europeans would face the potential danger of being exposed to river floods annually (Dottori et al., 2023).

In Norway, flood have occurred in various locations within its river network, causing damage to both natural and man-made assets. The occurrence of floods can result in significant economic losses although they typically do not lead to a high number of fatalities. The flood in Norway can be influenced by various factors: rainfall, snowmelt, topography, discharge, land-use, and geology. Meanwhile, the primary factor contributing to the occurrence of

significant floods in Norway is precipitation, frequently accompanied by the melting of snow. The magnitude of a flood is primarily influenced by the meteorological conditions specifically the distribution of precipitation and temperature levels. The water storage capacity of the vegetation, surface features, bedrock, lakes, and streams are an essential factor to consider. The vast climatic, topographical, and hydrographic variations in Norway cause river basins to vary greatly.

In western and northern Norway, along the coast and in the mountainous regions, precipitation is at its highest. Both spring and autumn are prime times for river flooding in Norway. In most cases, spring floods are caused by snowmelt or a combination of melting snow and precipitation. Large inlands river basins in mountainous and eastern Norway are particularly prone to these types of floods. Autumn floods, prevalent along the coastlines, are primarily caused by precipitation. The most significant flood in the study area occurred in late June 1927. The inundation was triggered by an extended period of intense rainfall. A rainfall of 76mm was recorded at the measuring station at Lifjell sanatorium in Bø on June 27th, 1927, among other observations. Furthermore, a significant flood occurred on May8, 1964 in Hørte, which was likely caused by a combination of rainfall and snowmelt (NVE 2007).

Given the current circumstances, it is of utmost importance to evaluate and categorise the risks associated with flooding disasters on a regional level. Although floods pose significant challenges in terms of prevention; however, it is possible to proactively anticipate and prepare for such catastrophic events. Efforts to mitigate and prevent the catastrophic consequences of floods are crucial for protecting lives, infrastructure, and ecosystems. Flood risk management plays a critical role in these endeavours, encompassing the evaluation of flood susceptibility. This procedure entails examining geographical and climatic variables to pinpoint regions that are most susceptible to risk. Through the identification of flood-prone areas, governments, planners, and communities can strategically implement measures such as enhancing drainage systems, building flood barriers, and enforcing land use policies that restrict development in high-risk zones. The prioritisation of resources and interventions, ultimately reduces the risk of catastrophic damage and improves community resilience against future flood events.

Flooding is a complicated phenomenon, with numerous human and natural elements contributing to the incidence and progression of floods. Climate change, for example, has a significant impact on the occurrence of extreme floods (Samson et al., 2015). For example, changes in climate may have an impact on land use and increase the risk of flooding (Emerton et al., 2017). Global research has recently been conducted on the effects of climate change on flood risk and frequency (Wu et al., 2010). Numerous researchers have carried out Flood Susceptibility Mapping (FSM) and natural hazard assessment using remote sensing (RS) and Geographic Information System (GIS) tools, greatly contributing to hazard analysis(Tehrany et al., 2015; White et al., 2010). Historically, the major goal of creating flood

models has been to accurately assess the discharge over the watersheds. To generate susceptibility maps, prediction methods combine various conditioning factors and weight their importance using decision-making rules.

Theoretically, FSM is capable of precisely identifying and defining potential flood hazards in the future, either deterministically or statistically. Both qualitative and quantitative analyses can be used to determine a region's susceptibility to flooding. Many scholars from around the world have studied flood disaster risks and proposed various solutions(Nguyen et al., 2023; Vojtek & Vojteková, 2019). Over the last ten years, Geographic Information Systems (GIS) and data from remote sensing have been used in FSM. Weights of evidence (Tehrany et al., 2015), Logistic regression (LR) (Tehrany et al., 2014), and Analytic Hierarchy Process (AHP) (Kazakis et al., 2015).

Among these methods and techniques, Multi-Criteria Decision Analysis (MCDA) is particularly well-suited for flood susceptibility mapping because:

- Integration of Diverse Factors: Multi-Criteria Decision Analysis (MCDA) facilitates the incorporation of various factors that influence flood risk, such as hydrological data, land use patterns, soil characteristics, topographical features, and climate conditions. The comprehensive assessment of flood is achieved by considering of a wide range of variables in MCDA.
- Flexibility in Weighting Criteria: The use of Multi-Criteria Decision Analysis (MCDA) allows experts to assign varying weights to different criteria, based on their relative importance in assessing flood risk. The flexibility of the system allows for a greater influence of critical factors on the outcome, resulting in more precise and customised flood susceptibility maps.
- Decision-Making Support: The Multi-Criteria Decision Analysis (MCDA) methodology facilitates decision-making processes by offering a well-defined framework that systematically assesses the potential consequences of various scenarios and interventions. The purpose of this solution is to assist stakeholders in making well-informed decisions regarding the allocation of resources for flood prevention and mitigation.
- Transparency and consistency: The methodological framework of Multi-Criteria Decision Analysis (MCDA) is designed to enhance transparency and ensure consistency in the analysis process. The process of selecting criteria, weighting them, and combining them is clearly defined at each step. This approach enhances the reliability and comprehensibility of the results for all stakeholders involved.
- Facilitates Stakeholder Involvement: The Multi- Criteria Decision Analysis (MCDA) processes typically encompass the participation of various stakeholders, such as government agencies, community representatives, and subject matter experts. The

incorporation of diverse perspectives and needs in the analysis helps to promote inclusivity, resulting in outcomes that are both widely accepted and effective.

- Scenario Analysis: Multi-Criteria Decision Analysis (MCDA) enables the simulation of various scenarios to assess the impact of modifications in one or more criteria on flood susceptibility. Understanding potential impacts of climate change and urban development on flood risks is crucial, and this capability plays a vital role in achieving that understanding.

The distinct domains of Geographical Information System (GIS) and Multi-Criteria Decision Analysis (MCDA) can collaborate to leverage the intersections between spatial representation and multiple influential factors (Çetinkaya et al., 2016). Geographic Information Systems (GIS) enable the integration of flood factors that are associated with specific locations on a map. On the other hand, Multi-Criteria Decision Analysis (MCDA) provides a structured approach to the design, evaluation, and prioritization of decisions. The relative importance of each component in relation to the flood issue is determined using the Analytical Hierarchy Process (AHP) method. It is recognized that each component does not contribute in the same proportion.

The process of GIS-based Multi-Criteria Decision Analysis (MCDA) involves two essential components: the calculation of factor weights using the Analytic Hierarchy Process (AHP) and the aggregation of weighted factors using the Weighted Linear Combination (WLC) method. These steps are employed to generate a flood risk map, as described by (Azareh et al., 2019) and Rahman et al. (2019). The use of Multi-Criteria Decision Analysis (MCDA) has been documented in several countries for flood risk assessment. For instance, in Greece, Papaioannou and Vasiliades (2014) employed MCDA for this purpose. Similarly, (Khosravi et al., 2019) utilized MCDA in the Republic of China, while Rincon Romero et al. (2018) applied MCDA in Canada. The metropolitan urban area of Athens was evaluated using the Analytic Hierarchy Process (AHP) and multi-criteria Geographic Information System (GIS) analysis to determine the locations that are susceptible to flash floods(Bathrellos et al., 2016). (de Brito & Evers, 2016) (Khosravi et al., 2019) conducted a study that revealed an 82% rise in the adoption of Multi-Criteria Decision Analysis (MCDA) for flood analysis since 2009. This increase was determined by examining advanced flood models. The MCDA technique enables the incorporation of social, environmental, and cultural factors into flood risk assessment, in contrast to other approaches that mainly focus on economic and physical risks (Meyer et al., 2009). The incorporation of socio-economic variability enables the identification of socially vulnerable communities and facilitates the development of more equitable policy decisions.

1.2 Research questions and Objective for the study

Aim: The purpose of this master's thesis is to comprehensively assess the effectiveness and practicality of Multi-Criteria Decision Making (MCDM) and Geographic Information Systems (GIS) techniques for fluvial flood susceptibility mapping in Telemark County, Norway.

1.2.1 In order to evaluate it, this study aims to:

1. Integrate Diverse Geospatial Data Sources in GIS: Utilize data from multiple sources, including topographic maps, hydrological data, and historical flood records, to create a comprehensive dataset for analysis.

2. Assess the Capability of MCDM and GIS: Determine how well MCDM integrated with GIS can map areas susceptible to flooding. This involves an analysis of various criteria that influence flood.

3. Develop a Flood Susceptibility Map: Create a detailed map that highlights areas in Bø and Seljord municipalities of Telemark County at different levels of flood susceptibility. This map may serve as a critical tool for local planners and decision-makers in implementing flood risk management strategies.

4. Analyse the Impact of Criteria weighting: examine how different weightings of criteria affect the outcomes of the flood susceptibility analysis. This includes sensitivity analysis to understand the robustness of the results.

5. Evaluate the model's accuracy by utilizing the ROC-AUC. The findings could be valuable to local governments and decision-makers in the field of catastrophic risk reduction.

1.2.2 Anticipated responses and results

Overall, the responses and results from this master's thesis are expected to contribute significantly to the field of disaster management, particularly in enhancing methodologies for flood risk analysis and mitigation planning.

1.Enhanced Flood Risk Identification: The application of MCDM and GIS is expected to yield a detailed and accurate flood susceptibility map that identifies areas at varying degrees of susceptibilities with a high level of spatial resolution. This map should highlight not only the

most vulnerable areas but also zones of potential risk that may not have been previously considered.

2.Validation of MCDM and GIS efficacy: The thesis aims to validate the effectiveness of various MCDM techniques in synthesizing intricate datasets into practical insights through a comparative analysis. The results should showcase the efficacy of these integrated methods in delivering unambiguous and dependable evaluations of flood risk, considering a wide range of criteria.

3. Insights into Criteria Weighting: The study will provide insights into the influence of various weightings of criteria on the outcomes of flood susceptibility mapping. This analysis could unveil the key factors, such as elevation, precipitation patterns, or land cover, that play a crucial role in determining the level of flood risk in Telemark County.

4. Policy and Planning Recommendations: This thesis should have the capacity to propose precise policies or planning measures derived from the identified flood-prone areas. These recommendations may encompass proposals for zoning regulations, enhancements to infrastructure, or strategies for emergency preparedness

5. Scalability and Adaptability Analysis: The result may also address the scalability and adaptability of the methods used in other regions or for different types of environmental risk assessments, potentially expanding the influence of the thesis beyond Telemark County.

6. Identification of Limitations and Future Research Directions: The thesis is expected to delineate any limitations encountered during the study, including issues related to data quality, methodological constraints, or difficulties in engaging stakeholders. Additionally, it proposes potential avenues for further investigation to enhance the evaluation and control of flood hazards.

1.3 Importance and value of the research

This research holds value not only due to its scientific rigor and practical application, but also because it has the potential to greatly improve communities' understanding, preparedness, and response to flood risks.

Scientific Contribution

Methodological Advancement: This research enhances the ongoing progress of combining methods in environmental science and disaster management by improving and evaluating the effectiveness of Multi-Criteria Decision Making (MCDM) and Geographic Information System (GIS). It enhances the scientific community's comprehension of how these technologies can be utilized to analyse and interpret intricate environmental data with greater efficiency.

Enhanced Analytical Precision: The study improves the precision of risk assessment models by prioritising the accuracy of flood susceptibility maps. This enhancement is essential for the advancement of more dependable predictions and evaluations in the field of environmental science.

Potential Impact

Improved Disaster Preparedness and Response: The flood susceptibility maps generated can be utilized by local authorities to enhance their preparedness and response strategies. This data aids in formulating more efficient evaluation strategies, implementing measures to safeguard infrastructure, and allocating resources effectively in the event of floods.

Policy Making and Planning: The findings of this research can provide valuable guidance to policy makers and planners in making informed decisions regarding land use, infrastructure development, and community zoning to minimize the effects of flooding.

Community Safety and Resilience: The research contributes directly to improving community safety and resilience by identifying areas that are prone to flooding. This is accomplished by implementing focused educational and awareness initiatives, enhancing early warning systems, and implementing adaptation strategies that involve the local community.

Economic Benefits

Cost Effectiveness: Efficient flood risk management can greatly diminish economic losses caused by property damage. Disruptions in business operations, and expenses related to recovery and reconstruction. The research assists in prioritizing investments in flood defense by offering precise data and predictive models.

Environmental Considerations

Environmental Conservation and Management: A comprehensive understanding of flood dynamics is essential for effectively managing natural resources, including water bodies and wetlands, which play a critical role in mitigating floods. This study can provide valuable guidance for environmental conservation efforts aimed at preserving or improving these natural mechanisms that protect against flooding.

Global Relevance

Scalability and Application in Other Regions: The research primarily examines Telemark County, but its methodologies and findings can be applied to other regions worldwide that encounter comparable flood hazards. The study's scalability enhances its global significance by offering a risk assessment model that can be customized and utilized in various regions across the globe.

1.4 The structure of the thesis

Section 2

This section provides the necessary foundation for comprehending the present condition of flooding and the endeavours undertaken by global authorities to formulate the most effective prediction methods. The study investigates the amalgamation of Geographic Information Systems (GIS) and Multi-Criteria Decision Analysis (MCDA) methodologies to forecast floods in areas with a high likelihood of risk.

Sections 3 and 4

These sections provide a comprehensive overview of the study area and in-depth analysis of data preprocessing steps. In addition, the report discusses several important aspects of flood susceptibility analysis. These include assessing the structural framework, using AHP-based grading, and weighting methods, ensuring consistency among the factors used, mapping flood susceptibility zones, evaluating the effectiveness of the AHP technique, and assessing the accuracy of the model.

Section 5

This section provides the results obtained from the thesis, which are depicted using figures, tables, maps, and graphs. Additionally, it provides a concise overview of the main findings pertaining to the five objectives of the thesis, emphasizing the most noteworthy observations.

Section 6

This section delivers a comprehensive analysis of the results obtained from the research.

Sections 7 and 8

These sections provide comprehensive conclusions derived from the research regarding the study area, summarizing the implications and insights obtained through the study.

2. Literature review

2.1 Definitions and concepts

2.1.1 Types and causes of flood

Floods are commonly referred to as the result of rivers exceeding their banks, which poses a threat of harm or destruction (Prinos et al., 2008). Floods are discussed when the volume of water reaches a specific level, even though this does not necessarily result in flooding. Some areas may experience high water levels and flooding, even if the water flow is not significantly large. Obstructed drainage outlets and the buildup of ricer ice are factors that can cause a river to exceed its banks. In highly populated regions, heavy rainfall or rapid snow melting can cause flooding, even if the water flow in the river basin is not at flood levels.

Floods are a prevalent natural disaster that has been increasingly encountered worldwide in recent times. The intensity and occurrence of flooding have experienced a predominance in recent years. There are various instances where Norway has experienced big flood events. Several of the most devastating floods in Norway are identified by their specific names. One of the most well-known flood events is the Storofsen, Ofsen, or Skriusommaren flood, which took place in July 1789 in eastern Norway and had devastating consequences. The flood that occurred in Glomma River between 1675 and 1773 are referred to as Storfloden. Prior to the

occurrence of Black Death, a significant flood resulted in substantial alterations at Vågåmo in River Otta. Additionally, the catastrophic flood that occurred in eastern Norway in December 1743 is referred to as Troeflaumen in Hardanger. The severe flood that occurred in South Norway in June 1860 is commonly known as Ofsen. The flood that occurred in 2011 and 2103 in River Glomma and River Gudbrandsdalsågen are collectively referred to as whit-Sunday flood (NVE 2021).

The primary factor contributing to significant floods in Norway is precipitation, frequently accompanied by the melting of snow (NVE 2000). The magnitude of floods is primarily influenced by weather conditions, specifically the distribution of precipitation and temperature levels. The water storage capacity of vegetation, bed rocks, lakes, streams, and rivers is a crucial factor to consider. The conditions of floods can also influence human activities. The process is achieved by implementing demanding development plans in areas adjacent to rivers by clearing forests and other vegetation. The emission of greenhouse gases is a less direct method of affecting flood conditions (NVE 2000). The increase in temperature can result in significant alterations to the weather. An outcome of this phenomenon could potentially manifest as a rise in the occurrence of floods, hurricanes, forest fires, and landslides. It can be argued that individuals bear responsibility for both the causes and consequences of floods.

Urban Flooding

Urban flooding is the term used to describe a flooding event caused by heavy precipitation, independent of an overflowing water body (Kundzewicz & Pińskwar, 2022). Urban drainage is the most prevalent form of pluvial flooding. In less developed areas, the natural environment naturally takes care of draining excess water. However, in developed areas, it becomes necessary to find methods to remove excess water that can seep into the ground because of impermeable surfaces (Prinos et al., 2008). Urban drainage involves the implementation of an enclosed network of channels to collect and remove surplus rainwater from the surface. This philosophy asserts that regardless of the intensity or duration of the rainfall, the drainage system must have the capacity to collect and eliminate the runoff (Ghanbari et al., 2024).

River flood

Flooding caused by rivers occurs when the amount of water in a river exceeds the capacity of the channels, whether they are natural or human-made, causing the water to overflow into nearby low-lying regions (Kundzewicz & Pińskwar, 2022). The changing patterns of floods by rivers vary according to the characteristics of the terrain. Runoff in mountainous areas can manifest within minutes following intense precipitation, whereas in flat and low-lying regions,

water accumulation may persist for days or even weeks. River flooding can be classified into distinct types: overbank flooding and flash flooding (Gruntfest & Handmer, 2001). Overbank flooding refers to the situation where the amount of water in a river or stream rises beyond its capacity and spills over into nearby flood areas. This typically happens as a result of surface water runoff following heavy rainfall, the release of water from dams, the melting of snow, or the formation of ice blocks(Enríquez de Salamanca, 2023). Meanwhile, flash flood refers to the rapid and perilous influx of a large amount of water into an area that is typically dry, or a sudden and significant increase in the water level of a stream or river beyond a pre-established flood threshold(Gruntfest & Handmer, 2001). It is defined as a rapid and forceful surge of water that occurs suddenly in a pre-existing river channel with minimal or no warning. Flash floods pose a greater threat to life and property compared to the overbank flooding due to their rapid onset and the significant number of debris they carry (Tockner & Stanford, 2002).

Coastal flooding

Coastal flooding occurs when intense storms or the other extreme weather conditions coincide with high tides, resulting in an elevation of sea levels above standard and the intrusion of seawater onto lands (Kundzewicz & Pińskwar, 2022). Flooding from storms and earthquakes are the primary causes of coastal flooding. A storm surge is the elevation of seawater above its usual tide levels caused primarily by the combination of low pressure in the atmosphere and the force of wind over a large area of open water. During a storm or hurricane, low pressure inside the eye of the storm generates suction, resulting in the formation of a water dome. If the storm is near land, the powerful winds within the storm propel the dome of water towards the land, resulting in a surge. Underwater earthquakes, resulting from the displacement of tectonic plates, cause significant shifts in the ocean floor (Doornkamp, 1998).

Types of floods in Norway

According to a report published by (NVE 2021), it has highlighted various types of causes of flooding in Norway. Snowmelt floods, rainfall floods, Ice run foods, slide-induced floods, and floods from glacial dams are some natural causes of flooding in Norway. Additionally, land use changes, effect of hydropower regulation are anthropogenic causes of floods in Norway. In Norway, there are four flood types that are relevant for significant flood risk:

- Fluvial floods refer to the floods that occur in the rivers.
- Flash floods refer to the sudden and rapid flooding that may happen beyond the usual river channel network.
- Storm water floods refer to the floods that occur in the urban areas.

- Coastal flooding

2.1.2 Spatial Scale of flood

The significance of flood processes and the level of detail in flood maps differ depending on their spatial scale. In accordance with (Moel et al., 2015), we also differentiate between local, regional, national, and supra-national scales. The selection of scales is frequently based on personal preference, but the following is a logical classification:

- **Large scale** pertains to limited geographical areas, such as towns or specific segments of a river. If the study area has a measurement, we classify it in this category if the area is less than 100 square kilometres.
- **Regional scale** refers to a defined geographic area such as a province, watershed, or a large city. Study areas with an area of less than 100000 square kilometres are within this scale.
- **National scale** pertains to evaluations of entire countries, utilizing consistent data. To eliminate small countries, the study area must exceed 100000 square kilometres.
- **Supra-national scales** refer to evaluations that encompass an entire continent or the entire planet.

2.1.3 Flood inventory

A flood inventory is a thorough collection of information regarding previous flood occurrences, including their scope, intensity, consequences, and destruction (Al-Abadi & Pradhan, 2020). The information provided usually consists of floodplain maps. Historical flood records, evaluations of damage, and details about measures taken to mitigate flood hazards. Through the systematic documentation and analysis of this data, authorities and stakeholders can acquire valuable insights into the patterns and characteristics of flooding in a specific region. This information can then be used to develop effective strategies for managing and reducing the risks associated with flooding (Haltas et al., 2021). Adopting a proactive approach is crucial in improving the ability of communities to withstand floods and reducing the resulting social, economic, and environmental consequences.

2.1.4 Flood susceptibility

Flood susceptibility is the probability or capacity of a particular area to undergo flooding, determined by the arrangement of geographical and environmental factors (Li et al., 2018). Flood susceptibility is determined by various factors, including topography, soil composition, vegetation cover, and hydrological features such as proximity to water bodies and drainage

patterns. Flood susceptibility does not forecast the timing of a flood, but rather identifies the regions that are more prone to being impacted by floods given appropriate circumstances (Rosmadi et al., 2023). Evaluating flood susceptibility is essential for disaster preparedness and management, enabling planners and authorities to enact preventive measures, devise effective mitigation strategies, and ensure swift response efforts to minimize the impact of floods on communities and infrastructure.

Flood susceptibility map assesses the likelihood of flooding in each area by analysing its physical attributes (Vojtek & Vojteková, 2019). This measure lacks quantitative analysis and does not assess any flood variables. Nevertheless, it can offer dependable information in the absence of quantitative data and can be utilized to conveniently evaluate areas at risk on a large scale. Flood susceptibility mapping is conducted by considering various factors, including topography, geography, and meteorology. These factors, such as altitude, slope, lithology, land use, and rainfall, are analysed and compared with historical flood events to determine the areas at risk. This analysis is conducted using multivariate techniques and Multi-Criteria Decision Analysis (Kazakis et al., 2015; Tehrany et al., 2014).

2.1.5 Flood Hazards

A Flood hazard is defined as the probability of potentially damaging flood events occurring in a given area within a specified time horizon (Nones, 2017). One way to get a hazard map is by using numerical methods (Dottori et al., 2022). This method does have some limitations, but it is generally useful. Fast and accurate flood simulations continue to be a challenge, despite the robustness and effectiveness of numerical methods for flood hazard modelling (Costabile et al., 2016). Several methods exist to make the simulations run faster. The latter is established by statistical analysis that takes flood frequency and intensity into account (Dottori et al., 2022). To create flood hazards maps, numerical models discretise the realm of computation and equations that govern how to replicate flood events.

2.1.6 Flood risk and vulnerability

Vulnerability refers to the susceptibility to harm when there is a lack of ability to adapt and exposure to stresses caused by changes in society and the environment. The awareness and mitigation of flooding repercussions for communities and ecosystems heavily rely on the assessment of flood risk and vulnerability. Flood risk is defined as the combined likelihood of an event and the potential negative impacts it can have on individuals, buildings, infrastructure, and the natural surroundings. The term vulnerability pertains to the susceptibility of these elements to potential harm or damage caused by flooding. This susceptibility is influenced by various factors, including socio-economic status, land use patterns, infrastructure resilience, and environmental conditions (Mitra et al., 2022).

Comprehending the concepts of flood risk and vulnerability is crucial in the development of efficient flood risk management strategies. These strategies encompass various aspects such as land-use planning, infrastructure investment, early warning systems, and community preparedness initiatives (Jongman et al., 2018).

2.2 Flood Susceptibility Mapping

Flood susceptibility mapping involves the identification and visualization of areas that are susceptible to flooding, considering a range of environmental and geographical factors. This mapping technique employs various data, including topography, soil types, land use, rainfall patterns, and proximity to water bodies, to evaluate the probability of different regions encountering flood events(Shokouhifar et al., 2022). The resultant maps classify areas based on their degree of vulnerability to flooding, ranging from low to high susceptibility.

These maps are indispensable instruments for urban planners, emergency management officials, and policymakers. They assist in the formulation of strategic plans for managing flood risks by providing guidance for land use decisions, informing the development of infrastructure, improving readiness for emergencies, and implementing measures to reduce the impact of floods. Flood susceptibility maps visually depict areas that are at risk of flooding, helping to improve comprehension and communication of flood risks to the public and stakeholders (Bajracharya et al., 2021). This enables more informed decision-making and strengthens community resilience to floods.

Furthermore, flood susceptibility mapping (FSM) often utilizes statistical analysis, fuzzy logic, hybrid methods, machine learning, and physical-based model (Kaya & Derin, 2023). Several techniques, including statistical analysis, can be employed to determine significant factors. Alternative approaches, such as fuzzy logic, offer the benefit of incorporating multiple parameters and accounting for inconsistencies in the data. Furthermore, machine learning algorithms possess the ability to acquire knowledge from data and reveal intricate connections between factors. The combination of various sources of data is necessary for the implementation of a flood susceptibility mapping (FSM). These data sources include hydrological, topographical, and meteorological data. Identifying appropriate techniques and factors is crucial to successfully incorporating and utilising these data sources to produce precise flood susceptibility maps.

2.2.1 Flood Indicators

Natural Catastrophes, such as floods, landslides, and erosion are predominantly influenced by the presence of various conditions in the specific area (Ali et al., 2019). To assess the flood susceptibility for any area, it is imperative to examine a range of flood-triggering factors, as well as their correlation with flooding (Sahana & Patel, 2019). The researchers in the reviewed articles utilised various flood indicators based on the applicability of the study area. Deciding on parameters for generating flood susceptibility maps is frequently regarded as a complex endeavour in the field of Flood Susceptibility Modelling (FSM) (Tariq et al., 2022). The choice of flood indicators is contingent upon the physical and natural attributes of the study area, as well as the accessibility of the data (Ullah & Zhang, 2020).

The researchers in the reviewed articles utilised a range of indicators for flood susceptibility mapping, with a maximum of 21 indicators and a minimum of 5 indicators. According to Table 1, it shows the number of flood indicators used in the reviewed articles. From the reviewed articles, it is found that most of the researchers prefer to have 10 indicators or less for the flood susceptibility mapping. Meanwhile, the preferred indicators for the research by the researcher include elevation, slope rainfall, LULC, TWI, geology, soil, and distance from river.

Table 1: *Review of flood indicators used for flood susceptibility mapping.* E: Elevation, S: Slope, A: Aspect, TWI: Topographic Wetness Index, DFR: Distance from river, DD: Drainage Density, NDVI: Normalized Difference Vegetation Index, LULC: Land use Land cover, G: Geology, C: Curvature, R: Rainfall, SPI: Stream Power Index, NDSI: Normalized Difference Snow Index, F: Flow Accumulation.

References	**Flood indicators**														
	E	S	A	TWI	DFR	DD	NDVI	LULC	G	Soil	R	C	SPI	NDSI	F
(Nguyen et al., 2021)	x	x	x	x	x	-	x	-	-	x	x	x	x	-	x
(Sahana & Patel, 2019)	x	x	x	x	x	x	-	x	x	x	x	x	-	-	-
(Tehrany et	x	x		x	x	-	-	-	x	x	-		-	-	-

al., 2015)															
(Bui et al., 2019)	x	x		x	x	-	x	x	x	x	x		-	-	-
(Khosravi et al., 2019)	x	x		x	x	-	x	x	x	x	x		x	-	-
(Yaseen et al., 2022)	x	x		x	x	x	x	x	x	x	x		x	-	-
(Vojtek & Vojteková, 2019)	x	x			x	x	-	-	x	-	-		-	-	-
(Rahmati et al., 2015)	x	x		x	x	x	-	x	x	x	-		-	-	-
(Nguyen et al., 2023)	x	x		x	-	-	x	x	x	x	x		x	x	x
(Al-Juaidi et al., 2018)	x	x		-	-	-	-	x	-	x	x		-	-	-
(Ali et al., 2019)	x	x		x	x	-	-	x	-	x	x		-	-	-
(Azareh et al., 2019)	x	x		x	x	x	-	x	-	x	-		-	-	-

2.2.2 Method and Techniques

When exploring studies on flood susceptibility in the literature, it becomes apparent that various methods are employed in susceptibility analysis. However, certain methods are more commonly favoured in practice over others. However, there is ongoing debate among scientists in this field regarding the superiority of commonly used methods over others. The literature commonly employs Multi-Criteria Decision-Making (MCDM) methods, physically based hydrological models, statistical methods, and various soft computing methods to evaluate flood sensitivity. Various methods proposed by researchers for creating more objective flood susceptibility maps differ in terms of their reliance on expert opinion and ease of application.

a. Multi-Criteria Decision-Making

The process of decision making involves selecting from a range of alternatives. Multi-Criteria Decision Making (MCDM), is a systematic process that enables the evaluating multiple criteria and the assigning values to alternatives in complex problems, such as disasters. MCDM methods are a set of techniques that facilitate the selection of the optional choice from a range of criteria applied simultaneously (Leake & Malczewski, 2000). Multi-Criteria Decision Analysis (MCDA) offers a comprehensive set of technical methodologies for organizing decision problems and developing, assessing, and ranking alternative decisions (Leake & Malczewski, 2000). The described approach is a decision-making method that enables decision-makers to select the most suitable decision based on the problem prevailing and relevant factors. It takes into consideration the effectiveness of numerous independent variables. Alternatively, there exist techniques that enable the assessment of inferences using a shared language in situations where conflicting factors arise or when factors cannot be quantified. The various MCDM techniques used by multiple scholars include the Analytical Hierarchy Process (AHP) (Kazakis et al., 2015), Analytical Network Process (ANP) (Dano et al., 2019), Weighted Linear Combination (WLC) (Azareh et al., 2019), and Decision-Making Trial and Evaluation Laboratory (DEMATEL) (Wang et al., 2018).

b. Statistical methods

The correlation between flood triggers and floods can be evaluated using statistical methods, which are indirect methods based on mathematical expressions (Dai). When assessing a building's vulnerability to flooding, bivariate and multi-variate statistical analyses are the tools of choice. Among other statistical analyses, the frequency ratio (FR) method is among the

most popular methods for determining how each class affects the flood. One common MSA is Logistic Regression (LR) (Tehrany et al., 2014), which is used to find the impact of each factor on flood formation. Research conducted by scholars (Rahmati et al., 2015) indicates that statistical analysis methods perform admirably when it comes to assessing flood susceptibility. Statistical methods typically use linear hypotheses to predict the variables; however, flooding is a complex phenomenon, so these variables are not always linear (Costache & Bui, 2019). Because floods are so complicated, researchers have begun to use cognitive approaches, which are more in line with easy computing, rather than conventional, precise, and inflexible methods.

c. Physical-based models

When it comes to flood modelling, real-world hydrological models work well (Dimitriadis et al., 2016). A few examples of these models are one-dimensional Mike 11, ISIS, and HEC-RAS, and two-dimensional TELEMAC-2D, RMA2, and SRH-2D (Tehrany et al., 2018). Physical-based models are not ideal for large-scale studies because they require fieldwork to collect data, a substantial budget, and significant computational capabilities (Rahmati et al., 2015; Tehrany et al., 2018). Both agree that alternative methods should not be used in place in conventional hydraulic modelling. Nevertheless, (Vojtek & Vojteková, 2019) note that these alternatives can be useful in scale analyses and in developing nations. Because of the methodological disparity, this thesis study did not include studies that included physical-based hydrological models and flood susceptibility analysis in their assessment.

d. Machine learning:

Recently, there has been a lot of interest in using machine learning techniques for flood susceptibility mapping. Many studies have been conducted to investigate different predictive models and their effectiveness in different geographical areas. A review of the literature reveals a strong trend toward employing advanced algorithms such as Support Vector Machines (SVM), Random Forests, and Artificial Neural Networks (ANNs) to enhance the accuracy and reliability of flood risk predictions. For instance, studies by (Tehrany et al., 2015) and (Lai et al., 2015) have shown that Random Forest outperforms traditional statistical methods in capturing intricate relationships among various flood-inducing factors, such as rainfall intensity, land slope, and soil type. The results emphasize the capability of machine learning to offer comprehensive spatial risk evaluations that are crucial for efficient disaster management and planning.

Additionally, the literature also discusses the difficulties related to implementing machine learning in flood susceptibility mapping, specifically concerning data accuracy and the

problem of model overfitting. The efficacy of machine learning models relies significantly on extensive superior datasets, encompassing past flooding occurrences, topographic information, and hydrological characteristics.

3 Materials and methods

3.1 Study Area

Telemark is the tenth largest county in Norway, with a total area of 15,299 square kilometres. The county is situated in the southeastern region of Norway which spreads to the ocean from the south and extends to the Hardangervidda plateau in the North. Additionally, the county has numerous hydropower resources because of its favourable climate and topography. Hence, it has 40 hydropower stations (Council 2016). Besides, the county is blessed with dynamic landscapes, mountains, valleys, rivers, and lakes.

However, the thesis research is centred on the Bø-Seljord catchment area, which is situated in the municipalities of Bø and Seljord. The study area covers a total of 1,058 square kilometres and is situated at elevations ranging from 15 meters to 1,536 meters above sea level. Located at 59.617º N and 8.6825º E. The Bø-Slejord catchment area is characterized by rugged mountains, deep valleys, and abundant waterways, creating a diverse and varied terrain. The topography of the region is shaped by the geological processes, primarily characterized by the presence of Precambrian rocks such as basalt, granitic gneiss, rhyolite, quartz slate, and lampro. The geological features present in this area offer a diverse and scenic environment that is well-suited for various activities. The soil composition of this area exhibits variation throughout its terrain, characterised by the presence of fertile soil in valley bottoms and the prevalence of rocky and infertile soils in mountainous regions.

The study area for the thesis is known for its abundant lakes, rivers, and waterfalls, such as Seljordsåna river, and Tinnelva river. The major population centres within the study area are Bø. Seljord, Nome, Hørte, Gvarv, and Lunde. Likewise, the land use and land cover of the research are mainly dominated by forest. The average annual precipitation of the study area is 137.46 mm with a substantial amount of snowfall in the winter. Telemark experiences a subarctic climate characterized by severe winters, the absence of dry season, and cool summers. The annual temperature of the County is 5.24º C, which is 0.21% higher than the average temperature in Norway. Meanwhile, the summer temperature may reach a maximum of 30º C, while it can drop as low as -25º C in winter.

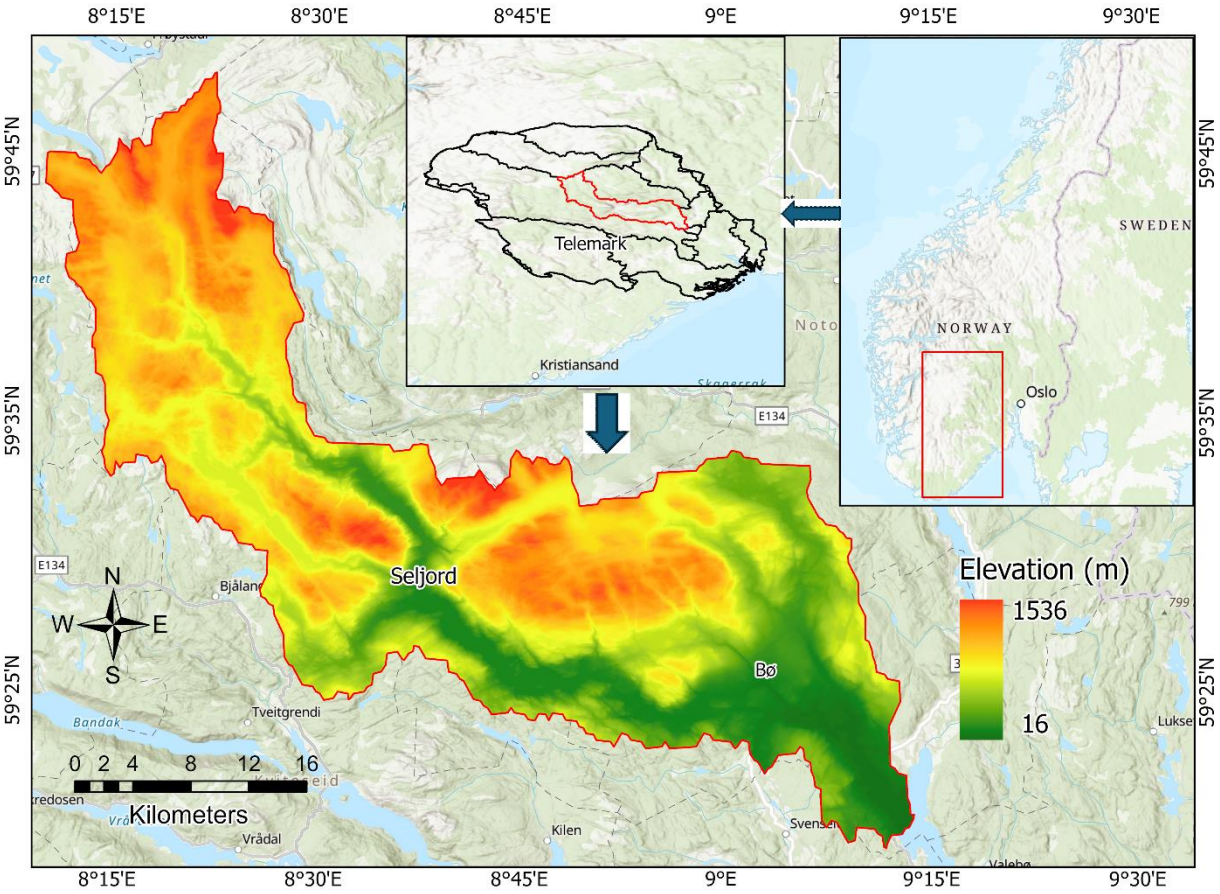

Figure 1: Study area within Bø and Seljord municipalities in Telemark County, Norway.

3.2 Data used

3.2.1 Fluvial food inventory map

The accuracy of flood susceptibility maps can be assessed using historical flood data, also known as flood inventories (Bui et al., 2019; Khosravi et al., 2019); therefore, flood inventory maps (FIM) are considered a crucial requirement in Flood Susceptibility Mapping (FSM) (Tehrany et al., 2015). Multiple techniques exist for the creation of the flood inventory map and the selection of a more suitable approach relies on various factors, including the objective of the analysis, the environmental circumstances of the research area, and the availability of Remote Sensing (RS) and Geographic Information System (GIS) data(Pradhan, 2009). For this thesis research, we used the reports provided by the Norwegian Water Resources and Energy Directorate (NVE). Reports published by the (NVE 2007), the document No.2, 2007 has provided information on the largest flood hit in the Seljord region. There were several flood events that occurred between 1892 and 1967 (NVE

2007). For this specific thesis research, a total of 64 flood points were taken for the analysis from the defined study area.

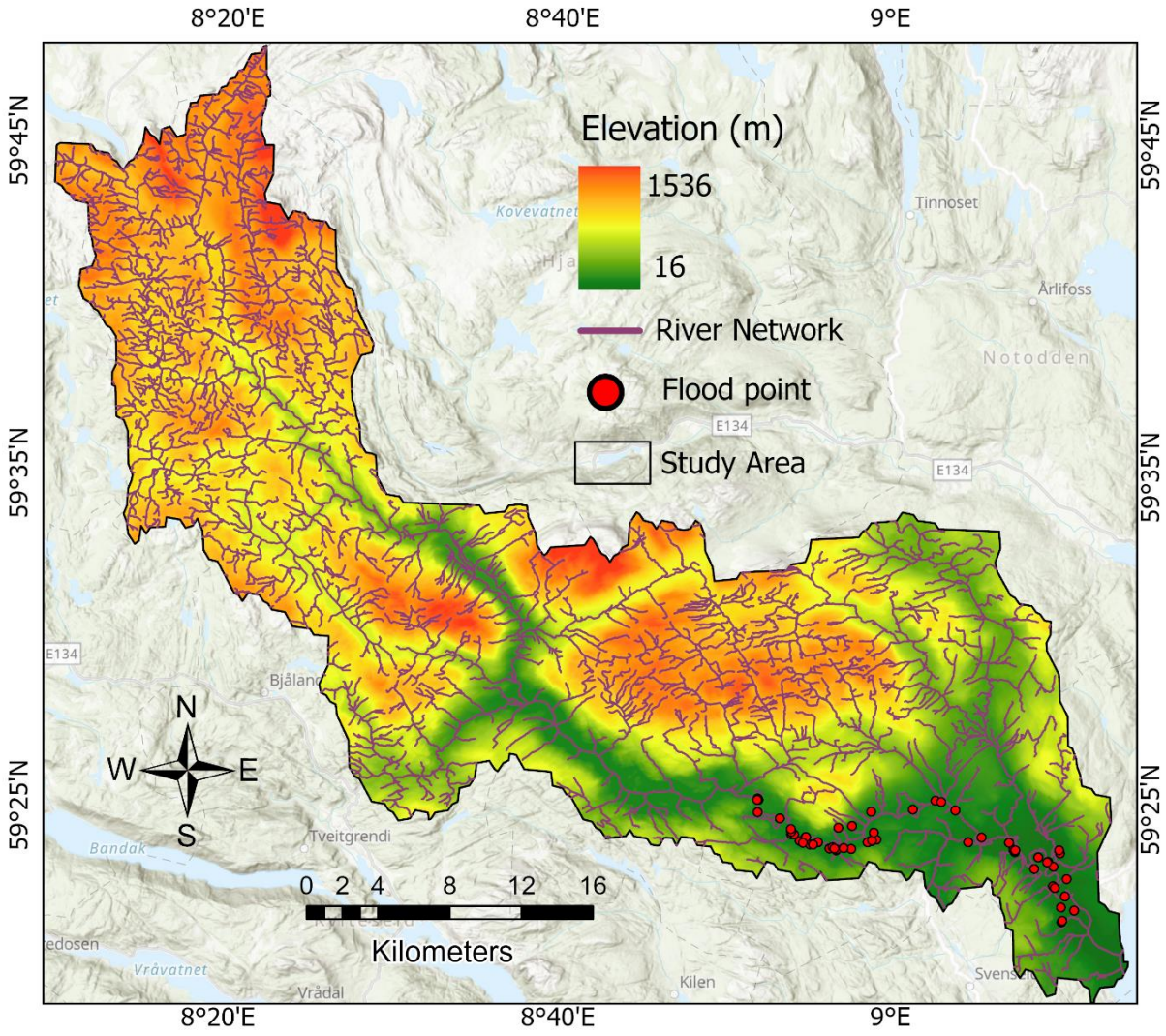

Figure 2: Study area with flood location within Bø and Seljord municipalities in Telemark County, Norway

3.1.2 Flood Indicators

Fluvial floods are the result of a multitude of geographically unique factors that contribute to their occurrence. Precise data regarding these conditioning factors are crucial for the precision and dependability of flood susceptibility mapping(Sahana & Patel, 2019). As of now, there is no universally accepted guideline for choosing flood-conditioning components for susceptible mapping (Dodangeh et al., 2019). The factors that contribute to the

occurrence of floods differ significantly between locations, depending on the physical characteristics and socio-economic conditions of each area. Hence, the flood indicator are usually chosen for the literature review, the specific site conditions, field investigation, and the expertise of experts(Chen et al., 2019; Sahana & Patel, 2019; Zeng et al., 2021). For this study, a comprehensive analysis was conducted on a total of ten factors that contribute to flood conditions. The factors considered in this study are: elevation, slope, distance from river, drainage density, Topographic Wetness Index, Normalized Difference Vegetation Index, Stream Power Index, Normalized Difference Snow Index, lithology, and Land Use Land Cover. Table 1 shows the data used in the thesis work.

The study utilized a substantial amount of raster and vector data, obtained in the form of shapefiles and TIFF files from various sources. Data were sourced from several freely available official sites, including NVE, Høydata.no, DIVA GIS, and ESRI, to support this thesis. Data processing and analysis were conducted using ArcGIS Pro 3.2 software. The data collected for this thesis are documented in Table 1.

Table 2: Data used in the thesis research

Data	Format	Source
Bø-Seljord watershed boundary	Shapefile	DIVA GIS (www.diva-gis.org)
Land use	Raster	ESRI (https://livingatlas.arcgis.com/landcover/)
Digital Terrain Model (DTM)	Raster	https://kartkatalog.geonorge.no/metadata/dtm-10-terrengmodell-utm33
Waterways	Shapefile	NVE (https://nedlasting.nve.no/gis/)
Geology	Shapefile	https://kartkatalog.geonorge.no/metadata/berggrunn-n1350
Sentinel-2	Raster	https://kartkatalog.geonorge.no/metadata/satellittdata-sentinel-2

a. Elevation

Elevation is a critical factor in flood susceptibility analysis because it determines the gravitational flow of water, affecting how water accumulates or drains in an area. Lower elevations are generally more prone to flooding as water naturally flows downhill and accumulates in these areas. Conversely, higher elevations are less likely to experience flooding (Dahri & Abida, 2017).The elevation map used in this study was generated from DEM data provided by GeoNorge, available at (https://kartkatalog.geonorge.no/metadata/dtm-10-terrengmodell-utm33) . The classification of elevations was performed using the manual -interval scale with surface analysis tool within the ArcGIS Pro. The data was classified into five distinct classes, each representing a specific range of values (Figure 3). These classes are as follows: 16 - 124m, 124 - 288m, 288 - 476m, 476 - 699m, 699 -1536m (Kazakis et al., 2015). They are labelled as classes 1 to 5, respectively.

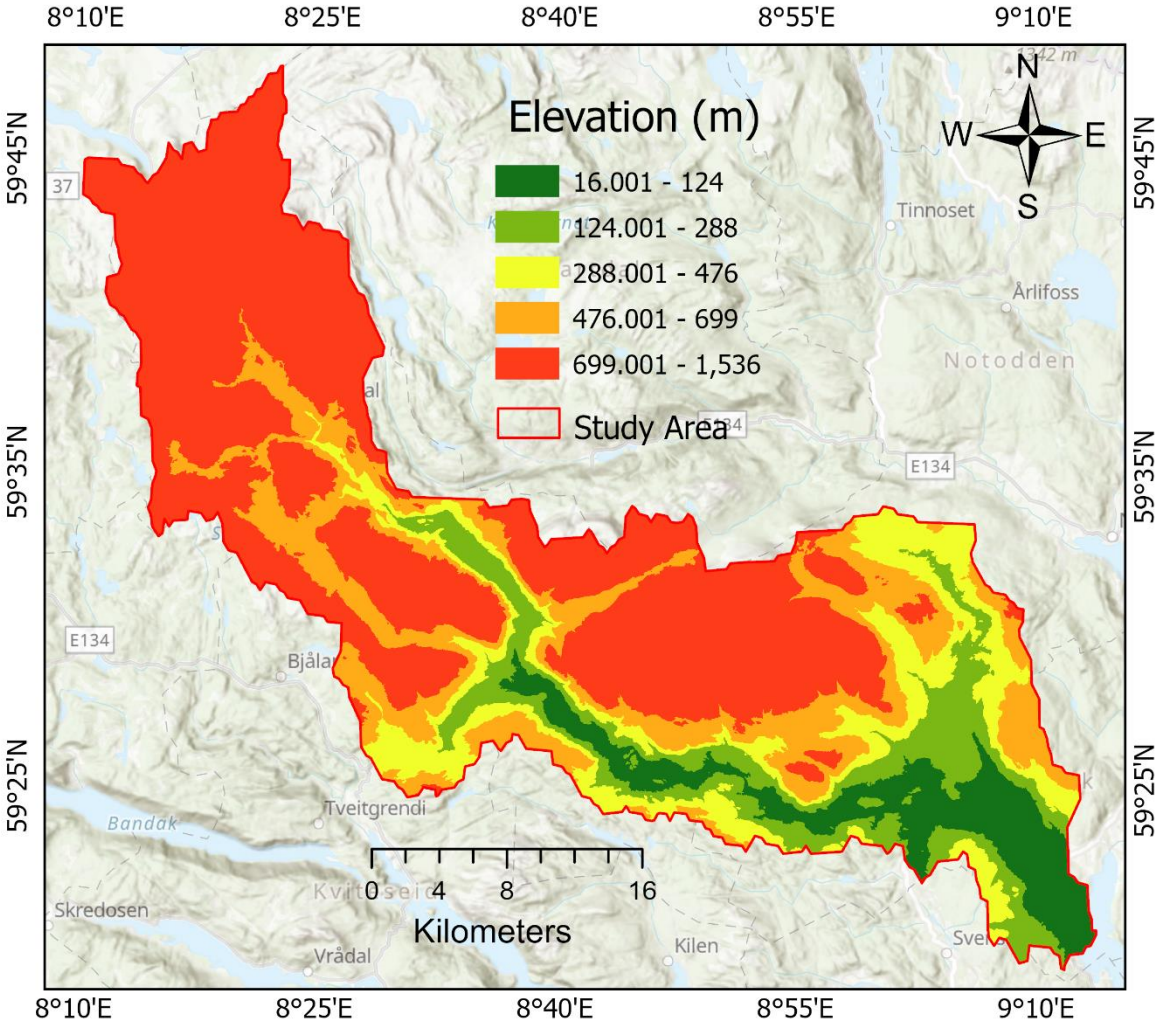

Figure 3: Elevation map for the study area

b. Slope

The slope of an area is significant factor in the regulation of surface runoff, infiltrations, and water retention. As a result, it has a direct impact on the susceptibility of an area to flooding. Previous research has indicated a noteworthy correlation bet ween the slope of the given area and runoff within the area (Fernandez et al., 2010). The surface runoff and infiltration processes that occur during flooding events or in hydrological studies are controlled by factors such as slope, duration of rainfall, and the geological characteristics of the area. The acceleration of the surface runoff caused by precipitation is attributed to steep slopes, resulting in a decrease in the absorption rate of the soil (Çelik et al., 2012; Das & Pardeshi, 2018). Consequently, regions characterized by low slope, such as lowlands, are prone to experiencing significant flooding. This is primarily attributed to the accumulation of substantial amounts of water, resulting in severe floods(Li et al., 2012; Pradhan, 2009). The slope of an area is a significant factor in the regulation of surface runoff, infiltrations, and water retention. As a result, it has a direct impact on the susceptibility of an area to flooding. Previous research has indicated a noteworthy correlation between the slope of the given area and runoff within the area(Fernandez et al., 2010). The slope map depicted in the figure was generated using the DEM within the ArcGIS Pro. The DEM layer is used as the input layer in the Slope tool under the Spatial Analyst tool. The layer is classified into five distinct classes (Figure 4) as follows:0º - 2º, 2º - 5º, 5º - 15º, 15º - 35º, 35º - 80º (Kazakis et al., 2015). Figure 5 shows the method to generate the slope map.

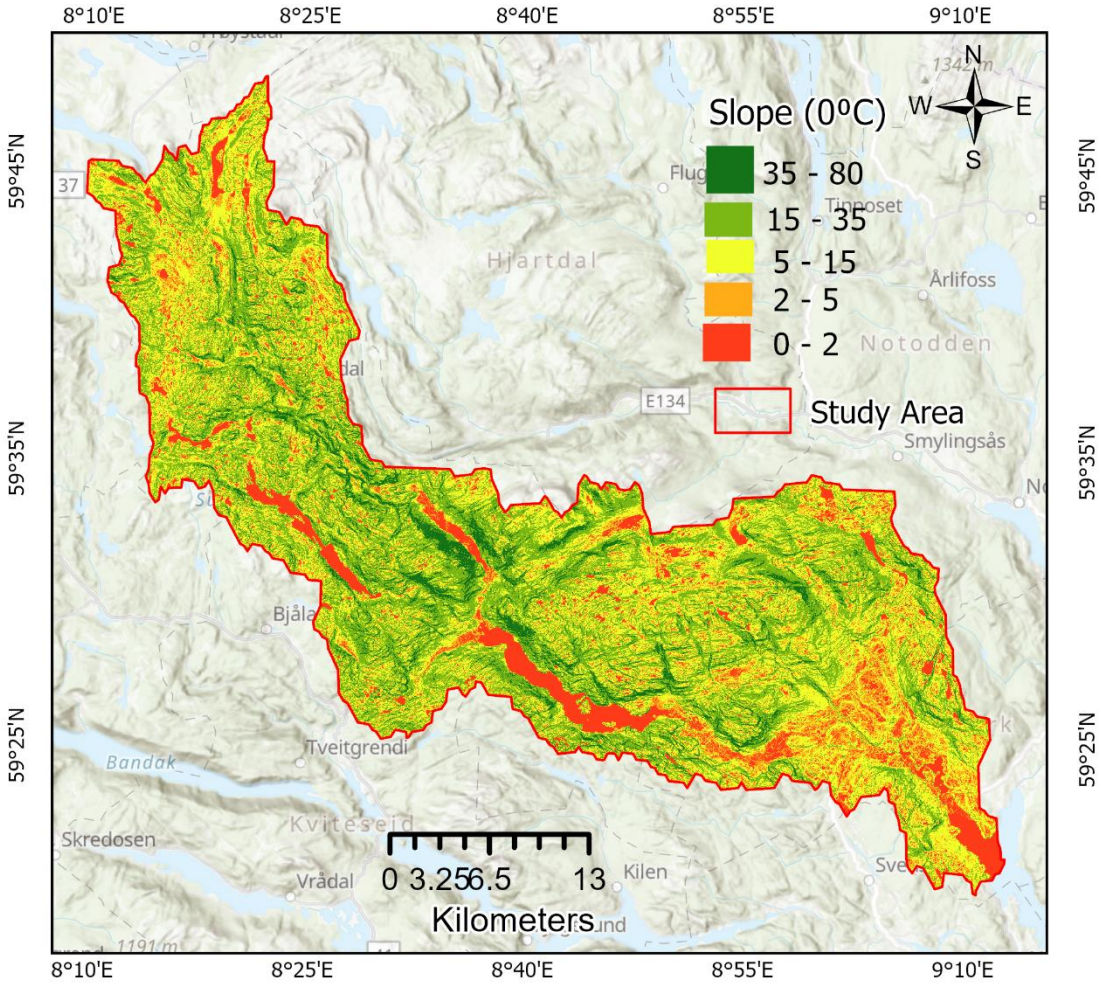

Figure 4: Slope map for the study area

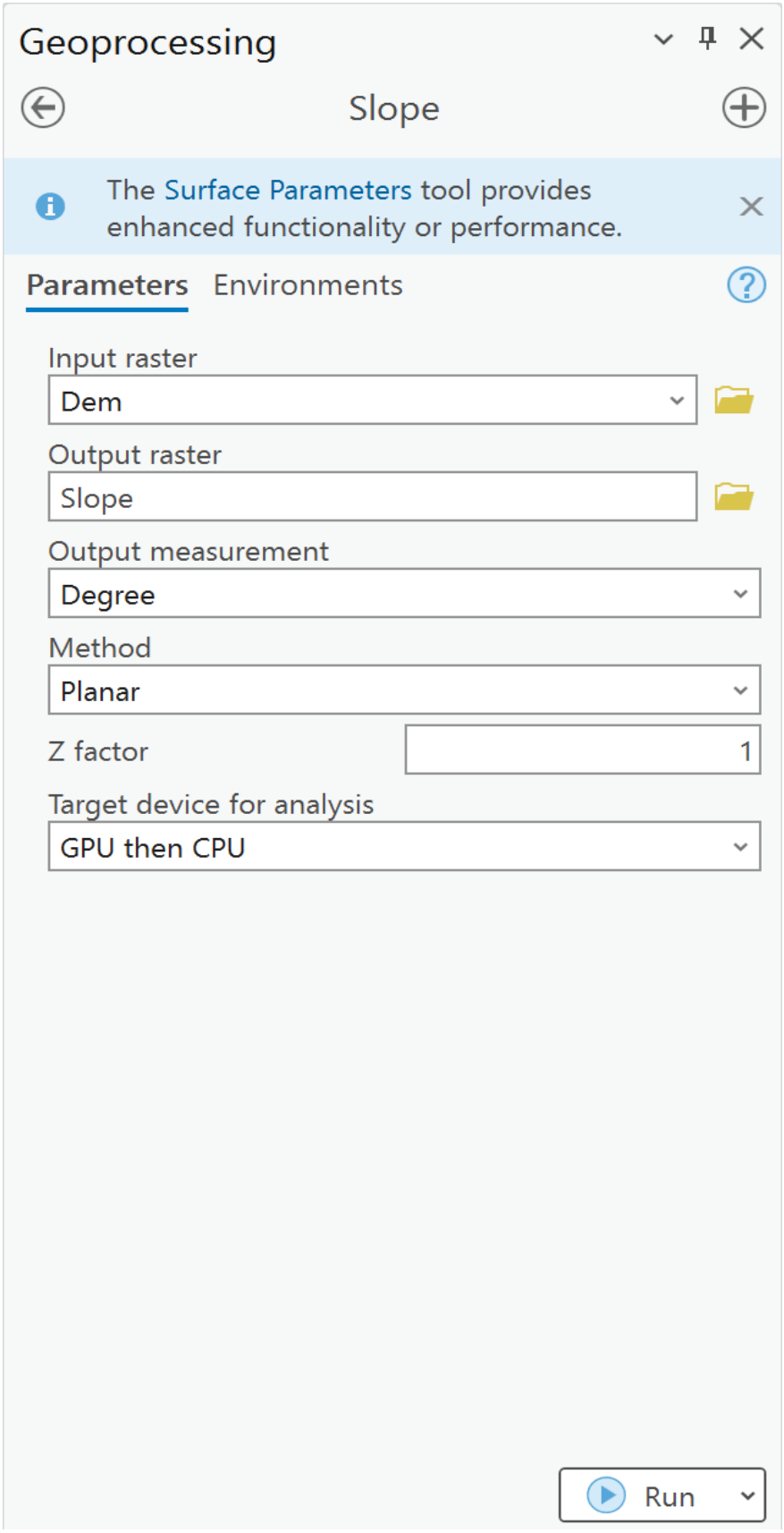

Figure 5: Slope tool for generating the slope map

c. Distance from the river:

Distance from the river is a crucial factor in flood susceptibility analysis because it directly influences how likely an area is to experience flooding (Kazakis et al., 2015). Proximity to rivers often correlates with increased risk, as areas closer to rivers are more susceptible to overflow and rapid water level rises during heavy rain or snowmelt. The distance from the river map was prepared with five classes (Figure 6): 0 - 200m, 200 - 500m, 500 - 1000m, 1000 - 1500m, 1500 - 2000m. In this research, the distance from the river layer is extracted using ArcGIS Pro 3.2. Meanwhile, the Norwegian Water Resources and Energy Directorate (NVE) provides the water network data in shapefile format, available at (https://nedlasting.nve.no/gis/). The water network shapefile and study area boundary were imported into ArcGIS Pro 3.2 software for analysis. The distance from the river map (Figure 6)is calculated using the Euclidean distance tool within the Spatial Analyst tool under the Geoprocessing tab.

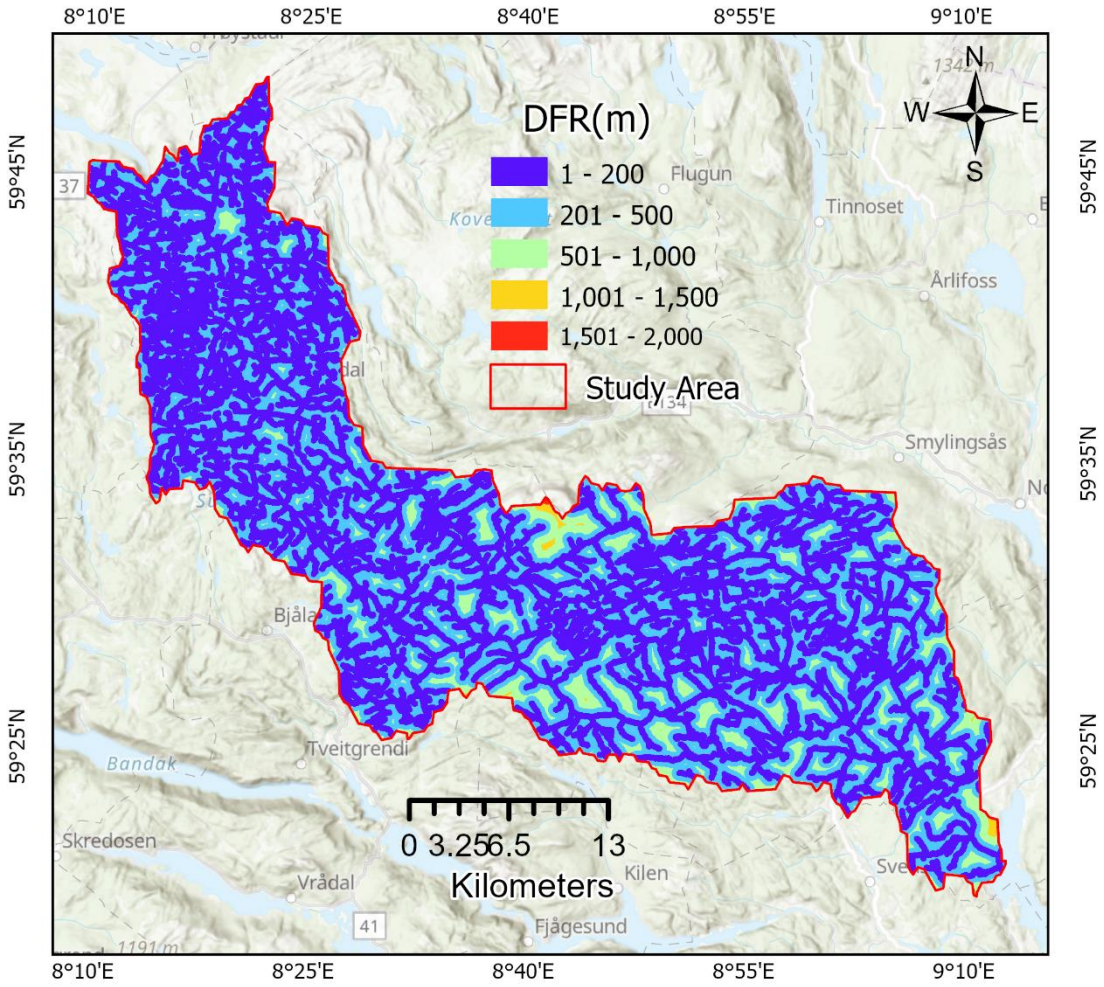

Figure 6: Distance from river map of the study area

d. Drainage density:

The drainage density is defined as the ratio of the sum of the lengths of all drainage channels within a cell to the area of that cell(Muchingami et al., 2019). Drainage density is a crucial factor to consider when conducting flood susceptibility analysis, as it serves as a reliable indicator of the area's ability to effectively remove excess amount of water. A high drainage density signifies an elevated probability of runoff concentration and accelerated water flow, resulting in an increased risk of flooding (Onuşluel Gül, 2013).The drainage density map is created in ArcGIS Pro 3.2 with DEM mentioned above. First, the watershed boundary is established through a series of steps (refer Figure 19). After delineating the watershed boundaries and stream order, both layers are imported into ArcGIS Pro. The drainage density is then calculated using the line density tool under the spatial analyst tool. The map (Figure 7) was classified into five distinct categories using a manual classification scheme as: 0.21 – 0.68, 0.69 – 1.72, 1.73 – 2.87, 2.88 – 3.21, 3.22 – 4.76 km/km².

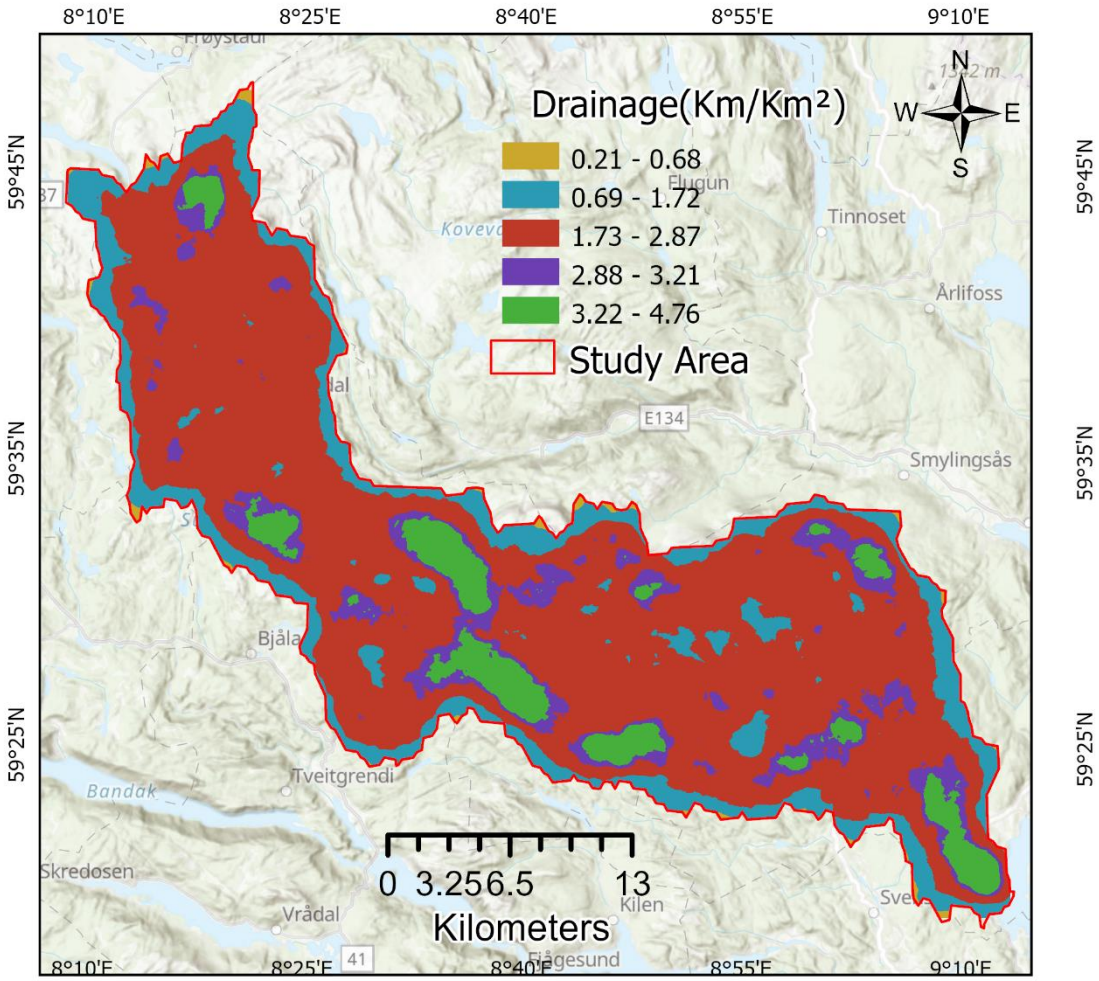

Figure 7: Drainage density map of the study area

e. Topographic Wetness Index:

Topographic Wetness Index (TWI) is the ideal choice for flood susceptibility analysis due to its ability to quantitatively assess how topography influences the accumulation and movement of surface water. TWI evaluates the likelihood of water accumulation in a specific location by considering the local drainage patterns and slope. Regions characterized by higher TWI values generally exhibit levels of moisture and are more prone to experiencing flooding events (Sahana & Patel, 2019). The index was computed by considering the upslope and slope of the cells using Equation (Moore et al., 1991), where α and β represent the cumulative upslope area and hydraulic gradient, respectively.

$$TWI = \ln\left(\frac{\alpha}{\tan(\beta)}\right) \quad (1)$$

In this research, the TWI map (Figure 8) was prepared using the DEM data. Figure 9 shows the various steps used in the preparation of TWI map used in this thesis research.

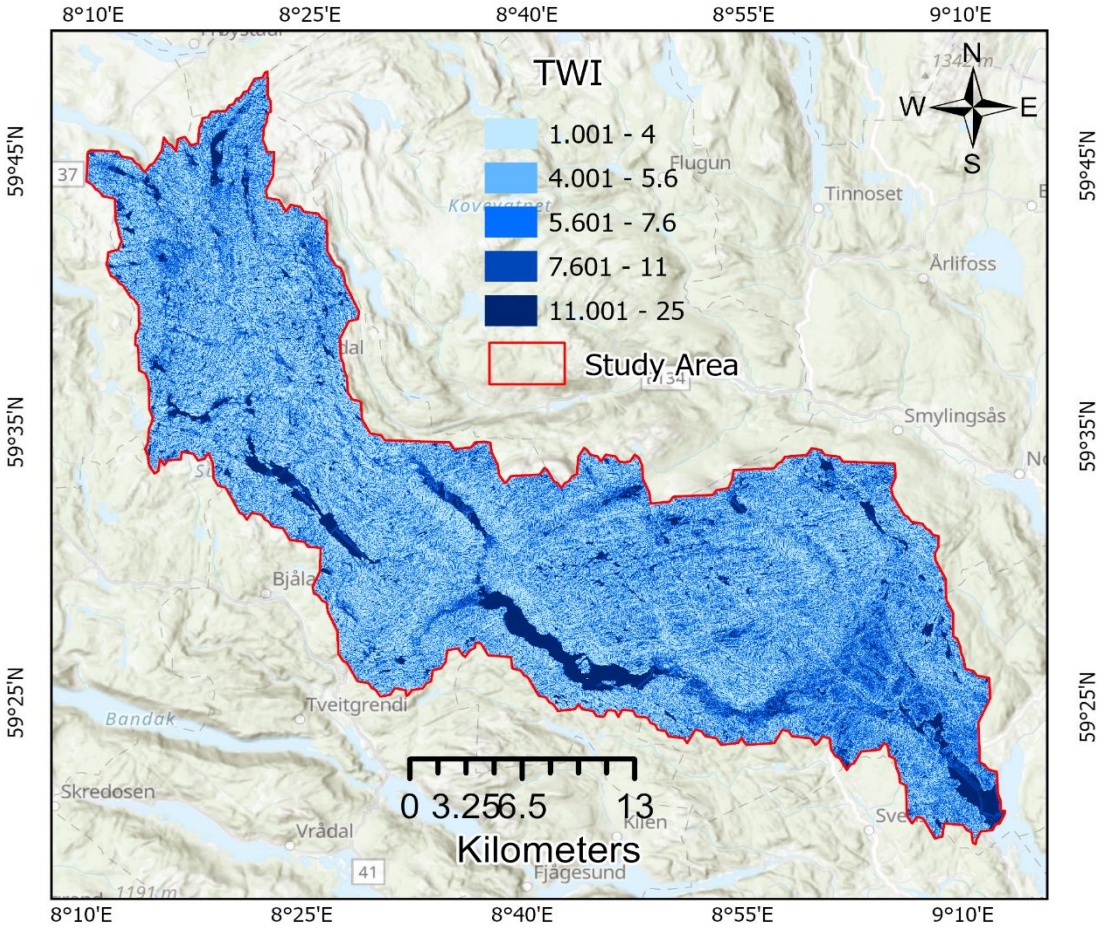

Figure 8: Topographic wetness index map of the study area

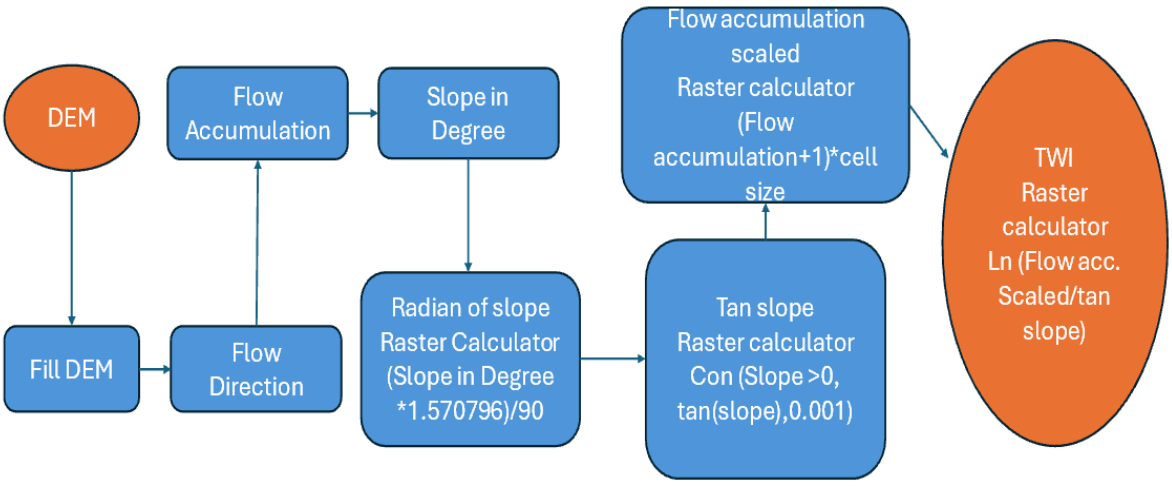

Figure 9: Procedure to generate TWI map

f. Normalized Difference Vegetation Index:

Normalized Difference Vegetation Index (NDVI) is the optimal choice for flood susceptibility analysis due to its ability to accurately quantify vegetation cover, which is vital for water absorption and soil stabilization. Regions characterised by abundant vegetation generally exhibit decreased vulnerability to flooding due to the capacity of plants and their root systems to absorb water and mitigate surface runoff. In contrast, regions with limited vegetation are more susceptible to flooding as they have less capacity to intercept and absorb rainfall. It plays a significant role in flood events(Khosravi et al., 2019). Its values range from -1 to +1. The NDVI values for the study area were calculated using the given equation, which is based on the sentinel-2 image.

$$NDVI=\frac{NIR-RED}{NIR+RED} \quad (2)$$

The NIR and Red refer to the spectral reflectance observations in the near-infrared and red bands of the electromagnetic spectrum, respectively. In the Sentinel-2 images, the near-infrared band corresponds to band 8, while the red bands correspond to band 4.

In this analysis, the NDVI map (Fig. 21) was generated using Sentinel-2 image, available at (https://kartkatalog.geonorge.no/metadata/satellittdata-sentinel-2. First, import the Sentinel-2 image into ArcGIS Pro 3.2, ensuring that the image is georeferenced with precision. Afterward, we navigate the Image Analysis window and select the band combination tool. To compute NDVI, it is typically recommended to choose the appropriate bands, such as the near-infrared (NIR) and red bands, which are band 8 and band 4 respectively. Once the composite image is created, we employ the Raster Calculator tool (Figure 11) to calculate the NDVI using the formula (Equation 2).

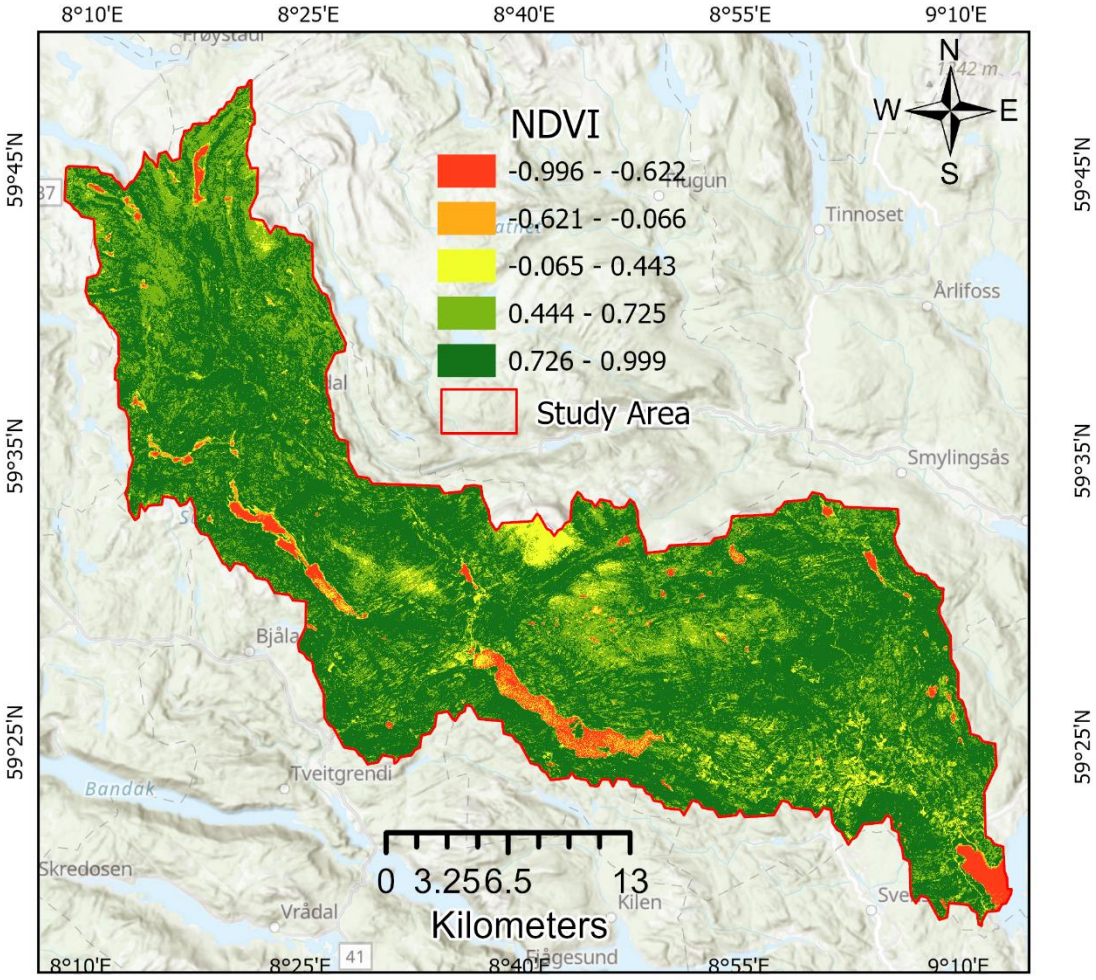

Figure 10: Normalized Difference Vegetation Index map of the study area

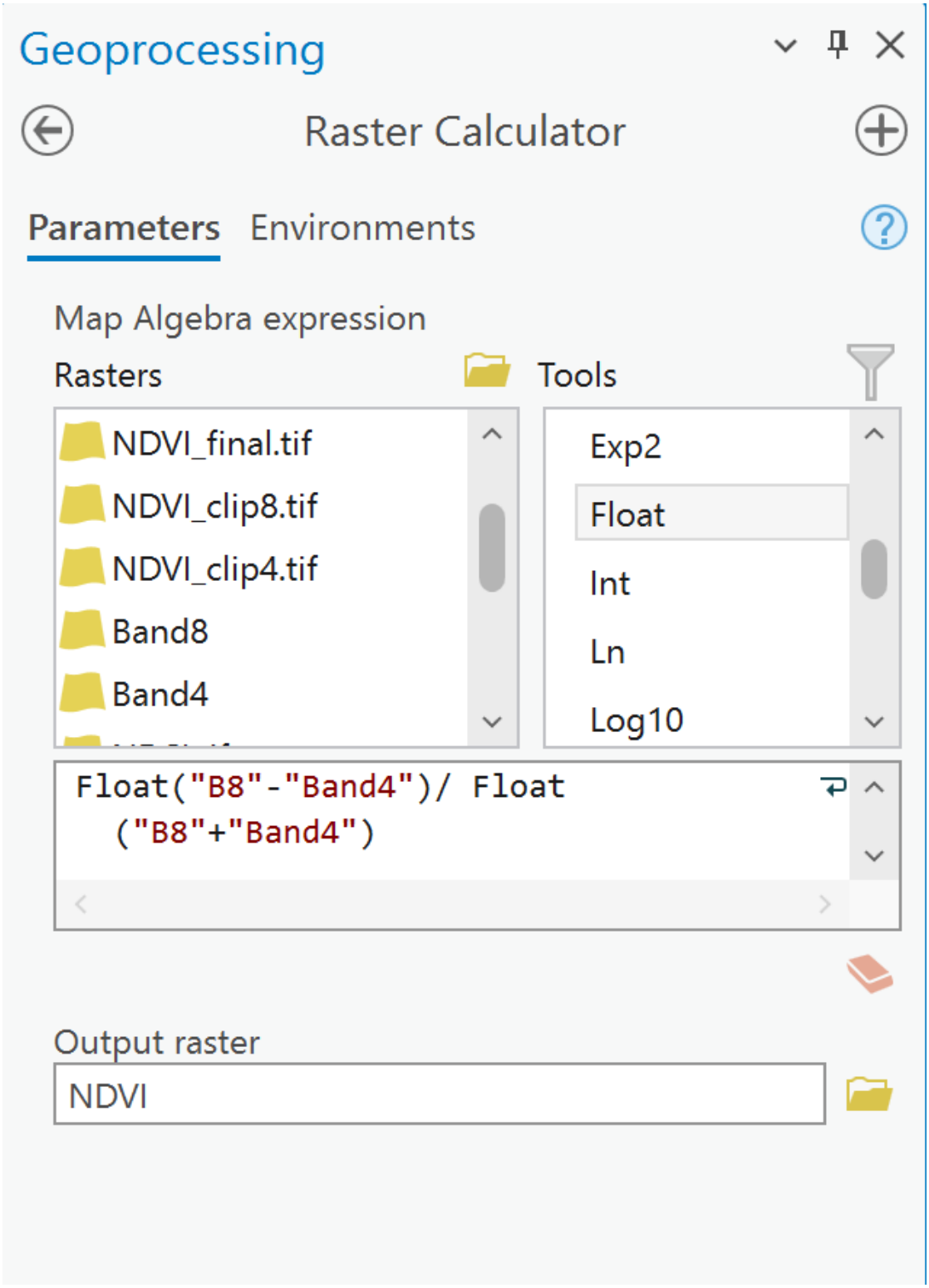

Figure 11: Raster Calculator Tool Generating NDVI map

g. Stream Power Index:

The Stream power index (SPI) is the recommended choice for flood susceptibility analysis due to its ability to quantify the erosive power of flowing water metric (Bui et al., 2019). This index considers the slope of the area and the upstream drainage area. A higher SPI indicates a stronger water flow and a greater potential for erosion. This, in turn, contributes to higher flood risks due to the increased likelihood of stream channel changes and greater sediment transport. It can be determined by applying Equation (3), which involves the specific catchment areas and the slope angle (β) measured in metre per square metre (m/m)

$$SPI = \ln(A_s \times \tan(\beta)) \quad (3)$$

In this analysis, the SPI map (Figure 12) was completed using the DEM) data with series of steps followed using ArcGIS Pr0 3.2. Figure 13 illustrates the various steps involved in the preparation of the SPI map used in this thesis research.

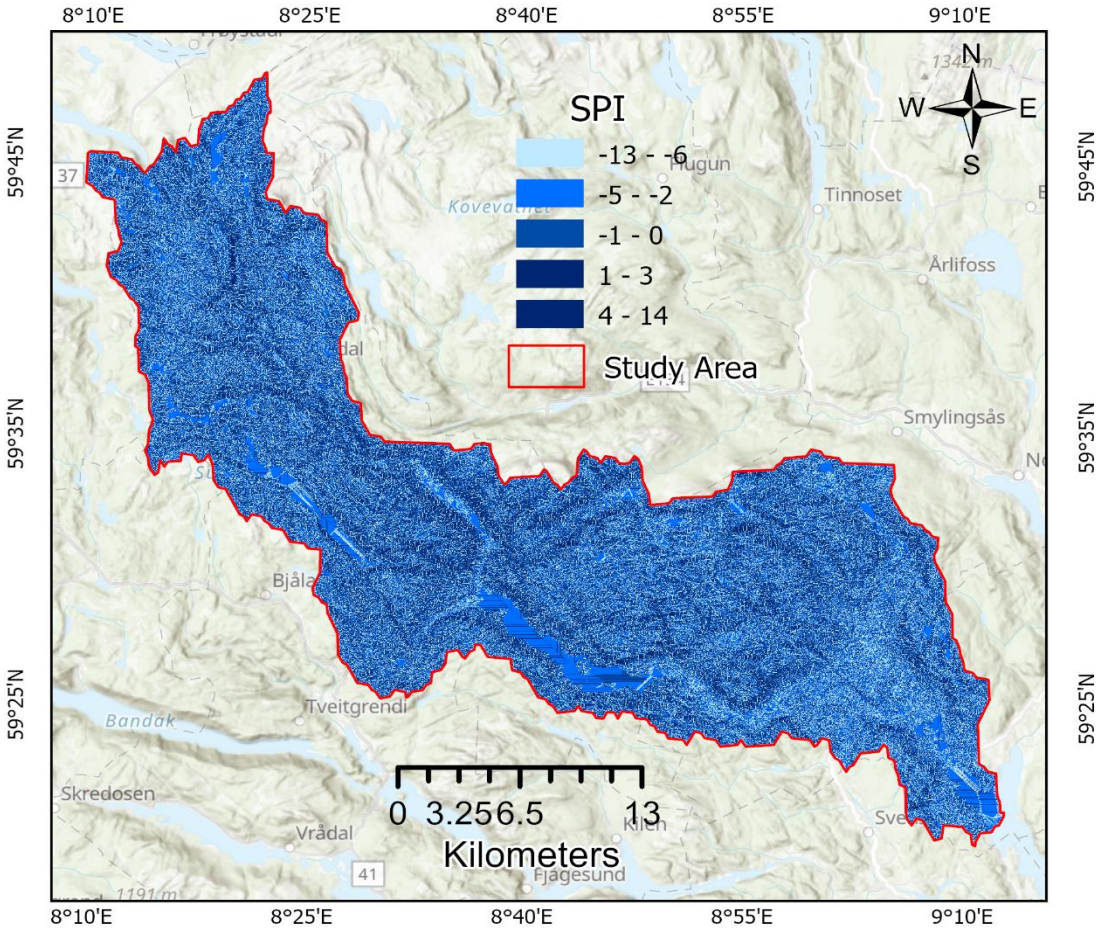

Figure 12: Stream Power Index map of the study area

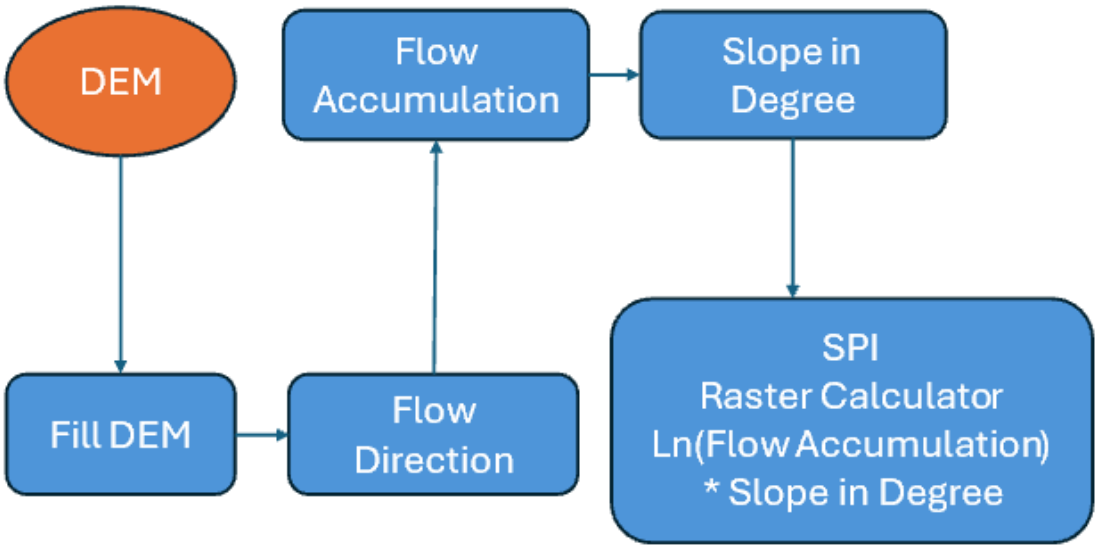

Figure 13: Procedure to generate SPI map

h. Normalised Difference Snow Index:

Normalized Difference Snow Index (NDSI) is a remote sensing spectral index used to detect snow cover. It works because snow has a distinct visible and near-infrared spectral signature compared to other earth features. It detects snow by comparing VIS and NIR reflectance. Its value ranges from -1 to +1. The selection of the Normalized Difference Snow Index (NDSI) is recommended for flood susceptibility analysis due to its capability to detect and monitor snow cover, which plays a critical role in flood risk assessment (Nguyen et al., 2023). The process of snow melting can lead to an increase in surface runoff, which in turn can raise the risk of flooding, particularly when snow melts rapidly

$$NDSI = \frac{B3 - B11}{B3 + B11} \quad (4)$$

In this analysis, the NDSI map (Fig. 23) was generated using the Sentinel-2 images mentioned above. First, import the Sentinel-2 image into ArcGIS Pro 3.2, ensuring that the image is georeferenced with precision. Afterward, we navigate to the Image Analysis window

and select the band combination tool. To compute NDSI, it is typically recommended to choose the appropriate bands, such as the Shortwave-infrared (SWIR) and green bands, which are band 11 and band 3 respectively. Once the composite image is created, we employ the Raster Calculator tool (Figure 15) to calculate the NDSI using (Eq. 4) above.

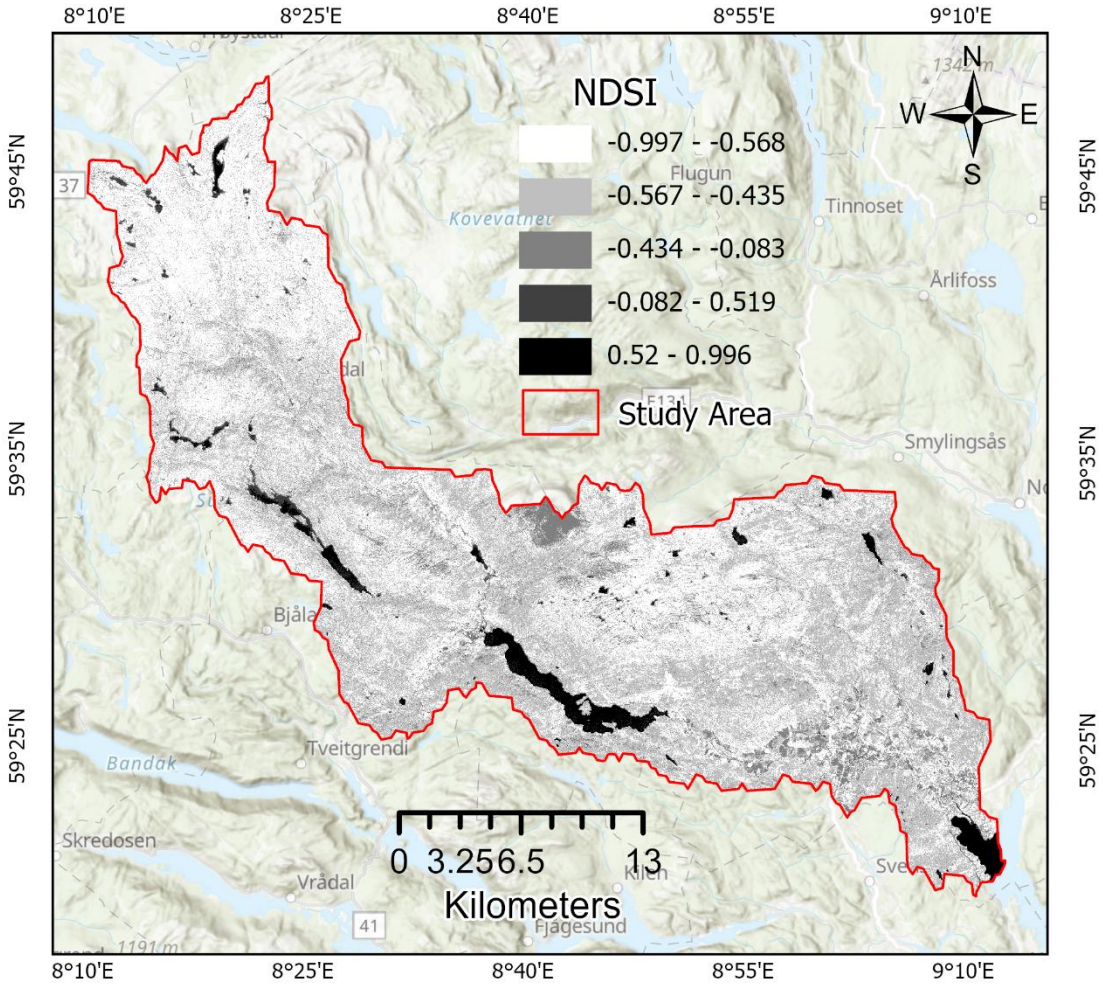

Figure 14: Normalized Difference Snow Index map of the study area

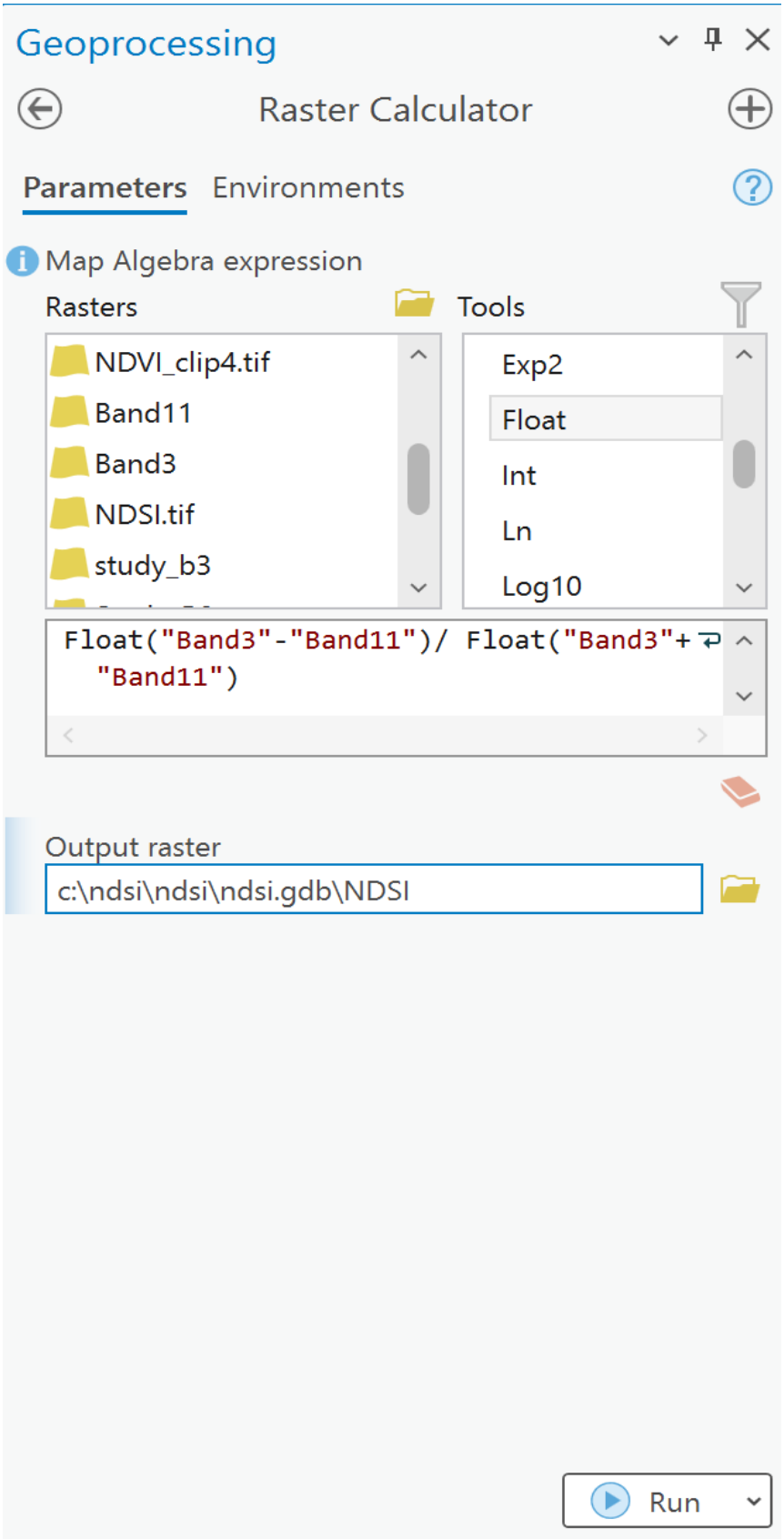

Figure 15: Raster Calculator tool for Generating NDSI map

i. Geology:

The selection of geology for flood susceptibility analysis is justified due to its influence on the permeability of the terrain and the behaviour of water flow. The comprehension of the geological composition of a specific area is essential for identifying regions that are susceptible to surface runoff, groundwater infiltration, or channelization. These factors play a crucial role in the flood risk assessment (Kazakis et al., 2015). The local geology contains valuable data on paleo-flood events, which can provide insight into the historical occurrence of flash floods(He et al., 2007). The infiltration process is accelerated by lithological units that have higher permeability. Conversely, an impermeable layer will amplify surface runoff, potentially leading to floods. The geological map (Figure 16) utilized for the Bø-Seljord region was prepared with five distinct geological features.

In this work, the geology map (Figure 16) created by using the geological data obtained from GeoNorge, available at https://kartkatalog.geonorge.no/metadata/berggrunn-n1350. After importing the shapefile into ArcGIS Pro 3.2, it is clipped according to the study boundary area and classified based on attributes called rock types.

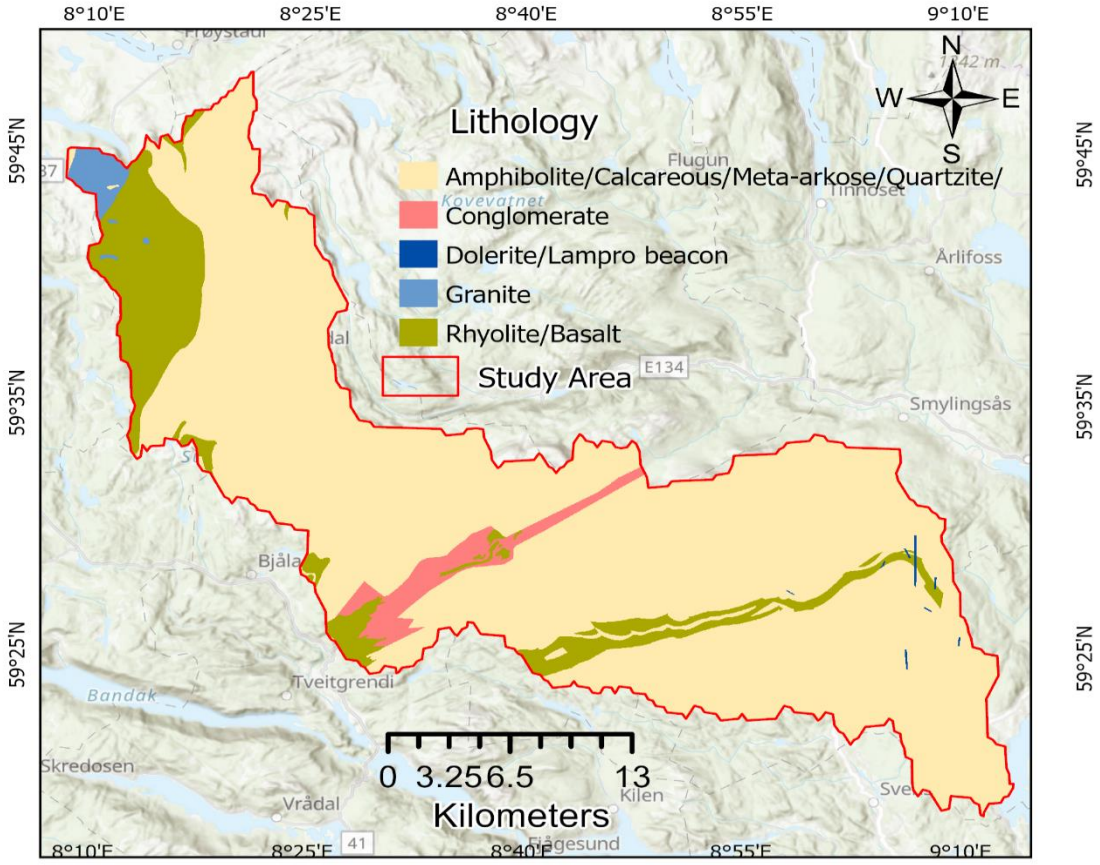

Figure 16: Geology map of the study area

j. Land-use and Landcover:

The selection of Land Use Land Cover (LULC) for flood susceptibility analysis is crucial due to its direct influence on the interaction between land and rainfall. Urban areas characterised by impervious surfaces, such as concrete, are associated with elevated runoff levels and heightened susceptibility to flooding (Norman et al., 2010). Conversely, regions featuring natural vegetation facilitate water absorption and mitigate runoff. The occurrence of floods in a particular area can be significantly affected by the surface cover or land-use patterns, as well as changes that occur in the area over time(Beckers et al., 2012). The LULC map (Fig. 25) with eight categories used in this study was prepared using a dataset extracted from ESRI, available at https://livingatlas.arcgis.com/landcover/. The data was then clipped according to the study boundary area in ArcGIS Pro.

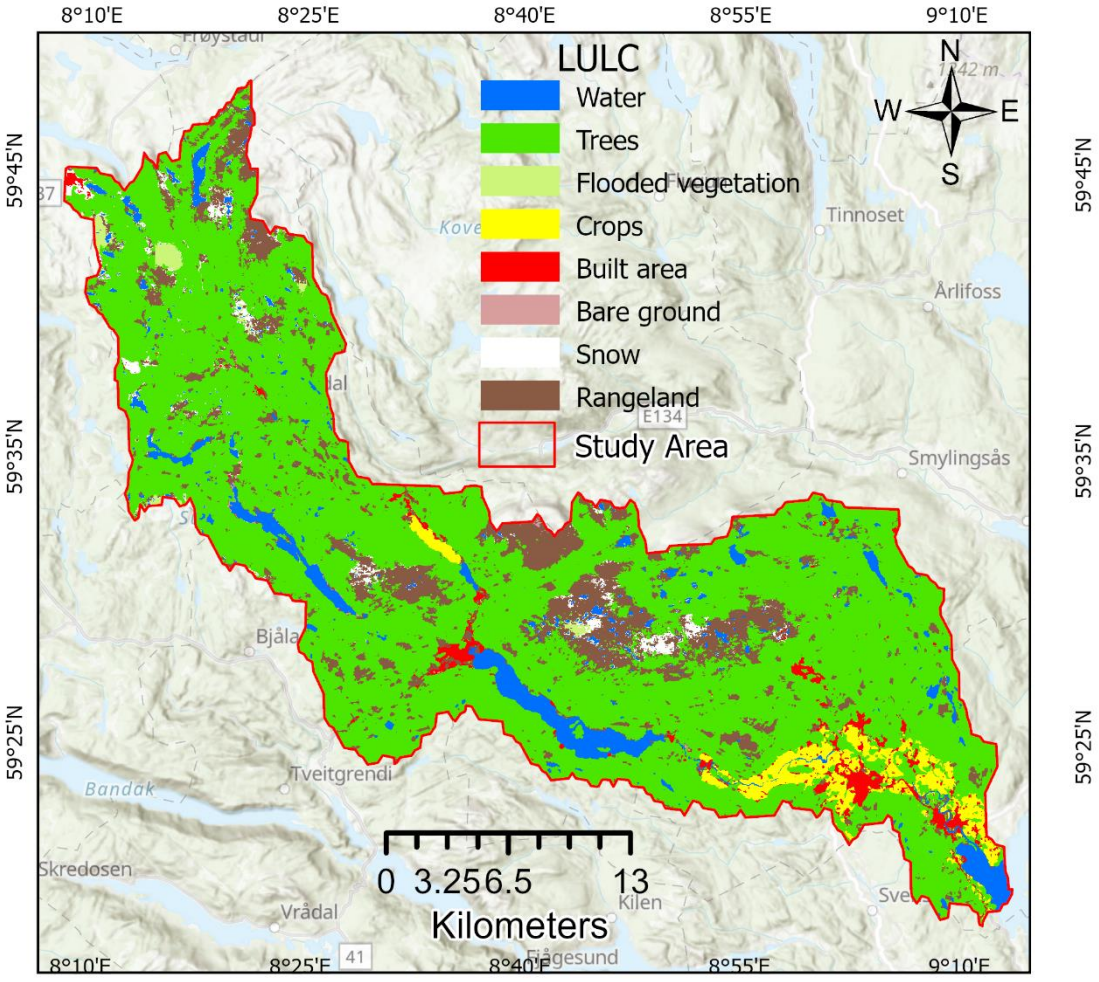

Figure 17: Land use and land cover map of the study area

3.3 Method Used

3.3.1 Analytic Hierarchy Process

In the late 1970s, Saaty introduced the Analytical Hierarchy Process (AHP) method, and now, it is the most widely used MCDA model for ranking decision alternatives on a global scale(Saaty, 1994). The term is commonly employed to assess and evaluate the components and their categories(Kumar & Anbalagan, 2016), making it a powerful method for resolving intricate problems(Souissi et al., 2019).The significance and applicability of this MCDA technique in relation to current issues have led to its widespread use in flood susceptibility mapping. Consequently, the current study used the AHP method to integrate the chosen thematic layers of flood susceptibility.

When preparing the susceptibility mapping, the relative importance of the flood indicators determines their respective weights. Furthermore, the pair-wise comparison matrices are utilized in AHP to compare the relative weight of each class that is contained within the same thematic layer. Additionally, thematic layers are compared to one another(Fenta et al., 2014). As a result, the relative weight of each layer has been determined employing Saaty's preference scale, which ranges from 1 to 9 (Table 3), as well as by utilizing literature review, field knowledge, and studies conducted in similar geographical regions that are comparable.

Table 3: Saaty's scale of relative importance

Saaty's scale of relative importance	
Intensity value	Description
1	Equally important
2	Equally important to moderately important
3	Moderately important
4	moderately to strongly important
5	strongly important
6	strongly to very strongly important
7	very strongly important
8	very strongly important to extremely strong important
9	extremely important

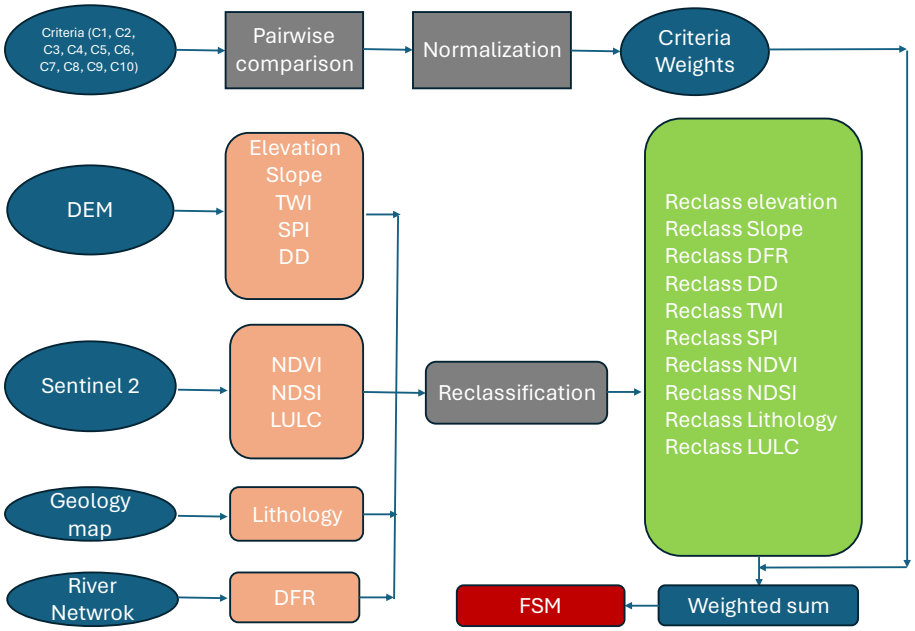

Figure 18: Multi-Criteria Decision Analysis procedure

When n number of criteria (flood indicators) for flood susceptibility mapping are to be compared, the AHP technique constructs a square matrix B=(b) to facilitate the comparison process. The following Equation 5 is represented below, and it is a condition that is satisfied regarding each b_{ij} of the matrix component.

$$b_{ij} = \frac{1}{b_{ji}} \tag{5}$$

when considering the reciprocal matrix, it is important to note that b_{ij} adheres to the equality, which is simply expressed as $b_{ij} = \frac{Mi}{Mj}$. Here, M_i represents the preference of the alternative i, as explained in the following Equation 6.

$$B = \begin{pmatrix} \frac{M_1}{M_1} & \cdots & \frac{M_1}{M_j} & \cdots & \frac{M_1}{M_n} & \cdots \\ \frac{M_i}{M_1} & 1 & \cdots & 1 & \cdots & \frac{M_i}{M_n} \\ \frac{M_n}{M_1} & \cdots & \cdots & \frac{M_n}{M_j} & \cdots & \frac{\ddot{M}_n}{M_n} \end{pmatrix} \quad (6)$$

The thesis research involved the construction of ten matrices for flood susceptibility thematic layers for the study area. The matrices have been computed for each class of the thematic layer to determine the AHP rating. The assignment of the weights or ratings involves the calculation of the relative ratio scale. This scale is derived from the pair-wise comparison reciprocal matrix of judgements, using the following method:

i)The sum of all the components that make up the j column in matrix b is shown in Equation 7 as follows:

$$\frac{M_1}{M_j} + \cdots + \frac{M_i}{M_j} + \cdots + \frac{M_n}{M_n} = \frac{\sum_{i=1}^{n} M_i}{M_j} \quad (7)$$

ii) The calculation of the normalized value involves dividing the comparison, which is denoted as $b_{ij}=M_i/M_j$ by following Equation 8:

$$\frac{\frac{M_i}{M_j}}{\frac{\sum_{i=1}^{n} M_i}{M_j}} = \frac{M_i}{M_j} \times \frac{M_j}{\sum_{i=1}^{n} M_i} = \frac{M_i}{\sum_{i=1}^{n} M_i} \quad (8)$$

iii) The weight or rating that is assigned to i^{th} row is referred, and it is determined by computing the average of the components within the Equation 9.

$$W_i = \left(\frac{M_i}{\sum_{i=1}^{n} M_i} + \cdots + \frac{M_i}{\sum_{i=1}^{n} M_i} \right) \times \frac{1}{n} \quad (9)$$

3.3.2 Verification of consistency

The consistency ratio, also known as CR, is utilized with the goal of evaluating the pair wise comparison of each parameter and the subcategories that they fall under. The following Equation 10 has been designated for use in the computation of the CR.

$$CR = \frac{CI}{RCI} \tag{10}$$

Where CR stands for the consistency index, CI, or the consistency index, and RCI or the random consistency index. For each of the different values of n, the RCI values remain the same(Saaty & Vargas, 1991), as described in Table 5, and the CI is computed using the Equation 11:

$$CI = \frac{(\lambda_{max} - n)}{n - 1} \tag{11}$$

Where the principal or largest eigenvalue of the pair-wise comparison matrix is denoted by the symbol λ_{max}. Equation 12 is used to determine the maximum value of k.

$$\lambda_{max} = \sum_{i=1}^{n} \left(W_i \times \frac{M_i}{\sum_{i=1}^{n} M_i} \right) \tag{12}$$

The AHP result is acceptable when the calculated consistency ratio value is less than or equal to 0.1. Nevertheless, if it is greater than 0.1, the result does not align with the continuation for further evaluation, and the method needs to be revised unless the threshold is met Table 4. A visual representation of the computed consistency ratio (CR) for flood susceptibility can be found in Table 4.

Table 4: Random Index to determine the consistency ratio for various matrices

Random Index to determine the consistency ratio for various matrices (Saaty and Vargas, 1991).											
1	2	3	4	5	6	7	8	9	10	11	12
0	0	0.58	0.9	1.12	1.24	1.32	1.41	1.45	1.49	1.51	1.48

4. Research Methodology

The objective of this thesis is to create a flood susceptibility map and provide flood prediction for the study area using Geographic Information Systems (GIS) and associated techniques and technologies. The project aims to achieve several objectives, including identifying areas prone to flooding and conducting a study on flood prediction. These objectives were successfully accomplished using GIS, Multi-Criteria Decision Analysis (MCDA), and various sensitivity analysis techniques. This chapter provides a comprehensive explanation of the methodology employed in this study. It is structured into the following sections:

- Determination of the catchment area
- Flood database
- Multicollinearity Test
- Multi-Criteria Decision Analysis (MCDA)
- Assessment of AHP technique using sensitivity analysis
- Software Used

GIS technology, along with the necessary data, will be employed to identify flood-prone areas within the study area. The collected data will be used for flood forecasting through the Analytical Hierarchy Process (AHP) method. The study and its accompanying maps can provide valuable assistance to the Bø and Seljord municipalities, which are responsible for planning and development in their respective areas.

4.1 Determination of the catchment area

The delineation of the catchment boundary was obtained from the Digital Terrain Model (DTM) with a resolution of 10 metres, extracted from https://kartkatalog.geonorge.no/metadata/dtm-10-terrengmodell-utm33. To delineate the catchment boundary, it is necessary to have a digital elevation model (DEM) without depressions. To achieve this, the sink tool in ArcGIS Pro hydrology is utilized to identify depression in the DEM, and the fill tool is then employed to fill these depressions. The flow direction tool is used to determine the direction in which water would flow for each cell. The flow accumulation tool calculates the number of cells that contribute to the flow of water into each cell of the filled digital elevation model (DEM). The areas exhibiting extremely high values may potentially correspond to perennial streams or major rivers, whereas areas displaying lower values may indicate sporadic streams. The flow accumulation grid enables

the calculation of the areas that contribute to the drainage of specific points on the DEM. Next, the Basin tool is employed to generate catchments. The Basin tool automatically identifies pour points and generates the catchment for the entire area. Figure 19 depicts the conceptual overview of catchment boundary delineation.

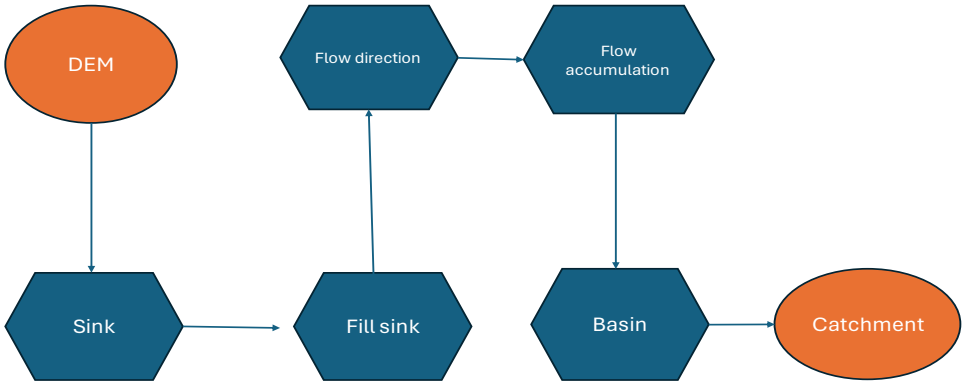

Figure 19: Process of delineating the catchment boundary

4.2 Flood database

The initial phase involves the creation of a flood database for the Bø-Seljord catchment area using ArcGIS Pro 3.2. The thesis study specified the use of the WGS 84 UTM Zone 32 N reference system for the database. This reference system uses the Transverse Mercator Projection. Subsequently, the ten flood indicators (elevation, slope, distance from river, drainage density, TWI, SPI, NDVI, NDSI, geology, and LULC) along with 64 flood locations derived from the (NVE Atlas) were imported into the database. The conversion of all ten flood parameters were performed, resulting in raster format with a resolution of 10 meters. It is important to mention that out of ten flood parameters, lithology, and land use land cover (LULC) fall into categorical parameters. Hence, a conversion process (Trọng et al., 2023)was employed to transform these parameters into continuous variables.

After delineation of the catchment boundary, the DEM boundary and other flood indicators used in the thesis research are clipped using ArcGIS Pro 3.2. To clip a raster layer in ArcGIS Pro, we need to define the extent or boundary within which we want to extract from the raster dataset. The clip raster tool in the Geoprocessing toolbox can be used for this purpose. Figure 10 shows the conceptual process of clipping the data per the boundary layer.

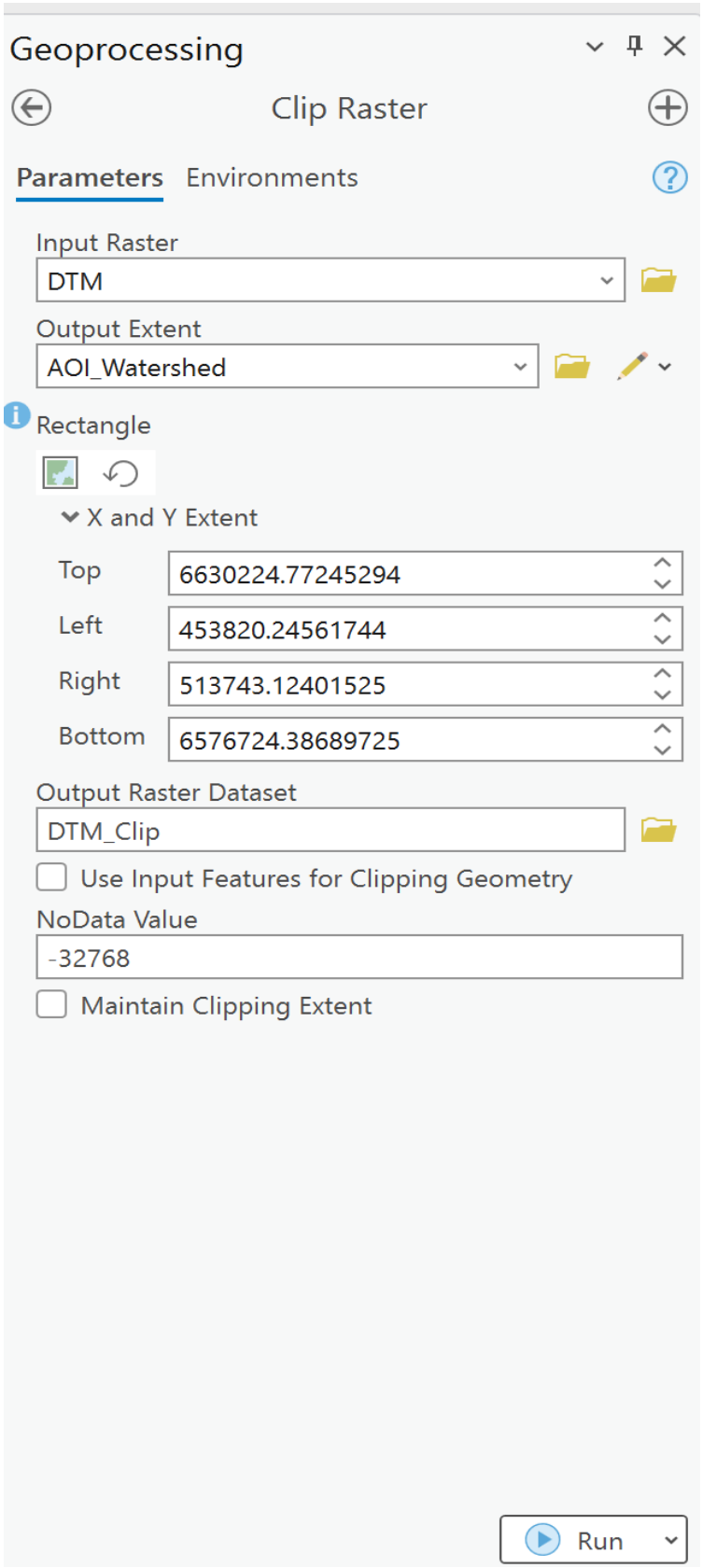

Figure 20: Clipping the DEM layer as per the extent of catchment boundary layer

Moreover, after clipping all the flood factors using ArcGIS Pro 3.2, all ten factors were reclassified using the reclassify tool under the Spatial Analyst Tool. Figure 21 shows the reclassification of DEM. Likewise, the other remaining flood factors were also reclassified.

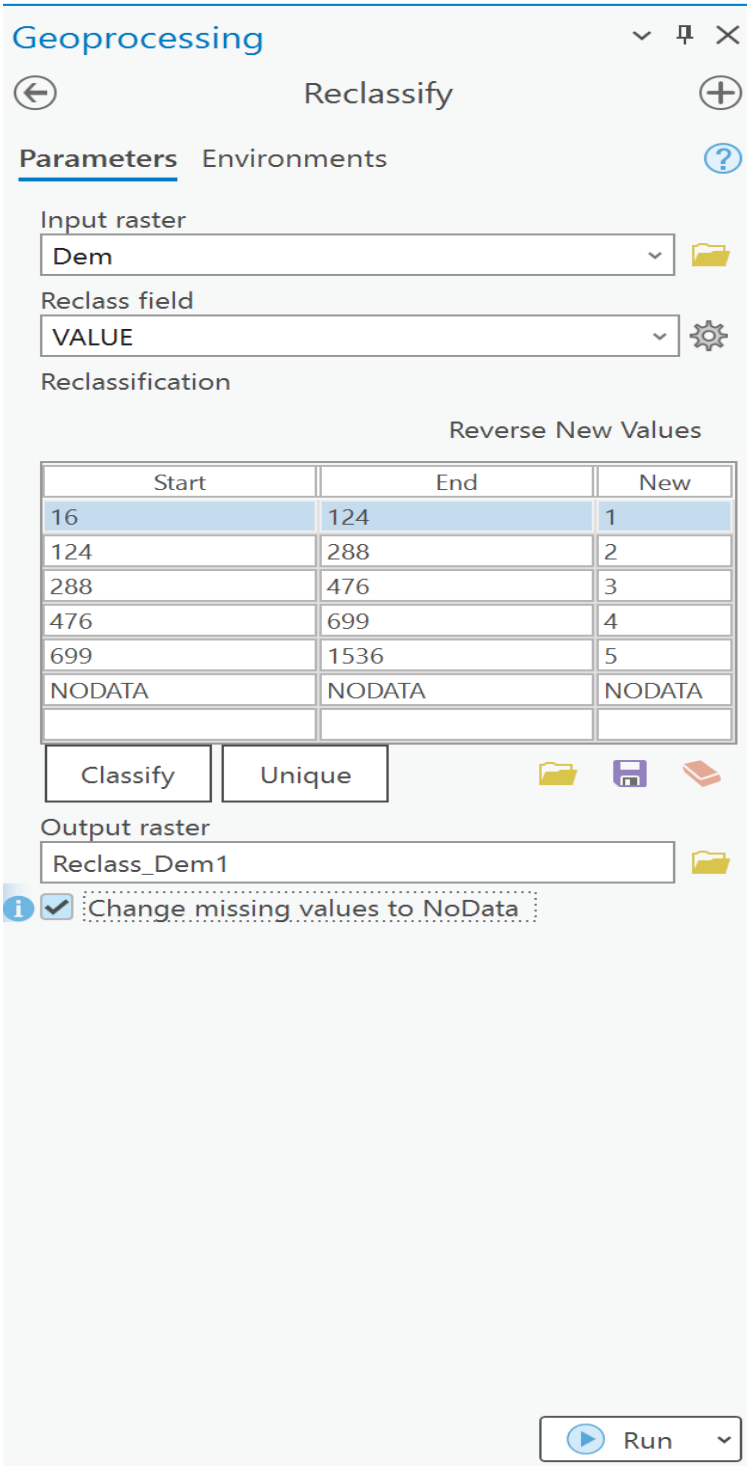

Figure 21: Reclassification process

After reclassifying all ten indicators, all the raster layers are converted into polygon using the raster to polygons tool under the conversion tool in the Geoprocessing tab in ArcGIS Pro 3.2. Figure 22 shows the process of converting a reclassified raster layer into polygon.

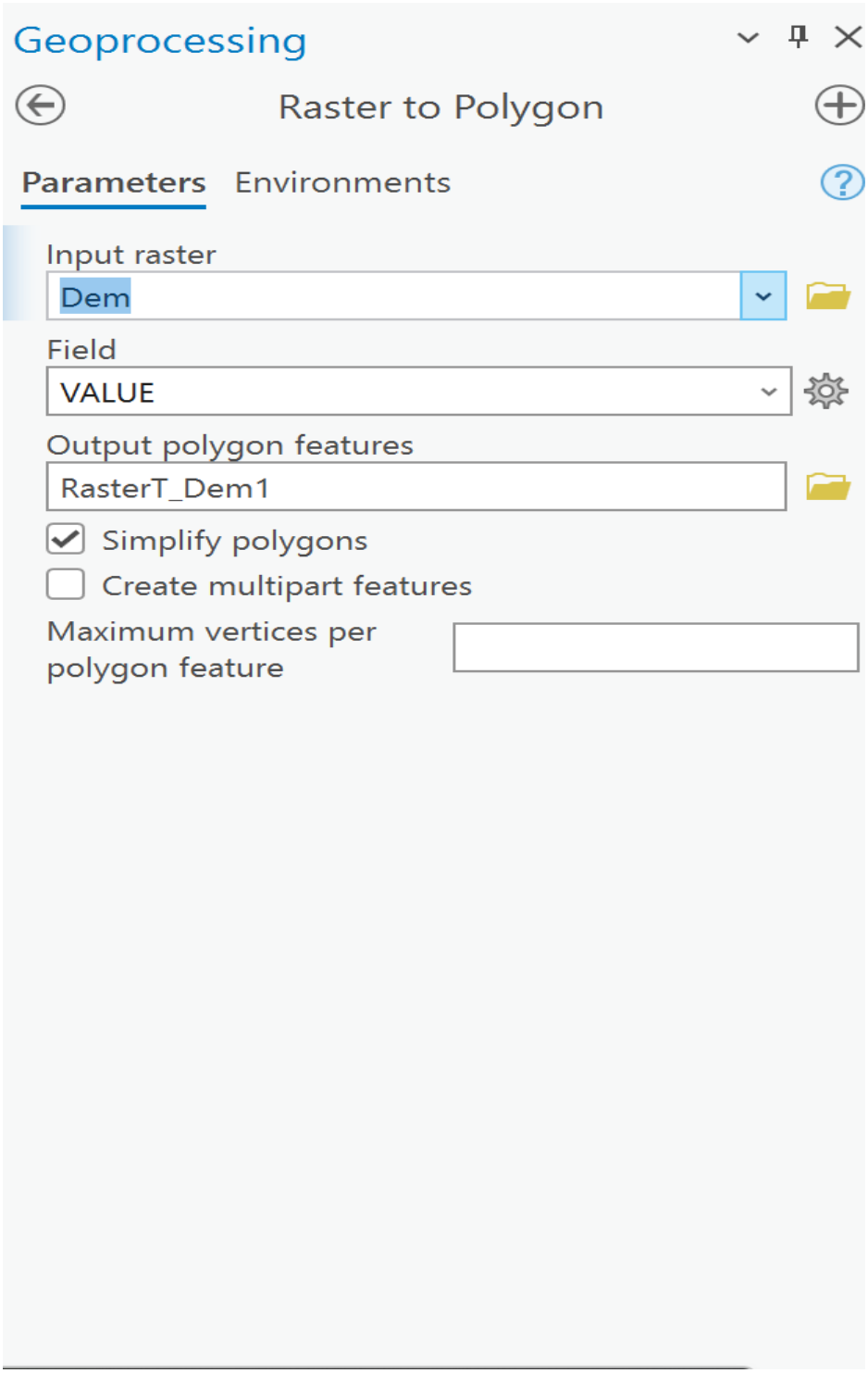

Figure 22: Raster to polygon tool for converting the raster layer to polygon.

After converting all the raster layers into polygons, each polygon layer is dissolved using the dissolve tool under Data management tool in geoprocessing tab using ArcGIS Pro 3.2. During the process of dissolving the polygon, under the dissolve field, a grid code must be selected. Figure 23 shows the process of dissolving the polygon.

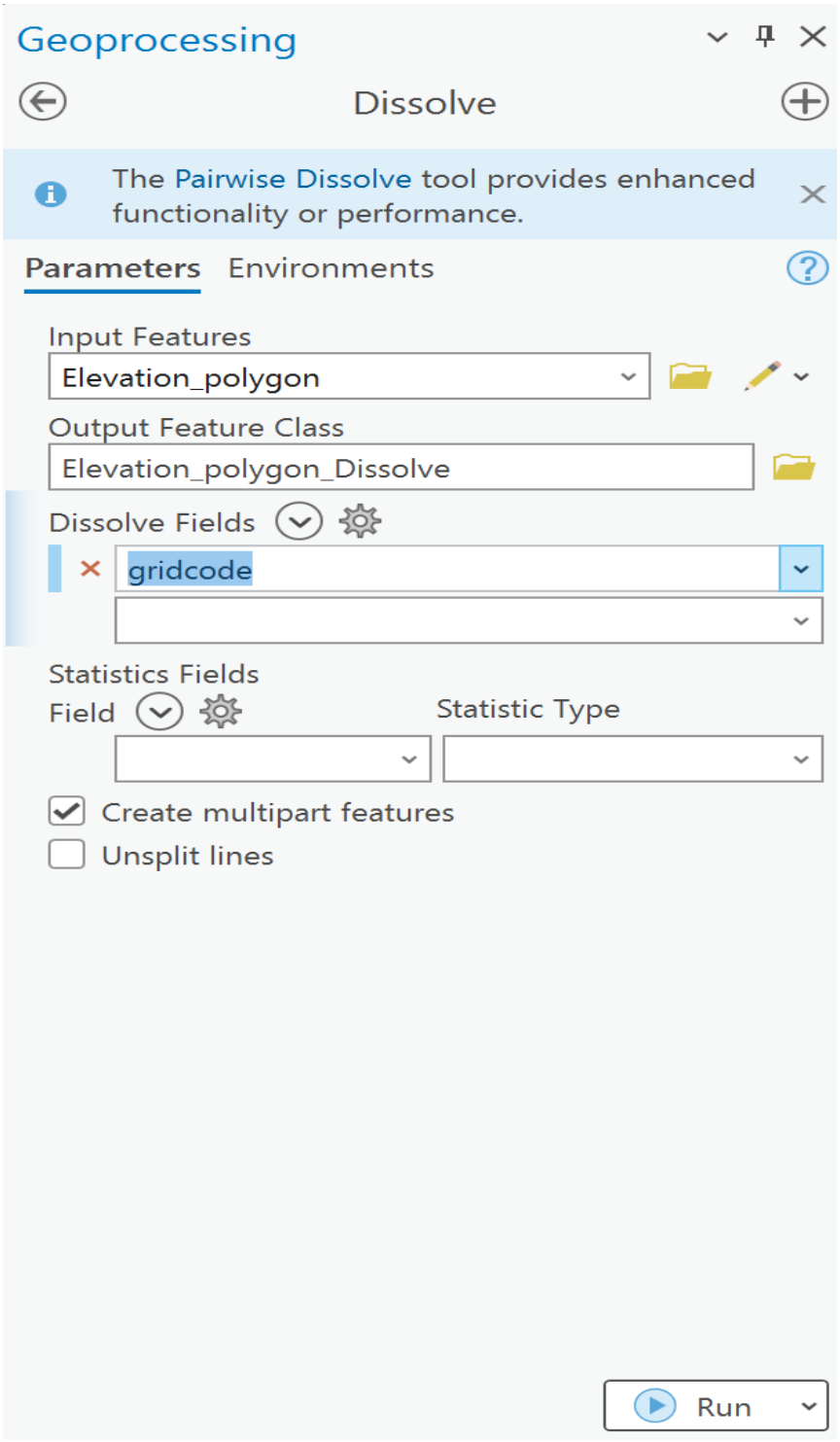

Figure 23: The Dissolving tool for processing the elevation polygon

Once all ten flood factors are dissolved, a field, named rating must be added to the attribute table of each dissolved layer, where the rating can be added to the reclass value obtained from the AHP sub-criteria analysis. Figure 24 shows the process of adding new fields and adding value to the field. Likewise, the same process is carried out for all the remaining nine indicators used in this thesis research.

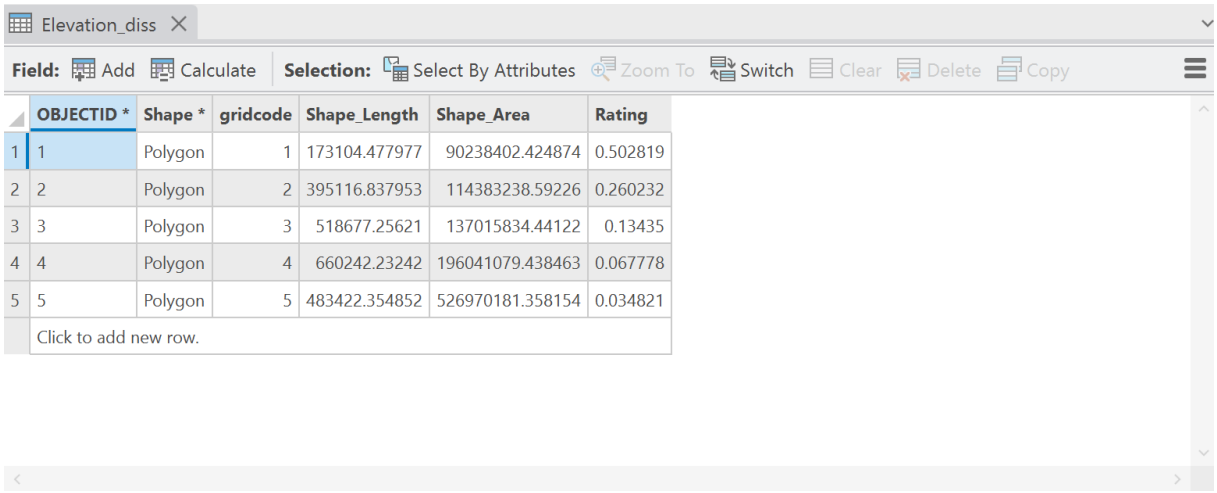

	OBJECTID *	Shape *	gridcode	Shape_Length	Shape_Area	Rating
1	1	Polygon	1	173104.477977	90238402.424874	0.502819
2	2	Polygon	2	395116.837953	114383238.59226	0.260232
3	3	Polygon	3	518677.25621	137015834.44122	0.13435
4	4	Polygon	4	660242.23242	196041079.438463	0.067778
5	5	Polygon	5	483422.354852	526970181.358154	0.034821
	Click to add new row.					

Figure 24: Adding the new field rating in the Elevation layer.

After adding the new field rating to each indicator used in flood analysis, all ten indicators were converted into a raster layers. A crucial step in this process was ensuring that the resolution of all raster layers was consistent. For this thesis research, we aimed to maintain a resolution of 10 meters for all indicators, saving them in a single geodatabase for further analysis. Consequently, all the new raster layers after conversion have a 10-meter resolution. Figure 25 illustrates the process of converting polygons to raster layers.

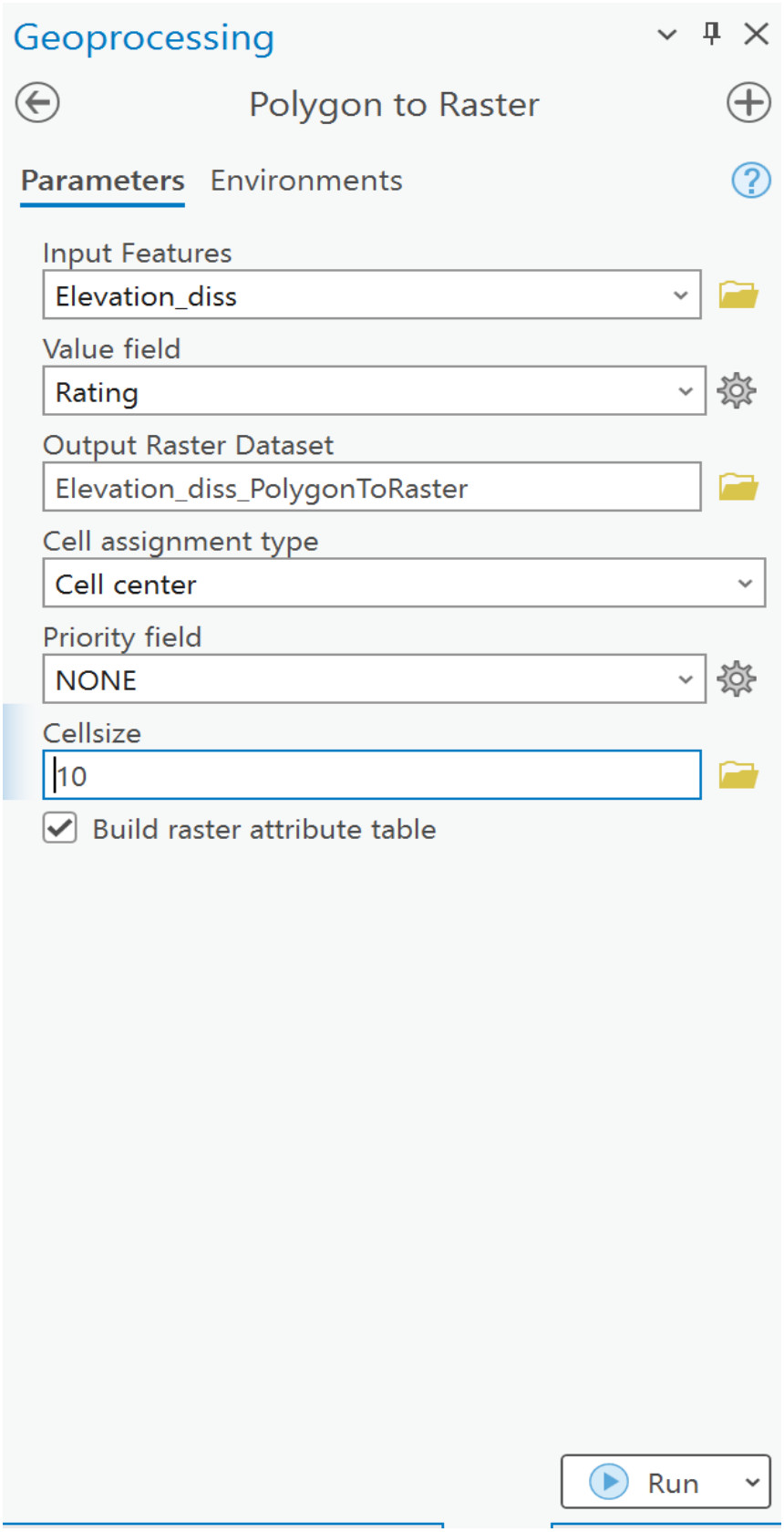

Figure 25: Polygon to raster tool

After creating a geodatabase with all required raster layers, the weighted sum overlay analysis is carried out using the weighted sum tool under the Spatial Analyst Tool in ArcGIS Pro. In the weighted sum tool, each indicator is selected simultaneously, and weights obtained from the AHP table for each indicator are employed in the weight field. Figure 26 shows the process of carrying out the overlay analysis.

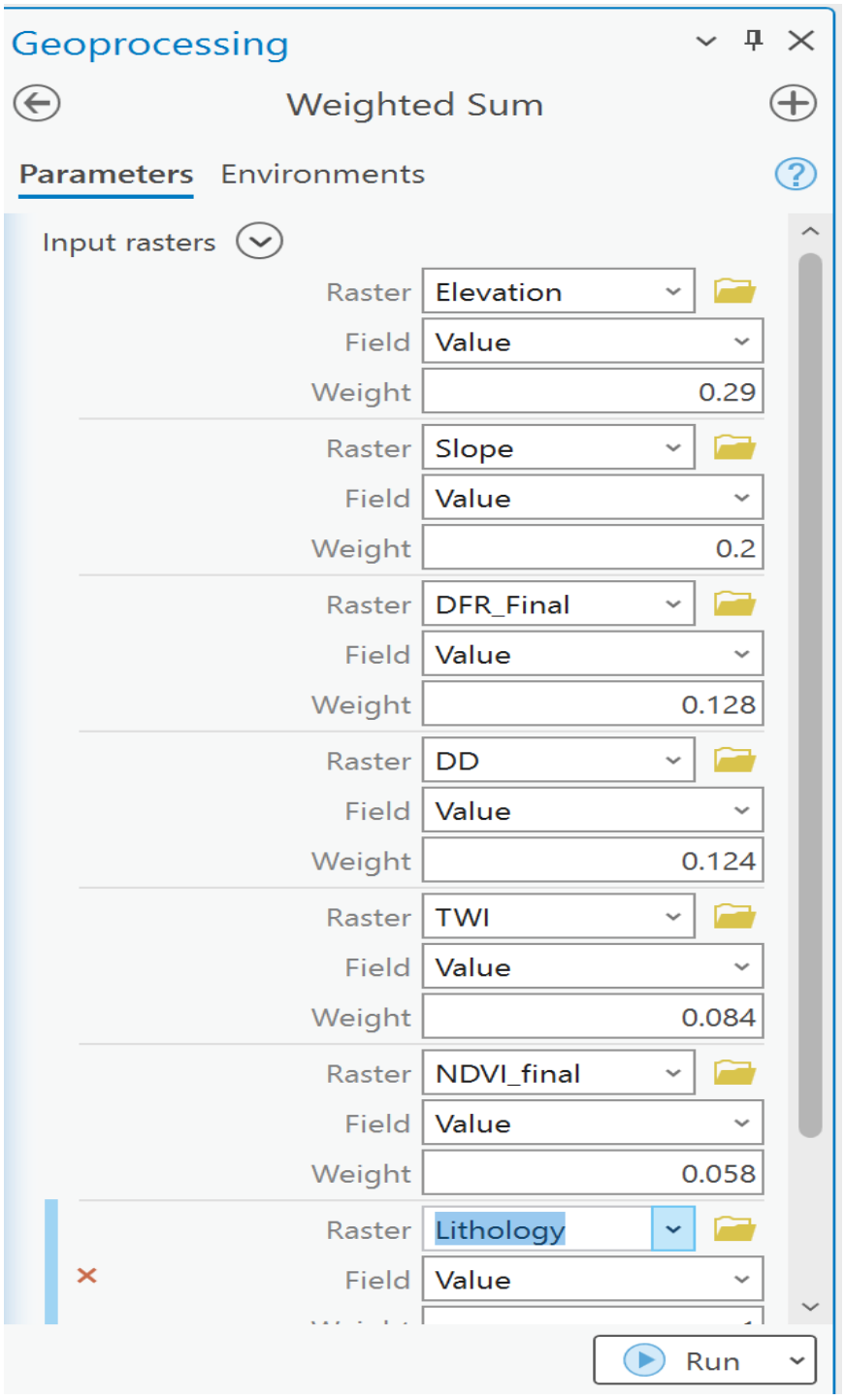

Figure 26: Process of weighted sum overlay analysis

4.3 Multicollinearity diagnosis

The multicollinearity diagnosis was determined to be a valuable tool as it did not adversely affect the predictability and reliability of the model. The flood susceptibility modelling involves conducting a multicollinearity test to identify any linear relationships between the variables(Al-Juaidi et al., 2018). Statistically, a strong correlation is observed between two or more independent variables(Mukherjee & Singh, 2020). As a result, correlation analysis is employed to identify specific independent variables that are strongly correlated. To analyse the multicollinearity among different independent variables, various methods were employed. For this research, the Variance Inflation Factor (VIF) method was utilized. The VIF (Myers et., 2010) was computed using the following formula:

The tolerance of the i^{th} predictor variable:

$$(\mathrm{T_i}) = 1 - \mathrm{R_i^2} \qquad (13)$$

Variance Inflation Factor of i^{th} predictor variable

$$(\mathrm{VIF_i}) = \frac{1}{\mathrm{T_i}} \qquad (14)$$

A Tolerance (TOL) value below 0.2 suggests potential multicollinearity, with severe multicollinearity occurring when TOL value drop below 0.1. The variance inflation factor (VIF), calculated as the reciprocal of tolerance (1/TOL), is used to assess multicollinearity. A VIF value exceeding 10 typically indicates significant multicollinearity (Bui et al., 2011).

4.4 Grading and weighting of flood indicators

The flood parameters selected for the study area are deployed to perform a pairwise comparison of criteria using the scale of 1 to 9 proposed by (Saaty, 1994). A square matrix is formed by performing the pairwise comparison of different criteria used in the thesis study. The flood analysis process involves decomposing the decision problem into a hierarchical structure consisting of goals and criteria. The objective of this thesis is to create a flood susceptible map by utilizing various indicators, including elevation, slope, distance from river, drainage density, TWI, NDVI, SPI, NDSI, lithology, and LULC. The estimation of the priorities of the decision criteria is then conducted. The individual priorities, based on the decision maker's choices, are converted into calculable values using a pairwise comparison matrix. This matrix plays a crucial role in the grading and weighting of flood parameters.

4.5 Verification of consistency

The consistency ratio (CR) is used to evaluate the pairwise comparisons of each parameter and their respective subcategories. The result obtained from verifying consistency determines whether the AHP results are acceptable. If the consistency ratio exceeds 0.1, the results are rejected, and the method is revised until the criterion is met. Table 5 shows the that the consistency ratio for the AHP results is below the threshold, making it acceptable for further analysis.

Table 5: Consistency assessment of aggregated for flood susceptibility in the study area

Lambda max	N	CI	CR
11.12	10	0.124	0.084

4.6 Flood susceptibility mapping

The preparation of the flood susceptibility zone is the most important task that the study ought to accomplish. The flood susceptibility parameters used for thesis research in the Bø-Seljord watershed area were assigned AHP weights (Table 11), and these weights were determined based on the priority among all the ten parameters employed in the study. Each of the mappings has been carried out with utilization of these weights. Through the utilization of the Spatial Analyst tool, the weighted sum method has been implemented within the ArcGIS Pro platform. For computing the FSM, the following Equation 15 is employed:

$$FSM = \sum_{i=1}^{n} W_i^S \times S_i^S \qquad (15)$$

Here, FSM refers to flood susceptibility mapping. W_i^Srepresents the weights assigned to susceptibility factors, while S_i^Sdenotes the weightage given to susceptibility sub-factors.

4.7 Sensitivity analysis

In the Analytic Hierarchy Process (AHP) assessment, the major drawback lies in the calculation of the weight of the input factors. Therefore, it is necessary to perform other analyses to verify the dependability and reliability of this method. Hence, sensitivity analysis is used to verify the assigned weights given to all the ten parameters obtained from the assessment through the Analytic Hierarchy Process (AHP). There are various sensitivity analyses to choose from, meanwhile the sensitivity analysis techniques used in this thesis work include Stillwell ranking methods, single parameter sensitivity analysis, and map removal sensitivity analysis.

4.7.1 Methods for ranking

The Stillwell ranking methods, also referred to as the Stillwell Technique, is a decision-making tool employed in the field of environmental impact assessment and land-use planning. The Stillwell ranking method is a systematic approach to decision making that assists stakeholders in evaluating and comparing the potential impacts of various alternatives in a structured manner. This method enables informed decision-making by considering multiple criteria and their respective importance. Hence, the method namely rank sum weight and reciprocal rank have been employed to compare with the AHP method. The rank sum weight $W_i(RS)$ and reciprocal rank weight $W_i(RR)$ can be calculated using following equations 16 and 17 (Stillwell & Seaver, 1981)

$$W_i(RS) = \frac{(n - R_j + 1)}{\sum_{k=1}^{n} (n - R_k + 1)} \tag{16}$$

$$W_i(RR) = \frac{\frac{1}{R_j}}{\sum_{k=1}^{n} \left(\frac{1}{R_k}\right)} \tag{17}$$

The normalized weight of each attribute, W_i, is determined based on the number of attributes, n. The attributes are ranked in ascending order, and R_j represents the direct rank of each attribute. Finally, each weight is normalized by $\sum_{k=1}^{n} (n - R_k + 1)$.

4.7.2 Single factor sensitivity analysis

Each flood indicator is tested using this sensitivity analysis. This method is employed to differentiate between the empirical weights assigned to each thematic layer in FSM maps obtained from the AHP and the actual of effective weights(Fenta et al., 2014; Mukherjee & Singh, 2020). The appropriate Equation to determine the effective weighting factor for FSM maps is:

$$W = \frac{P_r P_w}{\mathrm{FSM}} \times 100 \tag{18}$$

In the context where W denotes effective weight, P_r and P_w signify the rate and weight values of each layer, FSM signifies the mapping of flood susceptibility.

4.7.3 Map Removal Sensitivity analysis

An additional significant sensitivity analysis that can be essential to validate the weightage for parameters obtained from AHP is the map removal sensitivity analysis. This analysis seeks to examine the outcomes of removing any thematic layers utilized in the generation of the FSM maps. According to (Mukherjee & Singh, 2020), this method involves removing all thematic layers and then creating new FSM maps using the overlay analysis technique on top of the remaining layers. In this case, the sensitivity index is always calculated using following Equation:

$$\mathrm{SI} = \frac{\left|\left(\frac{\mathrm{FSM}}{\mathrm{N}}\right) - \left(\frac{\mathrm{FSM}'}{\mathrm{n}}\right)\right|}{\mathrm{FSM}} \times 100 \tag{19}$$

The sensitivity index associated with an excluded thematic layer is denoted as SI. FSM represents the flood susceptibility mapping of all the thematic layers. FSM' represents the flood susceptibility mapping of one excluded thematic layer. N represents the number of thematic layers in FSM maps, while n represents the number of thematic layers in FSM' maps.

4.8 Performance assessment

The resultant map obtained after the modelling must be verified to assess the reliability and accuracy. Validation of the data is one of the most important steps in ensuring the accuracy of any model post-development. Various methods have been utilized to validate MCDA models. In this thesis, verification of the Flood Susceptibility Map (FSM) was accomplished through the utilization of ROC-AUC (Mitra & Roy, 2022; Yaseen et al., 2022).

The ROC-AUC represents the trade-off between specificity and sensitivity in the field s of geomatics, natural hazards, and risk assessment. In the two-dimensional ROC graph, the x-axis represents the false positive rate, while the y-axis represents sensitivity, or the true positive rate. (Arabameri et al., 2019). The characteristics of the x-axis and the y-axis are expressed by Equations 20 and 21, where TN stands for true negative, FP stands for false positive, TP stands for true positive, and FN stands for false negative.

$$x = 1 - \text{ specificity } = 1 - \left[\frac{\text{TN}}{(\text{TN} + \text{FP})}\right] \quad (20)$$

$$y = \text{ sensitivity } = \left[\frac{\text{TN}}{(\text{TP} + \text{FN})}\right] \quad (21)$$

The performance of the Analytic Hierarchy Process (AHP) technique in the study region was quantitatively evaluated using the area under the receiver operating characteristics (ROC) curve(Nguyen et al., 2021). The FSM model that was prepared underwent verification using both flood and non-flood point data from the study area.

4.9 Software used

The Geographic Information System (GIS) software used for this study was ArcGIS Pro 3.2 ArcGIS, is developed by the Environmental Systems Research Institute (ESRI), is a geospatial information system designed for managing and analysing maps and geographic data. Microsoft Excel, part of the Microsoft Office suite, was utilized for conducting Analytic Hierarchy Process (AHP) calculations in the form of spreadsheets. SPSS software was employed to calculate the multicollinearity among the flood indicators used in the research. Endnote software was used to for referencing sources in the thesis report.

5. Results and analysis

5.1 Multicollinearity assessment

The current study involved the consideration of 1000 random points for flood susceptibility parameters during the assessment of multicollinearity. The collinearity statistics of the selected 10 flood parameters indicate that there is no evidence of a multicollinearity problem. The Variance Inflation Factor (VIF) and tolerance value for all susceptibility factors are less than 10 and greater than 0.1 respectively (refer Table 7). Hence, all the selected parameters can be used for further analyses in the thesis research to achieve the desired goal. The eigenvalue and condition index of all dimensions related to susceptibility indicate the absence of multicollinearity.

Table 6: Analysis of the relationship between flood susceptibility and collinearity

Flood susceptibility mapping		
Model	Eigenvalue	Condition Index
1	7.52	1.00
2	0.84	3.00
3	0.47	3.98
4	0.43	4.18
5	0.40	4.35
6	0.20	6.14
7	0.06	11.58
8	0.05	11.96
9	0.02	17.83
10	0.01	29.85

Table 7: Flood susceptibility statistics based on collinearity

Indicators	Tolerance	VIF
Elevation	0.72	1.37
Lithology	0.98	1.02
Distance	0.95	1.05
Drainage	0.92	1.08
LULC	0.88	1.14
NDSI	0.30	3.37
NDVI	0.27	3.74
Slope	0.47	2.14
SPI	0.51	1.97
TWI	0.34	2.92

5.2 Flood indicator analysis

The elevation in the area under research varies from 16m to 1536m at various points. Based on the elevation sub/classes, the highest percentage of the catchment area is covered by the high flood level category (9.71%), followed by the medium category (16.58%), the very high category (6.48%), the very low category (26.75%), and the low category (42.29%), as summarized in Table 11. As shown in Figure 3, the lower elevated lands are in the Midt-telemark, which is in the most southern part of the study area. A total of 29% of the total AHP weight was assigned to elevation, and higher ratings were given to the elevation classes that had lower ranges.

The slope of the catchment area varies from 0º to 80º (Figure 4), and it is weighted 21% in the AHP model. The lower slope values were given higher ratings and vice-versa. To prepare the flood susceptibility mapping flat (0º - 2º), gentle (2º - 5º), moderate (5º - 15º), moderately steep (15º - 35º), and steep (35º - 80º) terrains are classified as very high, high, moderate, low, and very low respectively.

In accordance with the representation shown in Figure 6, the parameter distance to the river is divided into five distinct sub-classes. The regions that are in the closest proximity to the river are the ones that are most likely to experience flooding problems. As a result, lower sub-classes were given greater weights within the overall ranking of subclasses in this parameter.

The region has a drainage density that ranges from 0.21 to 4.76 kilometres per square kilometre (Figure 7). The research found that areas with higher drainage density had higher weight, and vice-versa. This is because higher drainage density has been shown to indicate higher runoff.

The TWI values of the Bø-Seljord watershed region range from 3.62 to 25.13, and they are divided into five categories, as shown in Figure 8. The TWI exhibits a direct correlation with flooding. Consequently, when assigning ratings, higher TWI values are assigned higher values, while lower TWI values are assigned lower ratings for the sub-class rating of this parameter.

As shown in Figure 10, the different values of the study area region NDVI ranged from -0.0997 to 0.996. The probability of flooding was reflected by the fact that the NDVI value was negative. Since the NDVI value is moderate in the study area, the likelihood of flooding is moderate in the area. On the other hand, areas with a lower NDVI subclass were given higher ratings, and vice-versa.

The Stream Power Index (SPI) values for the study area are from -13 to 14 in Figure 12. The allocation of higher weights was based on the lower SPI values, and vice-versa. The lower SPI regions, as shown in Figure 12 are typically correlated with flooding events caused by water flow being either slow-moving or stagnant.

The Normalized Difference Snow Index (NDSI) is not a direct indicator of flooding. However, it is observed that higher values of NDSI are corelated with greater snow cover, which can potentially lead to increased flood risk due to the runoff from the snowmelt. The allocation of higher weights to the classes is based on higher NDSI values and vice-versa.

The lithological map of the catchment region is depicted in Figure 16. The classification is based on the Norwegian Water Resources and Energy Directorate (NVE) and consists of five distinct classes. The classification of flood susceptibility levels is based on the geological composition of the area. The highest flood susceptibility class, denoted as very high, is associated with amphibolite and calcareous rock types. The high flood hazard class is linked to basalt, while the medium flood hazard is linked to granite. Conglomerate is classified as a low flood susceptibility class. And dolerite is categorized as a very low class.

The land use and land cover (LULC) map of the study area is depicted in Figure 17. The classification consists of eight distinct classes. The association between flood hazard classes and the land cover types: the very high flood hazard class is associated with the built area, the high flood zone is linked to water and crops, the medium flood hazard class is associated with bare ground and snow, low flood class is with flooded vegetation and rangeland, and very low flood hazard class is associated with trees.

5.3 Flood susceptibility mapping result

Prior to executing the flood susceptibility model, the consistency ratio (CR) of each thematic layer and their respective sub-classes were calculated. The judgement matrices achieved a satisfactory level of consistency, with a CR value of less than 0.10. Subsequently, all ten reclassified layers of flood susceptibility indicators were processed in the ArcGIS Pro platform, utilising the respective weights assigned from the AHP model. The final flood susceptibility map (FSM) for the study area was generated using the weighted overlay method. The Bø-Seljord catchment area has been categorised into five flood susceptibility classes based on pixel values: very low, low, moderate, high, and very high (refer to Figure 28).

The distribution of susceptibility classes is represented as percentages using various methods, including natural break, geometrical mean method, quantile method, and equal interval method (Figure 27). The quantile deviation technique was used to generate the maximum areal coverage of very high and high flood susceptibility classes. On the other hand, an equal interval method was employed to generate maximum, medium and low classes. Lastly the geometrical interval method was utilized to generate the very low class.

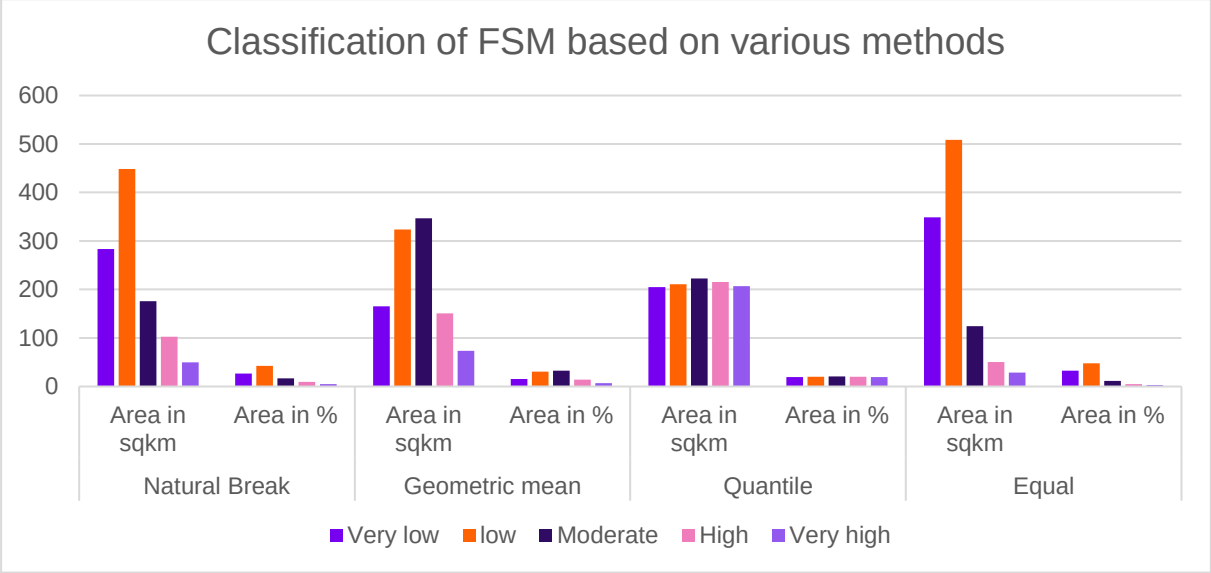

Figure 27: Classification of flood susceptibility mapping based on various classification methods

The generation of the FSM map of the Bø-Seljord watershed region involved assigning weights to various factors. The highest weight of 29% is allocated to elevation, followed by slope with 21%, drainage density with 12%, distance from river with 12%, TWI with 9%, NDVI with 6%, SPI with 4%, NDSI and lithology with 3%, and LULC with 2%. Floods in this study region typically occur in the riverside and water bodies and their adjacent areas. The flood susceptibility zones were determined based on several indicators including distance from the river, lower elevation, gentle slope, higher drainage density, TWI, and NDVI. These indicators collectively contribute to the identification of high to very high flood susceptibility zones in the defined study area.

Table 8: Pair-wise comparison matrix for the flood indicators. E: Elevation, S: Slope, DD: Drainage Density, DFR: Distance from River, TWI: Topographic Wetness Index, NDVI: Normalized Difference Vegetation Index, SPI: Stream Power Index, NDSI: Normalized Difference Snow Index, G: Geology, LULC: Land use and Land cover.

Preferred Over Other										
	E	**S**	**DD**	**DFR**	**TWI**	**NDVI**	**SPI**	**NDSI**	**L**	**LULC**
E	1	3	4	4	5	6	7	7	8	8
S	0.333	1	3	4	4	5	6	7	7	8
DD	0.250	0.333	1	1	3	4	5	6	7	7
DFR	0.250	0.250	1	1	3	4	5	6	6	7
TWI	0.200	0.250	0.333	0.333	1	3	4	5	5	6
NDVI	0.167	0.200	0.250	0.250	0.333	1	3	4	4	5
SPI	0.143	0.167	0.200	0.200	0.250	0.333	1	3	3	4
NDSI	0.143	0.143	0.167	0.167	0.200	0.250	0.333	1	1	3
G	0.125	0.143	0.143	0.167	0.200	0.250	0.333	1	1	3
LULC	0.125	0.125	0.143	0.143	0.167	0.200	0.250	0.333	0.333	1
Sum	2.736	5.611	10.236	11.260	17.150	24.033	31.917	40.33	42.330	52

Table 9: Normalized data for the flood indicators. E: Elevation, S: Slope, DD: Drainage Density, DFR: Distance from River, TWI: Topographic Wetness Index, NDVI: Normalized Difference Vegetation Index, SPI: Stream Power Index, NDSI: Normalized Difference Snow Index, G: Geology, LULC: Land use and Land cover.

Normalized Data											
	E	S	DD	DFR	TWI	NDVI	SPI	NDSI	L	LULC	Average
E	0.366	0.535	0.391	0.355	0.292	0.250	0.219	0.174	0.189	0.154	0.292
S	0.122	0.178	0.293	0.355	0.233	0.208	0.188	0.174	0.165	0.154	0.207
DD	0.091	0.059	0.098	0.089	0.175	0.166	0.157	0.149	0.165	0.135	0.128
DFR	0.091	0.045	0.098	0.089	0.175	0.166	0.157	0.149	0.142	0.135	0.125
TWI	0.073	0.045	0.033	0.030	0.058	0.125	0.125	0.124	0.118	0.115	0.085
NDVI	0.061	0.036	0.024	0.022	0.019	0.042	0.094	0.099	0.094	0.096	0.059
SPI	0.052	0.030	0.019	0.018	0.015	0.014	0.031	0.074	0.071	0.077	0.040
NDSI	0.052	0.026	0.016	0.015	0.012	0.010	0.010	0.025	0.024	0.058	0.025
G	0.046	0.026	0.014	0.015	0.012	0.010	0.010	0.025	0.024	0.058	0.024
LULC	0.046	0.022	0.014	0.013	0.009	0.008	0.008	0.008	0.008	0.019	0.016
Sum	1	1	1	1	1	1	1	1	1	1	1

Table 10: Consistency vector for the flood indicators. LM: Lambda max, CV: Consistency Vector. E: Elevation, S: Slope, DD: Drainage Density, DFR: Distance from River, TWI: Topographic Wetness Index, NDVI: Normalized Difference Vegetation Index, SPI: Stream Power Index, NDSI: Normalized Difference Snow Index, G: Geology, LULC: Land use and Land cover.

Lambda Calculation											SUM	Consistency Vector
	E	**S**	**DD**	**DFR**	**TWI**	**NDVI**	**SPI**	**NDSI**	**L**	**LULC**		
E	0.292	0.62	0.514	0.498	0.423	0.353	0.281	0.173	0.191	0.12	3.471	11.872
S	0.097	0.21	0.385	0.498	0.338	0.294	0.241	0.173	0.167	0.12	2.526	12.199
DD	0.073	0.07	0.128	0.125	0.254	0.235	0.201	0.148	0.167	0.11	1.509	11.753
DFR	0.073	0.05	0.128	0.125	0.254	0.235	0.201	0.148	0.143	0.11	1.468	11.786
TWI	0.058	0.05	0.043	0.042	0.085	0.176	0.16	0.124	0.119	0.09	0.952	11.262
NDVI	0.049	0.04	0.032	0.031	0.028	0.059	0.12	0.099	0.095	0.08	0.633	10.765
SPI	0.042	0.03	0.026	0.025	0.021	0.02	0.04	0.074	0.072	0.06	0.416	10.366
NDSI	0.042	0.03	0.021	0.021	0.017	0.015	0.013	0.025	0.024	0.05	0.254	10.261
L	0.037	0.03	0.018	0.021	0.017	0.015	0.013	0.025	0.024	0.05	0.246	10.295
LULC	0.037	0.03	0.018	0.018	0.014	0.012	0.01	0.008	0.008	0.02	0.166	10.665
Lambda max												**11.122**

Table 11: Selected factors for flood susceptibility of Bø-Seljord watershed area in Telemark County. CBD: Conglomerate/Basalt/Dolerite; CMA: Granitic gneiss/meta akrose; ACQ: Amphibolite/Calcareous/Quartz slate; LGQ: Lampro/Granite/Quartzite

Selected flood susceptibility parameters for the study area					
Parameters	**Weight**	**Class range**	**Reclass Value**	**Flood Level**	**Rating**
Elevation	0.29	16-124	1	Very high	0.503
		124-288	2	High	0.260
		288-476	3	Moderate	0.134
		476-699	4	Low	0.068
		699-1536	5	Very low	0.035
Slope	0.21	0-2	1	Very high	0.457
		2-5	2	High	0.257
		5-15	3	Moderate	0.150
		15-35	4	Low	0.087
		35-80	5	Very low	0.049
DFR	0.13	0-200	1	Very high	0.524
		200-500	2	High	0.222
		500-1000	3	Moderate	0.132
		1000-1500	4	Low	0.076
		1500-2000	5	Very Low	0.046
DD	0.12	0.205-1.491	1	Very Low	0.035
		1.492-2.098	2	Low	0.068
		2.099-2.599	3	Moderate	0.134
		2.6-3.207	4	High	0.260
		3.208-4.762	5	Very High	0.502
TWI	0.08	-13.81--6.32	1	Very low	0.044
		-6.31--1.91	2	Low	0.076
		-1.9-0.19	3	Moderate	0.144
		0.2-2.83	4	High	0.268
		2.84-14.3	5	Very high	0.468
NDVI	0.06	-0.996--0.622	1	Very high	0.416
		-0.621--0.066	2	High	0.262
		-0.065-0.443	3	Moderate	0.161
		0.444-0.725	4	Low	0.099
		0.726-0.999	5	Very Low	0.062
SPI	0.04	-13--6	1	Very high	0.503
		-5--2	2	High	0.260
		-1-0	3	Moderate	0.134
		1-3	4	Low	0.068
		3-14	5	Very low	0.035
NDSI	0.03	-0.0997--0.568	1	Very high	0.467
		-0.567--0.435	2	High	0.256
		-0.0434--0.083	3	Moderate	0.148
		-0.082-0.519	4	Low	0.083
		0.52-0.996	5	Very Low	0.044
Lithology	0.02	CBD	1	Very high	0.498

		GMA	2	High	0.263
		ACQ	3	Moderate	0.136
		Rhyolite	4	Low	0.067
		LGQ	5	Very low	0.037
LULC	0.02	Water	1	Very high	0.155
		Trees	2	Very low	0.043
		Flooded vegetation	3	Low to medium	0.087
		Crops	4	High	0.154
		Built Area	5	Extreme high	0.241
		Bare ground	6	Medium to high	0.136
		Snow	7	Medium	0.111
		Rangeland	8	Low	0.073

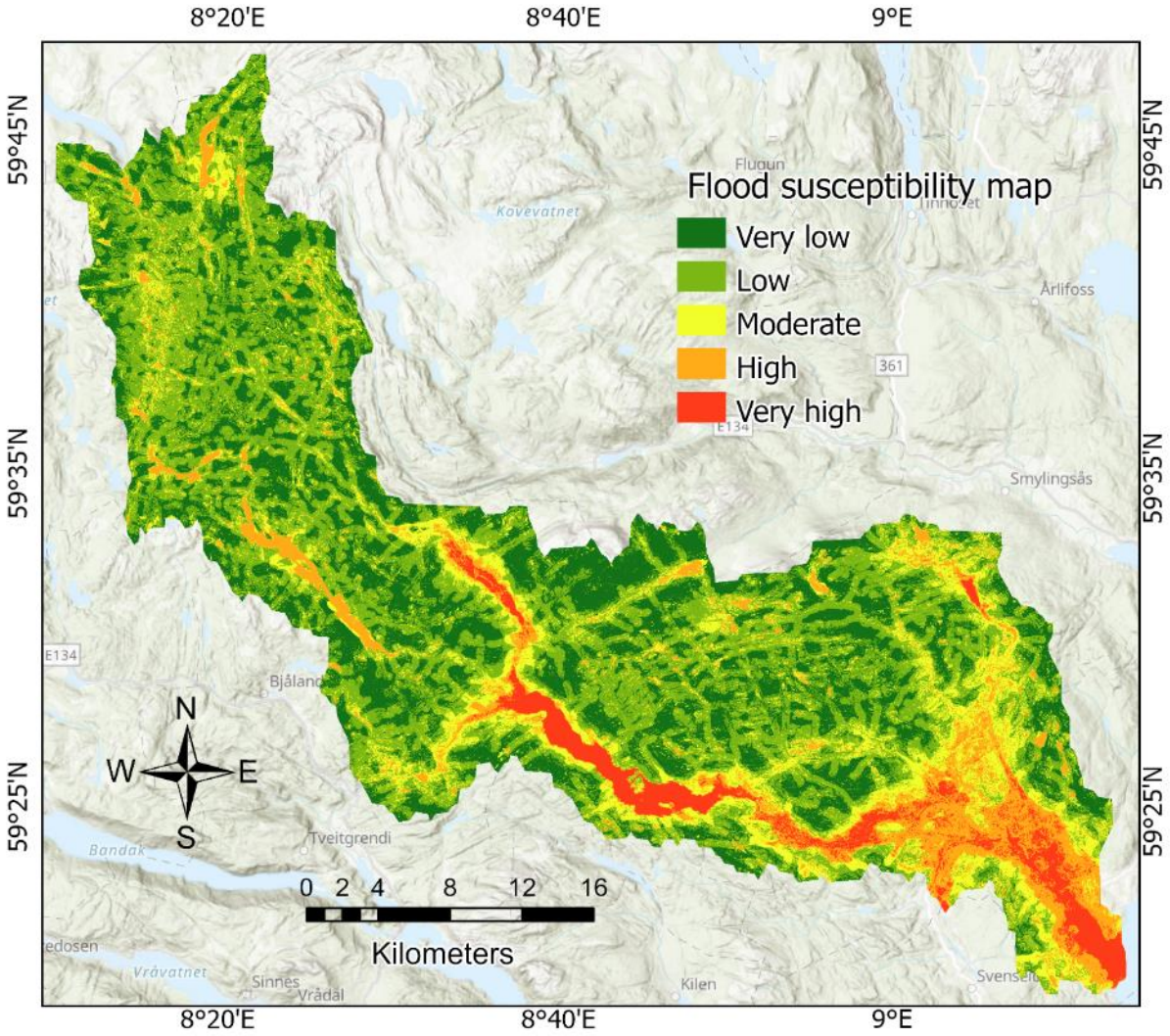

Figure 28: Flood susceptibility mapping of study area

Table 12: Area of flood susceptibility of the study area

Area of flood susceptibility		
Level	**Area in Sq.km**	**Area in percent (%)**
Very Low	283.614	26.740
Low	448.547	42.290
Moderate	175.890	16.584
High	102.943	9.706
Very High	49.6403	4.680

5.4 Sensitivity analysis

In this study, a sensitivity analysis was conducted to gain a better understanding of the important thematic layers of the acquired FSMs (Flood Susceptibility Map), as well as the impact of the assigned rank and weights on each and thematic layer(Mukherjee & Singh, 2020). The study provided by (Fenta et al., 2014) insights into the relative importance of different maps determining the values of the output map. Specifically, it identifies the most and least significant maps in this regard. To better understand the importance of the flood indicators and the impact of the ranking and weighting, a sensitivity analysis was conducted.

5.4.1 Stilwell ranking result

The weightage comparison between the Saaty (1980) and Stillwell (1981) for Flood Susceptibility Mapping (FSM) is illustrated in Table 13. The output obtained after the calculation of the AHP model by Saaty (1980) and Stillwell's ranking method (1981) demonstrates minimal changes in the ranking of the criteria. This clearly shows that the weights assigned to the parameters used in this study through the AHP model are reliable and accurate to some extent.

Table 13: Weightage comparison using AHP method and Stilwell ranking method. E: Elevation, S: Slope, DD: Drainage Density, DFR: Distance from River, TWI: Topographic Wetness Index, NDVI: Normalized Difference Vegetation Index, SPI: Stream Power Index, NDSI: Normalized Difference Snow Index, G: Geology, LULC: Land use and Land cover.

	Direct rank	Saaty (1988)	Stillwell ranking method (1981)			
		Pair-wise	Ranking Sum		Reciprocal Rank	
		AHP weight	$(n - rj + 1)$	$(n - rj - 1)/\sum n - rk + 1)$	$(1 /rj)$	$(1/rj) /\sum\left(\frac{1}{rk}\right)$
E	1	0.29	10	0.159	1.000	0.313

S	2	0.21	9	0.143	0.500	0.157
DD	3	0.13	8	0.127	0.330	0.103
DFR	3	0.12	8	0.127	0.330	0.103
TWI	4	0.08	7	0.111	0.250	0.078
NDVI	5	0.06	6	0.095	0.200	0.063
SPI	6	0.04	5	0.079	0.170	0.053
NDSI	7	0.02	4	0.063	0.140	0.044
L	7	0.02	4	0.063	0.140	0.044
LULC	8	0.02	2	0.032	0.130	0.041

5.4.2 Sensitivity analysis for flood indicator

Regarding susceptibility analysis in the selected study area, the parameter elevation is assigned the highest empirical weight of 29%, obtained from the AHP model. However, based on the statistical output obtained through sensitivity analyses for each parameter, it has a mean effective weight of 15.59% (Table 14).

Table 14: Descriptive statistics for single parameter sensitivity analysis. SD: Standard Deviation, E: Elevation, S: Slope, DD: Drainage Density, DFR: Distance from River, TWI: Topographic Wetness Index, NDVI: Normalized Difference Vegetation Index, SPI: Stream Power Index, NDSI: Normalized Difference Snow Index, G: Geology, LULC: Land use and Land cover.

Flood Indicators	Empirical weight in %	Effective weight in %			
		Min	Max	Mean	SD
E	29	2.88	68.06	15.59	11.72
S	21	3.10	66.37	18.89	8.03
DFR	13	1.78	63.06	31.92	12.73
DD	12	1.03	53.28	11.26	6.93
TWI	8	0.83	36.77	6.14	4.02
NDVI	6	0.83	17.23	3.17	1.54
SPI	4	0.31	26.79	5.60	4.54
NDSI	3	0.19	16.14	4.08	1.92
G	2	0.16	13.90	1.47	1.73
LULC	2	0.19	6.19	0.74	0.36

The distance from the river corresponds to the highest mean effective weight at 31.95%. In contrast, the empirical weight for this parameter, obtained from the AHP model, is only 13%, resulting in maximum observed deviation. Geology and land-use and land cover categories have the lowest mean effective weights, specifically 1.5% and 0.7%, respectively. The mean effective weights calculated from single parameter sensitivity analysis and the empirical

weights calculated from the AHP model exhibits a high degree of similarity for the slope, SPI, NDSI, DD, geology, and TWI variables. Figure 28 depicts all the effective weights assigned to ten flood susceptibility indicators used in this thesis research.

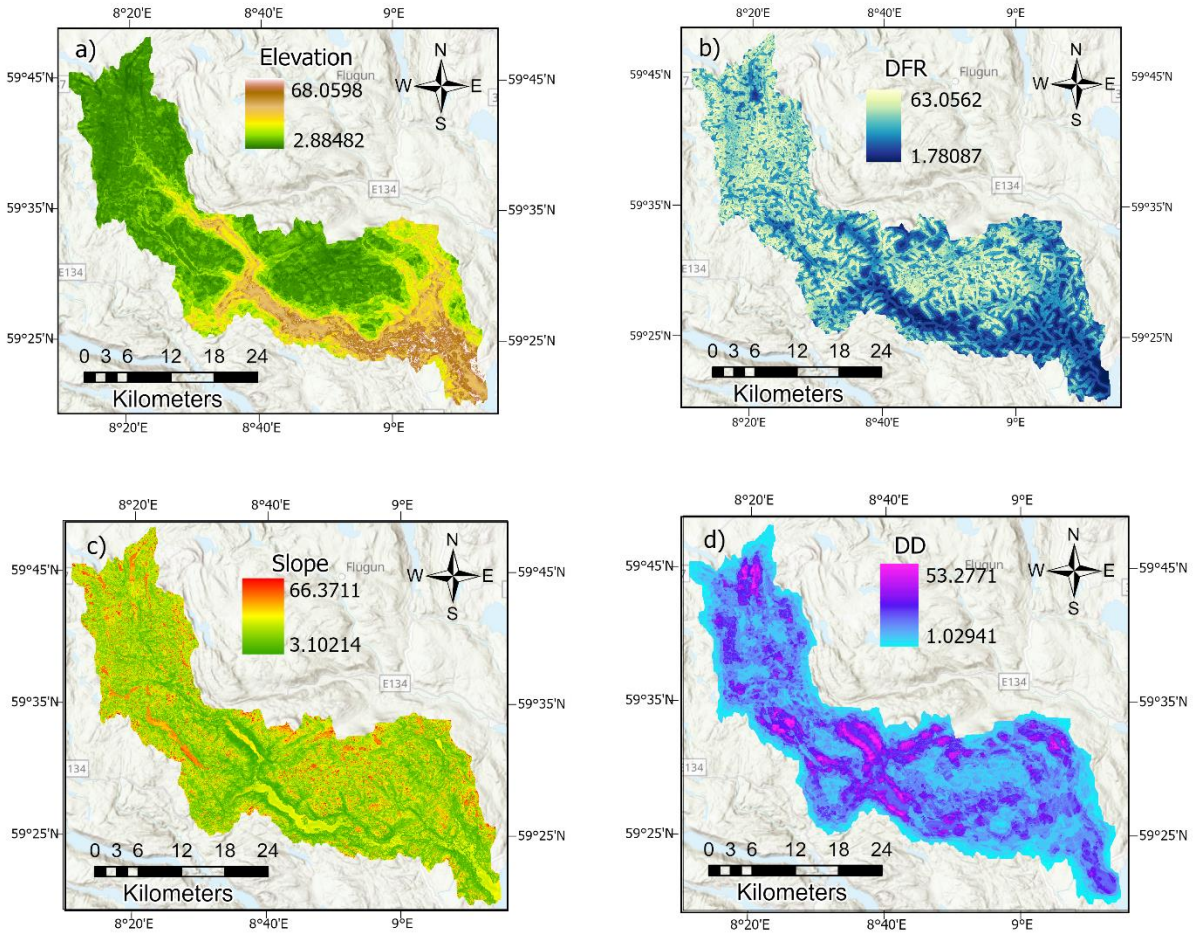

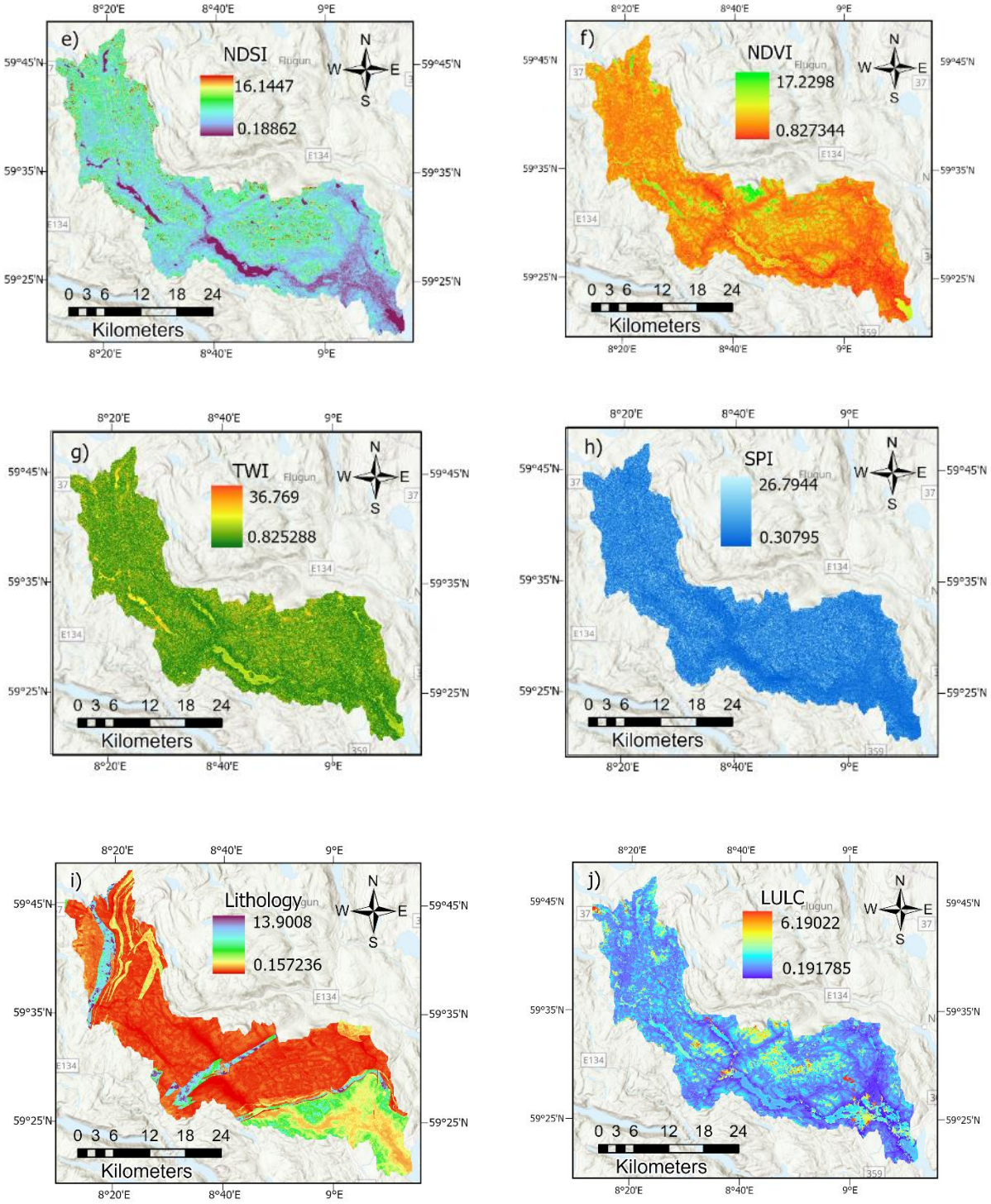

Figure 29: Effective weight for Flood susceptibility factor: a) Elevation, b) DFR, c) Slope, d) DD, e) NDSI, f) NDVI, g) TWI, h) SPI, i) Lithology, and j) LULC

5.4.3 Map Removal Sensitivity Analysis

The result of the map removal sensitivity analysis is shown in Table 15. It could be seen that. the output shows a certain variation when removing a single parameter sensitivity while considering the susceptibility indicators (Table 15). The highest Sensitivity Index (SI) value, with a mean variation of 3.48%, was observed when removing the elevation layer. Conversely, the lowest SI value, with a mean variation of 0.88% (Table 15). The difference between the highest and lowest SI values is 2.6%. The sensitivity parameter index (SI) of all the flood parameters used in the study area is illustrated in Figure 30.

Table 15: Descriptive statistics of map removal sensitivity analysis of flood susceptibility mapping. E: Elevation, S: Slope, DD: Drainage Density, DFR: Distance from River, TWI: Topographic Wetness Index, NDVI: Normalized Difference Vegetation Index, SPI: Stream Power Index, NDSI: Normalized Difference Snow Index, G: Geology, LULC: Land use and Land cover.

Flood indicators	% Variation in SI			
	Min	Max	Mean	SD
E	0.000	5.878	3.480	1.557
S	0.000	5.087	1.924	0.904
DFR	0.000	5.042	1.523	1.094
DD	0.000	13.930	1.693	1.072
TWI	0.000	2.873	1.629	0.520
NDVI	0.026	2.684	1.641	0.243
SPI	0.000	2.564	1.151	0.496
NDSI	0.000	1.620	0.886	0.268
G	0.253	2.162	1.507	0.217
LULC	0.689	1.760	1.362	0.118

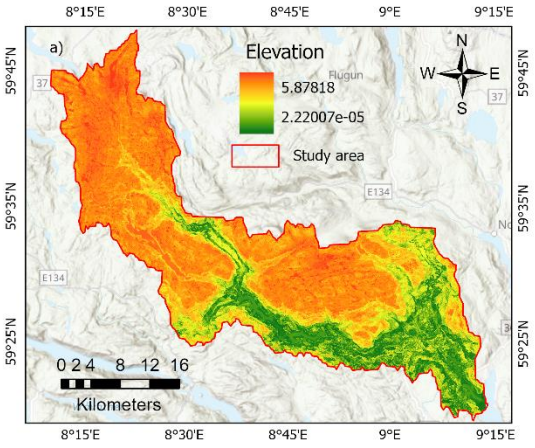
a)
Elevation
5.87818
2.22007e-05
Study area
Flugun
N
W
E
S
0 2 4 8 12 16
Kilometers
8°15'E
8°30'E
8°45'E
9°E
9°15'E
59°45'N
59°35'N
59°25'N

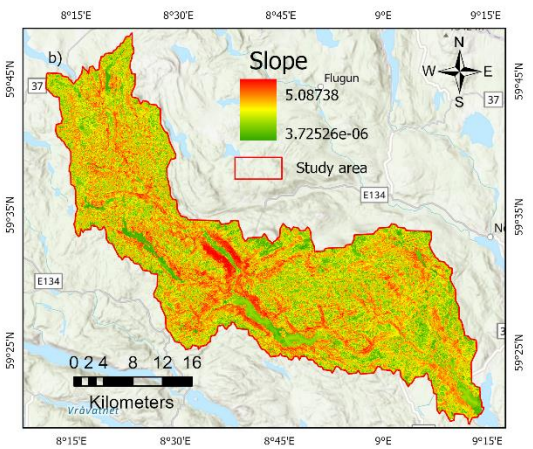
b)
Slope
5.08738
3.72526e-06
Study area
Flugun
N
W
E
S
0 2 4 8 12 16
Kilometers
8°15'E
8°30'E
8°45'E
9°E
9°15'E
59°45'N
59°35'N
59°25'N

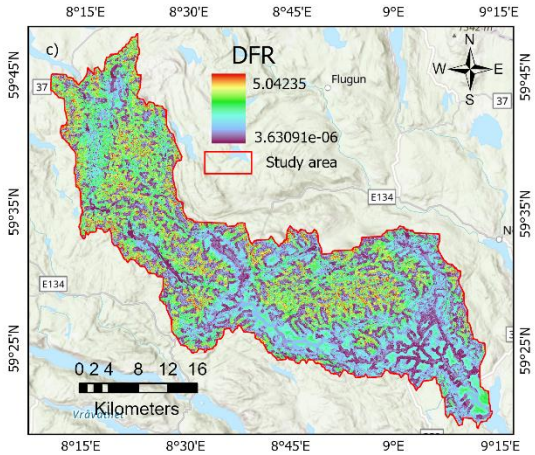
c)
DFR
5.04235
3.63091e-06
Study area
Flugun
N
W
E
S
0 2 4 8 12 16
Kilometers
8°15'E
8°30'E
8°45'E
9°E
9°15'E
59°45'N
59°35'N
59°25'N

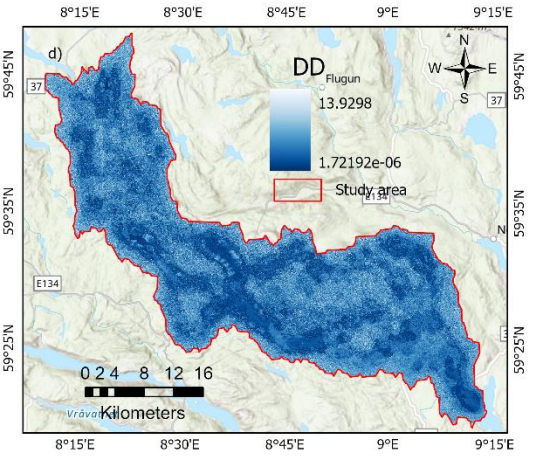
d)
DD
13.9298
1.72192e-06
Study area
Flugun
N
W
E
S
0 2 4 8 12 16
Kilometers
8°15'E
8°30'E
8°45'E
9°E
9°15'E
59°45'N
59°35'N
59°25'N

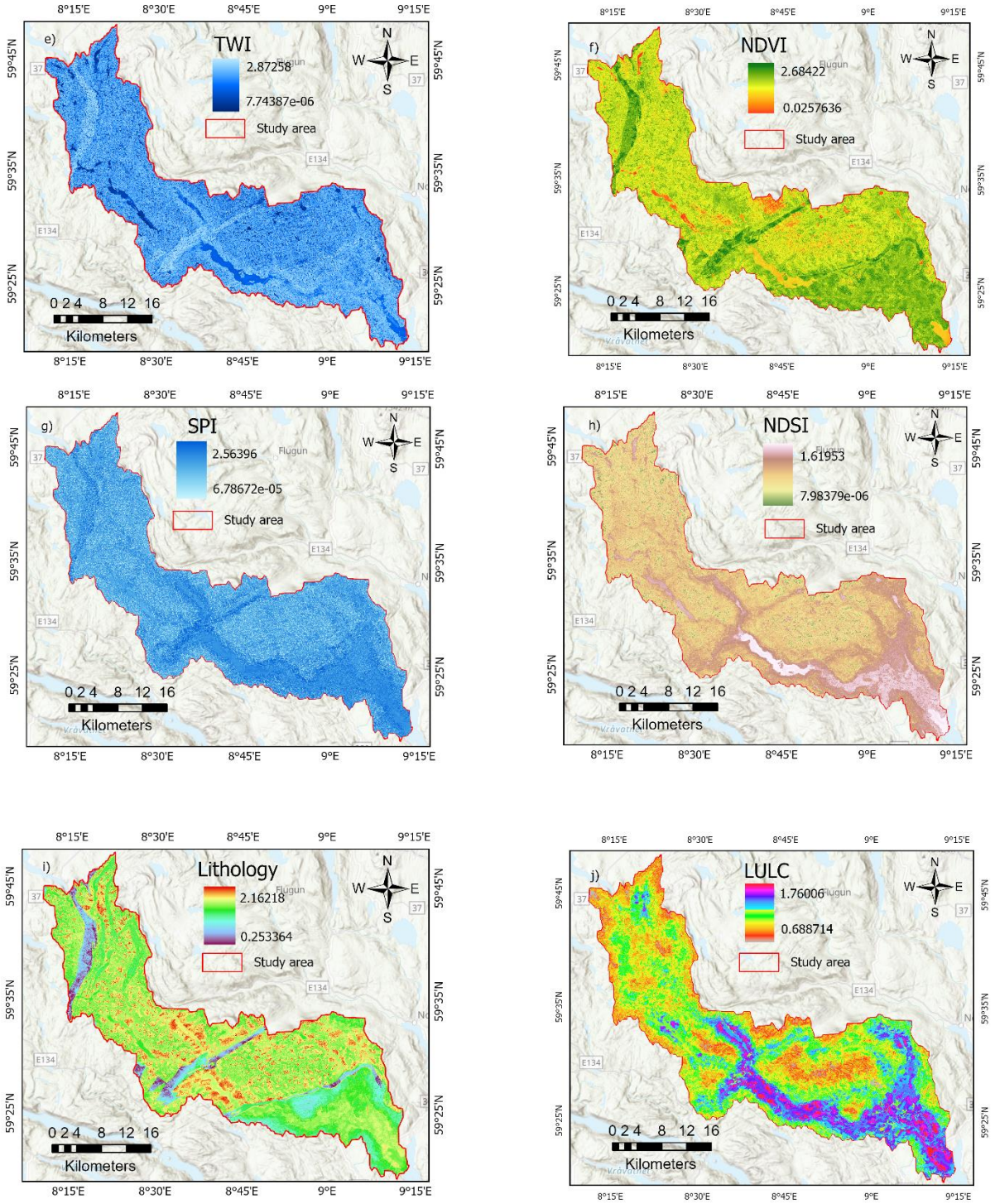

Figure 30: Sensitivity Index parameters for the Flood Susceptibility Map of the study area: a) Elevation, b) Slope, c) DFR, d) DD, e) TWI, f) NDVI, g) SPI, h) NDSI, i) Lithology, and j) LULC

In addition, an analysis was further conducted to determine the percentage of changes in Flood Susceptibility Mapping (FSM) when each flood indicator was removed. The results of this analysis are shown in Table 16 and Figure 30. The removal of each flood indicator layer has resulted in significant variation in the percentage of produced FSM maps.

Table 16: Percentage of changes in flood susceptibility mapping related to the removal of each flood indicator. E: Elevation, S: Slope, DD: Drainage Density, DFR: Distance from River, TWI: Topographic Wetness Index, NDVI: Normalized Difference Vegetation Index, SPI: Stream Power Index, NDSI: Normalized Difference Snow Index, G: Geology, LULC: Land use and Land cover.

Flood Indicators	% Change in FSM with map the removal				
	Very Low	Low	Moderate	High	Very high
E	-15.31	-17.40	58.18	-7.76	55.73
S	-20.47	-7.27	41.08	-0.95	41.08
DFR	61.66	-27.90	-14.44	-18.18	-10.69
DD	-13.20	4.13	2.37	10.72	11.19
TWI	1.58	2.40	0.06	-20.53	13.29
NDVI	-3.93	-3.45	7.34	5.90	16.06
SPI	1.57	4.80	-6.97	-8.87	-8.39
NDSI	3.26	1.08	-4.20	-4.60	-3.29
G	7.31	-2.12	-4.64	-2.31	-0.74
LULC	5.83	1.65	-3.52	-5.81	-2.88

The exclusion of distance from the river resulted in the highest increase in areas classified as very low, low, moderate, high, and very high flood susceptibility, with a percentage increase of 61.66%. The exclusion of the Stream Power Index (SPI) resulted in 4.80% increase, the removal of elevation layer resulted in a 51.18% increase, and the exclusion of Drainage Density (DD) resulted in a 10.72% increase. Conversely, the flood susceptibility of area classified as very low, low, moderate, high, and very high decreased the most when elevation layer was removed, by 15.31%, followed by the distance from river layer, by 27.9%, the Stream Power Index (SPI) layer, by 20.53%, and the drainage density layer, by 10.69%. this analysis shows that “distance from the river” is the most sensitive layer in the Flood Susceptibility Mapping (FSM) compared to the other layers.

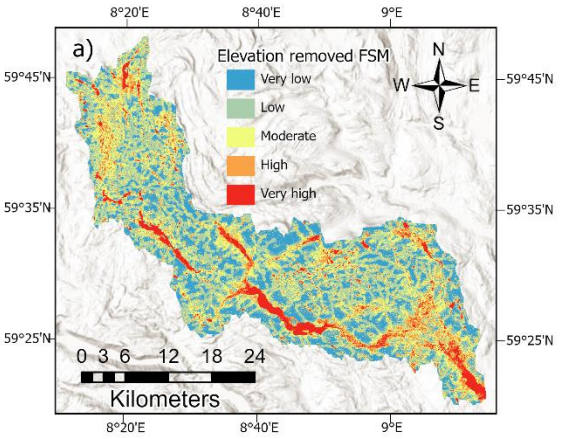
a)
Elevation removed FSM
Very low
Low
Moderate
High
Very high
N
W
E
S
8°20'E
8°40'E
9°E
59°45'N
59°35'N
59°25'N
0 3 6 12 18 24
Kilometers

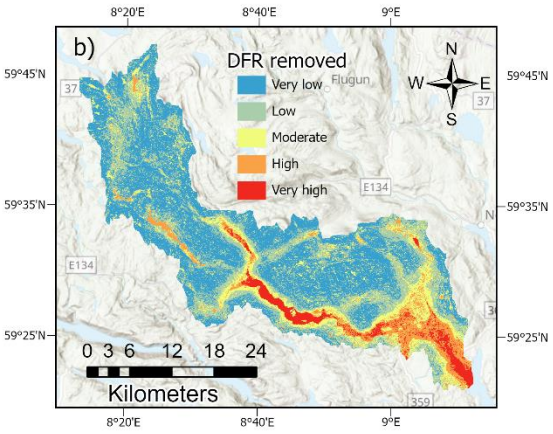
b)
DFR removed
Very low
Low
Moderate
High
Very high
Flugun
E134
N
W
E
S
8°20'E
8°40'E
9°E
59°45'N
59°35'N
59°25'N
0 3 6 12 18 24
Kilometers

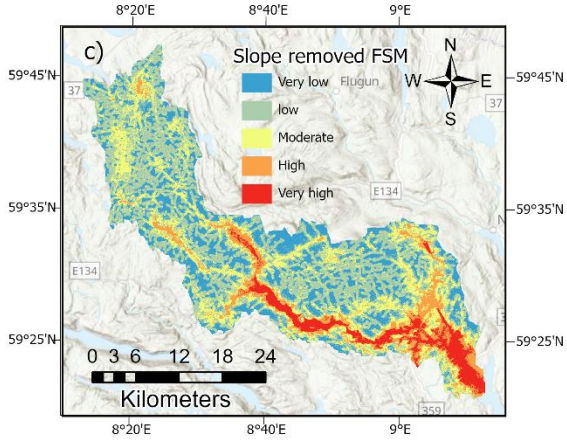
c)
Slope removed FSM
Very low
low
Moderate
High
Very high
Flugun
E134
N
W
E
S
8°20'E
8°40'E
9°E
59°45'N
59°35'N
59°25'N
0 3 6 12 18 24
Kilometers

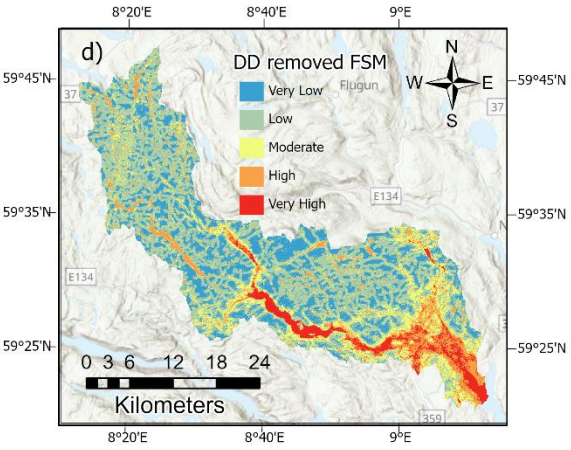
d)
DD removed FSM
Very Low
Low
Moderate
High
Very High
Flugun
E134
N
W
E
S
8°20'E
8°40'E
9°E
59°45'N
59°35'N
59°25'N
0 3 6 12 18 24
Kilometers

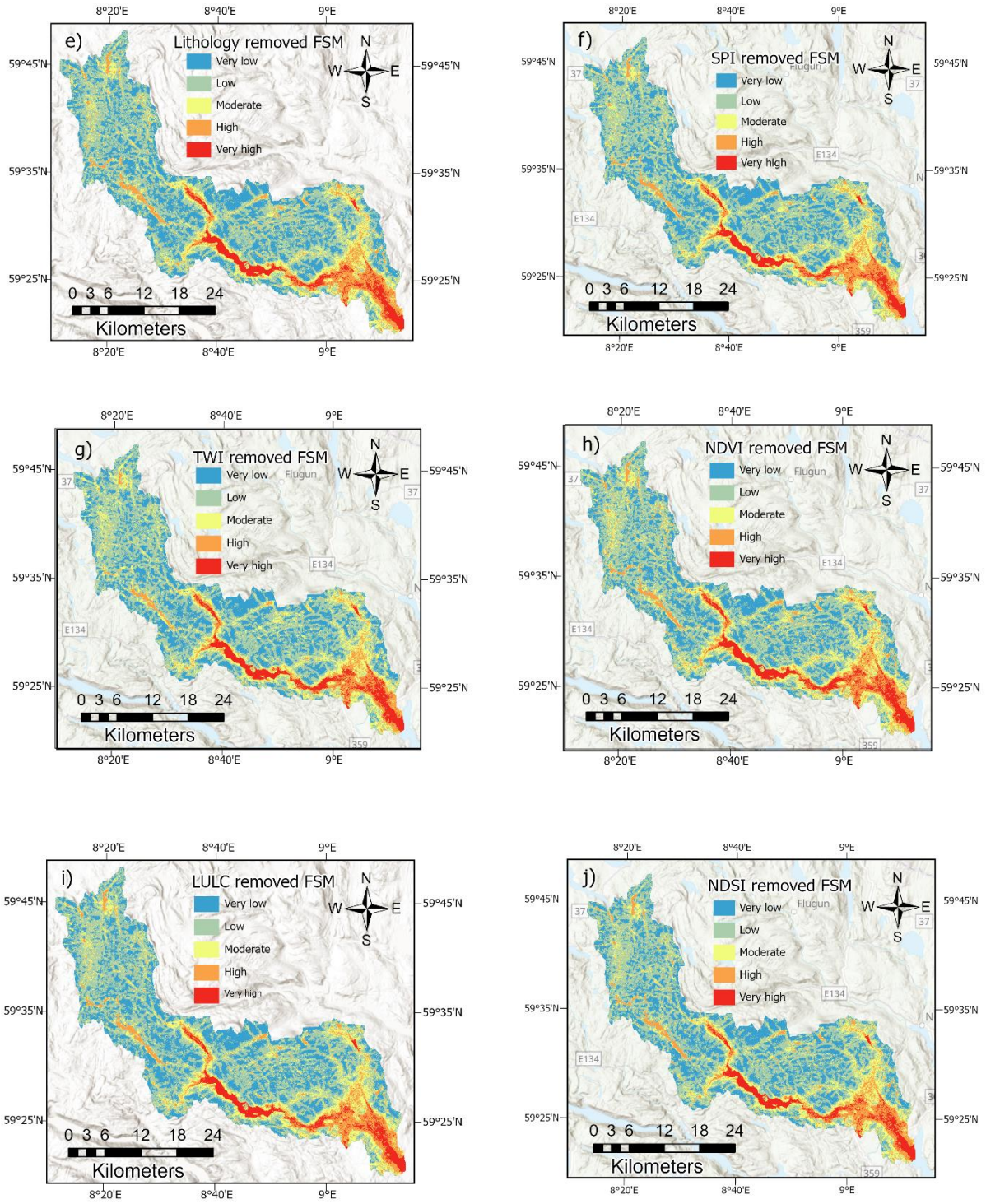

Figure 31: Flood susceptibility map after the removal of each indicator, a) elevation, b) distance from river, c) slope, d) drainage density, e) lithology, f) SPI, g) TWI, h) NDVI, i) LULC, and j) NDSI

6 Model validation

The resultant map of the study area, obtained through the application of Analytic Hierarchy Process (AHP) must be validated to determine its accuracy. Consequently, this thesis research conducted quantitative assessments to verify the accuracy of the AHP model output by comparing it to the flood inventory map, which is derived from historical flood records in the study area. The Receiver Operating Characteristics Area Under the Curve (ROC-AUC) was calculated by comparing the Flood Susceptibility Mapping (FSM) map of the study area with flood and non-flood points within the study area using 'ArcSDM' tool in ArcGIS software.

Figure 31 shows the Receiver Operating Characteristics (ROC) curves and the Area Under the Curve (AUC) for the AHP model. The AUC represents the accuracy rate of the Flood Susceptibility Mapping model and can be classified into four categories: excellent (>0.9), acceptable (0.8-0.9), good (0.7-0.8), and considerable (0.5-0.7). The study found that the AHP technique achieved an observed accuracy of 0.957 (95.70%). Based on this scale, the model demonstrates efficient performance in producing the FSM map, resulting in an excellent outcome.

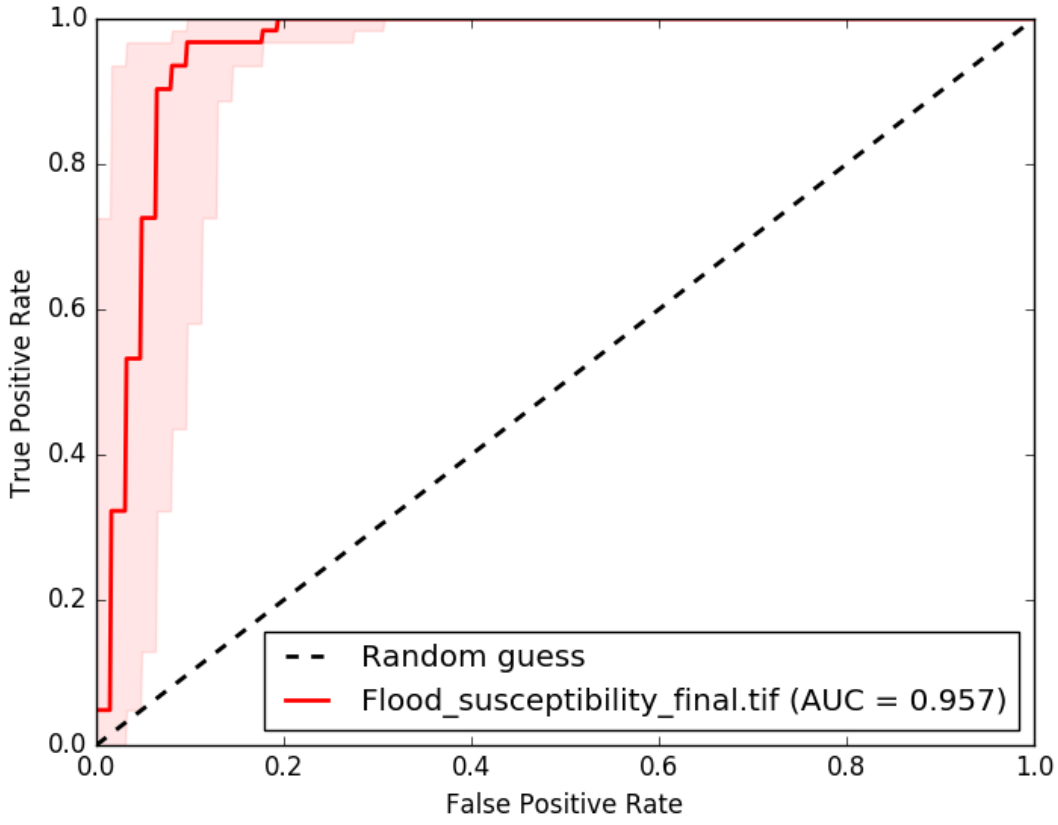

Figure 32: ROC-AUC assessment

7. Discussion

The current study comprehensively assesses the effectiveness and practicality of multi-Criteria Decision Making (MCDM) and Geographic Information Systems (GIS) techniques for fluvial flood susceptibility mapping in Bø-Seljord catchment region of Telemark County, Norway. Flood susceptibility mapping is a widely technique for flood prediction and serves as an essential tool for flood control, research, and the implementation plans globally. The AHP is frequently used due to its effectiveness and reliability in delineating FSM, providing alternative solutions for natural hazard assessment and flood management.

The study identified the key indices that significantly influence the mapping of flood susceptibility in the specified zone. These indices include elevation, slope, distance from river, drainage density, and topographic wetness index (TWI). The analysis incorporates geomorphological and hydraulic characteristics in relation to flood intensity. Indicators such as elevation, slope, distance from rivers, TWI, Normalized Difference Vegetation Index (NDVI), Stream Power Index (SPI), Normalized Difference Snow Index (NDSI), geology, and land use and land were analysed. The study assigned the weightages of over 70% to four parameters: Elevation, slope, distance from rivers, and drainage density. Previous studies have examined flood susceptibility using various indices and models, such as frequency ratio, support vector machine, and fuzzy logic models, to achieve better predictive results.

(Rahman et al., 2019) has provided a concise overview of the models employed in flood susceptibility assessment and delineated a framework for future research. Recently, GIS-based Multi-Criteria Decision Analysis (MCDA) methods have played a vital role in understanding the behaviour and limitations of flood susceptibility models. However, rankings in MCDA often involve a high degree of uncertainty due to factors such as raw data, data processing, criterion selection, and thresholds. The weights assigned to criteria can be subject to significant debate and uncertainty, often due to lack of awareness of decision makers' preferences or the unknown nature and scope of the criteria (Chen et al., 2019).

A significant flaw in the AHP technique lies in the computation of weights. Therefore, it is necessary to perform sensitivity analyses to validate the assigned weights for the AHP (Mukherjee & Singh, 2020). Sensitivity analysis focuses on the relationship between the inputs and outputs of the modelling application, evaluating the resilience of end results to minor variations in the raw data. This research utilised three types of sensitivity analysis to cross-validate the weights assigned in the AHP method. The AHP weights assigned to flood susceptibility indicators were validated using Stillwell ranking methods. Discrepancies between empirical and effective weights were observed during the sensitivity analysis of each indicator. The statistical results of the map removal sensitivity analysis demonstrated variability in the Sensitivity Index (SI) across indicators. The SI was calculated by considering

the rate, weight, and impact of other thematic layers (Fenta et al., 2014). The AHP method effectively met the research objectives, as shown by the cross-verification results using ROC-AUC.

The devastating effects of flooding on people's homes, businesses, and way of life are a global issue demanding attention. Numerous methods for assessing flood susceptibility have been developed, all aiming to improve predictions and inform decision-making.

8. Conclusion and Limitations

8.1 Conclusion

Multi-Criteria Decision Making (MCDM) and Geographic Information Systems (GIS) techniques for fluvial flood susceptibility mapping was employed. Assessing the sensitivity of a solution is crucial to determine its reliability utilizing the AHP methodology. It provides evaluators or modelers with more accessible feedback, making it easier for non-experts to understand. This approach allows for a thorough exploration of the decision-making problem while also offering insights into how changes in criteria weights impact evaluation outcomes both spatially and quantitatively. Ongoing advancements in this field, such as conducting thorough analyses of criteria threshold adjustments, modifying the relative importance of criteria, and consequently adjusting the preference matrix, will enhance the successful application of GIS and MCDA to real-world land management challenges.

The research is distinguished by its sensitivity analyses of the AHP method, which have the potential to be applied to other geographical areas. A precise susceptibility model provides land-use planners and government authorities with an invaluable tool for implementing effective risk-reduction strategies. In this region, the results of this thesis research may be applied to land-use determination prior to flood control. Therefore, this research introduces a novel aspect to studies that utilizing multiple MCDA techniques for modelling purposes. Another significant aspect of this research is the identification of high flood-risk areas, which can assist the local government in determining the necessity for additional monitoring within the defined study area.

Thus, it is imperative to implement a comprehensive flood risk strategy to effectively enhance the region resilience. Additionally, it is recommended to employ both structural and non-structural flood defence techniques in high-risk areas. Mitigation measures for reducing flood-prone areas include prohibiting settlement expansion, implementing sustainable floodplain management practices, and prioritising public awareness. The flood susceptibility map generated form this analysis will provide valuable assistance to local governments and

public protection agencies in evaluating areas that could potentially be impacted by future flood events.

8.2 Limitations of the study

The study's limitations pertain to the subjective nature of the MCDA technique, which can introduce uncertainty and bias while employing the AHP model. To address these limitations, it is highly recommended to incorporate high resolution data and explore alternative techniques more suitable for this specific area. The research could enhance model evaluation by incorporating additional sensitivity analyses. Additionally, decision-making can be improved by utilising various machine learning techniques, such as frequency ratio, weight of evidence, and logistic regression, to gain a deeper understanding of flood susceptibility. Despite its imperfections, the MCDA approach can serve as a valuable tool for examining practical issues in regions with limited data availability, especially with respect to flood records. However, the current thesis study has limited information on past flood events in the defined study area, and the accuracy could be improved with more flood points. The present research holds potential value for policymakers, local administrative authorities, environmentalists, and engineers, and can be applied to numerous flood-prone locations worldwide.

References

Al-Abadi, A., & Pradhan, B. (2020). In flood susceptibility assessment, is it scientifically correct to represent flood events as a point vector format and create flood inventory map? *Journal of Hydrology*, *590*. https://doi.org/10.1016/j.jhydrol.2020.125475

Al-Juaidi, A., Nassar, A., & Al-Juaidi, O. (2018). Evaluation of flood susceptibility mapping using logistic regression and GIS conditioning factors. *Arabian Journal of Geosciences*, *11*, 1-10. https://doi.org/10.1007/s12517-018-4095-0

Ali, S. A., Khatun, R., Ahmad, A., & Ahmad, S. (2019). Application of GIS-based analytic hierarchy process and frequency ratio model to flood vulnerable mapping and risk area estimation at Sundarban region, India. *Modeling Earth Systems and Environment*, *5*. https://doi.org/10.1007/s40808-019-00593-z

Arabameri, A., Rezaei, K., Cerdà, A., Conoscenti, C., & Kalantari, Z. (2019). A comparison of statistical methods and multi-criteria decision making to map flood hazard susceptibility in Northern Iran. *Science of The Total Environment*, *660*, 443-458. https://doi.org/10.1016/j.scitotenv.2019.01.021

Azareh, A., Rafiei Sardooi, E., Choubin, B., Barkhori, S., Shahdadi, A., Adamowski, J., & Band, S. (2019). Incorporating multi-criteria decision-making and fuzzy-value functions for flood susceptibility assessment. *Geocarto International*, *36*, 1-21. https://doi.org/10.1080/10106049.2019.1695958

Bajracharya, S., Khanal, N., Nepal, P., Rai, S., Ghimire, P., & Pradhan, N. (2021). Community Assessment of Flood Risks and Early Warning System in Ratu Watershed, Koshi Basin, Nepal. *Sustainability*, *13*. https://doi.org/10.3390/su13063577

Bathrellos, G., Karymbalis, E., Skilodimou, H., Gaki-Papanastassiou, K., & Baltas, E. (2016). Urban flood hazard assessment in the basin of Athens Metropolitan city, Greece. *Environmental Earth Sciences*, *75*. https://doi.org/10.1007/s12665-015-5157-1

Beckers, A., Detrembleur, S., Dewals, B., Gouverneur, L., Dujardin, S., Archambeau, P., Erpicum, S., & Pirotton, M. (2012). *Relative impacts of climate and land use changes on future flood damage along River Meuse in Wallonia*.

Bui, D., Khosravi, K., Shahabi, H., Daggupati, P., Adamowski, J., Melesse, A., Pham, B., Pourghasemi, H., Mahmoudi, M., Bahrami, S., Pradhan, B., Shirzadi, A., Chapi, K., & Lee, S. (2019). Flood Spatial Modeling in Northern Iran Using Remote Sensing and GIS: A Comparison between Evidential Belief Functions and Its Ensemble with a Multivariate Logistic Regression Model. *Remote Sensing*, 11. https://doi.org/10.3390/rs11131589

Bui, D., Löfman, O., Revhaug, I., & Dick, Ø. (2011). Landslide susceptibility analysis in the Hoa Binh province of Vietnam using statistical index and logistic regression. *Natural Hazards*, *59*, 1413–1444. https://doi.org/10.1007/s11069-011-9844-2

Çelik, H., Coskun, H. G., Cigizoglu, H., Ağıralioğlu, N., Aydın, A., & Esin, I. (2012). Erratum to: The analysis of 2004 flood on Kozdere Stream in Istanbul. *Natural Hazards*, *63*. https://doi.org/10.1007/s11069-012-0249-7

Çetinkaya, C., Özceylan, E., Erbas, M., & Kabak, M. (2016). GIS-based Fuzzy MCDA Approach for Siting Refugee Camp: A Case Study for Southeastern Turkey. *International Journal of Disaster Risk Reduction*, *18*. https://doi.org/10.1016/j.ijdrr.2016.07.004

Chen, W., Li, Y., Xue, W., Shahabi, H., Li, S., Hong, H., Wang, X., Bian, H., Zhang, S., Pradhan, B., & Ahmad, B. B. (2019). Modeling flood susceptibility using data-driven approaches of naïve Bayes tree, alternating decision tree, and random forest

methods. *Science of The Total Environment*, *701*. https://doi.org/10.1016/j.scitotenv.2019.134979
Costabile, P., Costanzo, C., & Macchione, F. (2016). Performances and limitations of the diffusive approximation of the 2-d shallow water equations for flood simulation in urban and rural areas. *Applied Numerical Mathematics*, *116*. https://doi.org/10.1016/j.apnum.2016.07.003
Costache, R.-D., & Bui, D. (2019). Spatial prediction of flood potential using new ensembles of bivariate statistics and artificial intelligence: A case study at the Putna river catchment of Romania. *Science of The Total Environment*, *691*, 1098-1118. https://doi.org/10.1016/j.scitotenv.2019.07.197
Dahri, N., & Abida, H. (2017). Monte Carlo simulation-aided analytical hierarchy process (AHP) for flood susceptibility mapping in Gabes Basin (southeastern Tunisia). *Environmental Earth Sciences*, *76*, 302. https://doi.org/10.1007/s12665-017-6619-4
Dano, D. U. L., Balogun, A.-L., Matori, A., Wan Yusof, K., Rimi Abubakar, I., Said, M., Aina, Y., & Pradhan, B. (2019). Flood Susceptibility Mapping Using GIS-Based Analytic Network Process: A Case Study of Perlis, Malaysia. *Water*, *11*, 615. https://doi.org/10.3390/w11030615
Das, S., & Pardeshi, S. (2018). Comparative analysis of lineaments extracted from Cartosat, SRTM and ASTER DEM: a study based on four watersheds in Konkan region, India. *Spatial Information Research*, *26*, 47-57. https://doi.org/10.1007/s41324-017-0155-x
de Brito, M., & Evers, M. (2016). Multi-criteria decision-making for flood risk management: A survey of the current state of the art. *Natural Hazards and Earth System Sciences*, *16*, 1019-1033. https://doi.org/10.5194/nhess-16-1019-2016
Dimitriadis, P., Tegos, A., Oikonomou, A., Pagana, V., Koukouvinos, A., Mamassis, N., Koutsoyiannis, D., & Efstratiadis, A. (2016). Comparative evaluation of 1D and quasi-2D hydraulic models based on benchmark and real-world applications for uncertainty assessment in flood mapping. *Journal of Hydrology*, *534*. https://doi.org/10.1016/j.jhydrol.2016.01.020
Dodangeh, E., Choubin, B., Najafi, A., Nabipour, N., Panahi, M., Band, S., & Mosavi, A. (2019). Integrated machine learning methods with resampling algorithms for flood susceptibility prediction. *Science of The Total Environment*, *705*, 135983. https://doi.org/10.1016/j.scitotenv.2019.135983
Doornkamp, J. (1998). Coastal flooding, global warming and environmental management. *Journal of Environmental Management - J ENVIRON MANAGE*, *52*, 327-333. https://doi.org/10.1006/jema.1998.0188
Dottori, F., Alfieri, L., Bianchi, A., Skøien, J., & Salamon, P. (2022). A new dataset of river flood hazard maps for Europe and the Mediterranean Basin. *Earth System Science Data*, *14*, 1549-1569. https://doi.org/10.5194/essd-14-1549-2022
Dottori, F., Mentaschi, L., Bianchi, A., Alfieri, L., & Feyen, L. (2023). Cost-effective adaptation strategies to rising river flood risk in Europe. *Nature Climate Change*, *13*, 1-7. https://doi.org/10.1038/s41558-022-01540-0
Enríquez de Salamanca, A. (2023). Contraction of the fluvial territory in the Jarama River (Spain). *Earth Surface Processes and Landforms*, *48*. https://doi.org/10.1002/esp.5578
Fenta, A., Kifle, A., Gebreyohannes, T., & Hailu, G. (2014). Spatial analysis of groundwater potential using remote sensing and GIS-based multi-criteria evaluation in Raya Valley, northern Ethiopia. *Hydrogeology Journal*. https://doi.org/10.1007/s10040-014-1198-x
Fernandez, D., Lutz, M., Geológico, S., Argentino-Delegación, M., Tucumán, M., Lillo, & p. (2010). Author's personal copy Urban flood hazard zoning in Tucumán Province, Argentina, using GIS and multicriteria decision analysis. *Engineering Geology*.
Ghanbari, M., Dell, T., Saleh, F., Chen, Z., Cherrier, J., Colle, B., Hacker, J., Madaus, L., Orton, P., & Arabi, M. (2024). Compounding effects of changing sea level and rainfall

regimes on pluvial flooding in New York City. *Natural Hazards*. https://doi.org/10.1007/s11069-024-06466-8
Gruntfest, E., & Handmer, J. (2001). Dealing with Flash Floods: Contemporary Issues and Future Possibilities. In (Vol. 77, pp. 3-10). https://doi.org/10.1007/978-94-010-0918-8_1
Haltas, I., Demir, I., Yildirim, E., & Oztas, F. (2021). A Comprehensive Flood Event Specification and Inventory: 1930-2020 Turkey Case Study. *International Journal of Disaster Risk Reduction*, *56*, 102086. https://doi.org/10.1016/j.ijdrr.2021.102086
He, B., Xu, Y.-G., Huang, X., Luo, Z.-Y., Shi, Y., Yang, Q.-J., & Yu, S.-Y. (2007). Age and duration of the Emeishan flood volcanism, SW China: Geochemistry and SHRIMP zircon U-Pb dating of silicic ignimbrites, post-volcanic Xuanwei Formation and clay tuff at the Chaotian section. *Earth and Planetary Science Letters*, *255*, 306-323. https://doi.org/10.1016/j.epsl.2006.12.021
Jongman, B., Ward, P., & Aerts, J. (2018). Global exposure to river and coastal flooding: Long term trends and changes.
Kaya, C., & Derin, L. (2023). Parameters and methods used in flood susceptibility mapping: a review. *Journal of Water and Climate Change*, *14*. https://doi.org/10.2166/wcc.2023.035
Kazakis, N., Kougias, I., & Patsialis, T. (2015). Assessment of flood hazard areas at a regional scale using an index-based approach and Analytical Hierarchy Process: Application in Rhodope–Evros region, Greece. *Science of The Total Environment*, *538*, 555–563. https://doi.org/10.1016/j.scitotenv.2015.08.055
Khosravi, K., Shahabi, H., Pham, B., Adamawoski, J., Shirzadi, A., Pradhan, B., Dou, J., Ly, H.-B., Grof, G., Loc, H., Hong, H., Chapi, K., & Prakash, I. (2019). A Comparative Assessment of Flood Susceptibility Modeling Using Multi-Criteria Decision-Making Analysis and Machine Learning Methods. *Journal of Hydrology*, *573*. https://doi.org/10.1016/j.jhydrol.2019.03.073
Kumar, R., & Anbalagan, R. (2016). Landslide Susceptibility Mapping Using Analytical Hierarchy Process (AHP) in Tehri Reservoir Rim Region, Uttarakhand. *Journal of the Geological Society of India*, *87*. https://doi.org/10.1007/s12594-016-0395-8
Kundzewicz, Z., & Pińskwar, I. (2022). Are Pluvial and Fluvial Floods on the Rise? *Water*, *14*, 2612. https://doi.org/10.3390/w14172612
Lai, C., Chen, X., Zhao, S., Wang, Z., & Wu, X. (2015). A flood risk assessment model based on Random Forest and its application. *Shuili Xuebao/Journal of Hydraulic Engineering*, *46*, 58-66. https://doi.org/10.13243/j.cnki.slxb.2015.01.008
Leake, C., & Malczewski, J. (2000). GIS and Multicriteria Decision Analysis. *The Journal of the Operational Research Society*, *51*, 247. https://doi.org/10.2307/254268
Li, C., Liu, M., Hu, Y., Shi, T., Zong, M., & Walter, M. (2018). Assessing the Impact of Urbanization on Direct Runoff Using Improved Composite CN Method in a Large Urban Area. *International Journal of Environmental Research and Public Health*, *15*, 775. https://doi.org/10.3390/ijerph15040775
Li, K., Wu, S., Dai, E., & Xu, Z. (2012). Flood loss analysis and quantitative risk assessment in China. *Natural Hazards*, *63*. https://doi.org/10.1007/s11069-012-0180-y
Melgar-García, L., Martínez-Álvarez, F., Bui, D., & Troncoso, A. (2023). A novel semantic segmentation approach based on U-Net, WU-Net, and U-Net++ deep learning for predicting areas sensitive to pluvial flood at tropical area. *International Journal of Digital Earth*, *16*, 3661-3679. https://doi.org/10.1080/17538947.2023.2252401
Merz, B., Kundzewicz, Z. W., delgado, J., Hundecha, Y., & Kreibich, H. (2012). Detection and Attribution of Changes in Flood Hazard and Risk. *IAHS-AISH Publication*, 435-458. https://doi.org/10.1201/b12348-29
Meyer, V., Scheuer, S., & Haase, D. (2009). A multicriteria approach for flood risk mapping exemplified at the Mulde river, Germany. *Natural Hazards*, *48*, 17-39. https://doi.org/10.1007/s11069-008-9244-4

Mishra, A., & Kumar, G. (2020). Climate change will affect global water availability through compounding changes in seasonal precipitation and evaporation. *Nature Communications*, *11*. https://doi.org/10.1038/s41467-020-16757-w
Mitra, R., & Roy, D. (2022). Delineation of groundwater potential zones through the integration of remote sensing, geographic information system, and multi-criteria decision-making technique in the sub-Himalayan foothills region, India. *International Journal of Energy and Water Resources*, *7*. https://doi.org/10.1007/s42108-022-00181-5
Mitra, R., Saha, P., & Das, J. (2022). Assessment of the performance of GIS-based analytical hierarchical process (AHP) approach for flood modelling in Uttar Dinajpur district of West Bengal, India. *Geomatics, Natural Hazards and Risk*, *13*, 2183-2226. https://doi.org/10.1080/19475705.2022.2112094
Moel, H., Jongman, B., Kreibich, H., Merz, B., Penning-Rowsell, E., & Ward, P. (2015). Flood risk assessments at different spatial scales. *Mitigation and Adaptation Strategies for Global Change*, *20*. https://doi.org/10.1007/s11027-015-9654-z
Moore, I., Grayson, R., & Ladson, T. (1991). Digital Terrain Modeling: A review of hydrological, geomorphological, and biological applications. *Hydrological Processes*, *5*, 3-30. https://doi.org/10.1002/hyp.3360050103
Muchingami, I., Chuma, C., Gumbo, M., & Hlatywayo, D. (2019). Review: Approaches to groundwater exploration and resource evaluation in the crystalline basement aquifers of Zimbabwe. *Hydrogeology Journal*, *27*. https://doi.org/10.1007/s10040-019-01924-1
Mukherjee, I., & Singh, U. K. (2020). Delineation of groundwater potential zones in a drought-prone semi-arid region of east India using GIS and analytical hierarchical process techniques. *CATENA*, *194*, 104681. https://doi.org/10.1016/j.catena.2020.104681
Nguyen, H., Nguyen, Q.-H., Du, Q., Ha Thanh, N., Nguyen, G., & Bui, Q.-T. (2021). A novel combination of Deep Neural Network and Manta Ray Foraging Optimization for flood susceptibility mapping in Quang Ngai province, Vietnam. *Geocarto International*, *37*, 1-22. https://doi.org/10.1080/10106049.2021.1975832
Nguyen, L., Bui, D., & Seidu, R. (2023). A Comparative Flood Susceptibility Assessment in a Norwegian Coastal City Using Feature Selection Methods and Machine Learning Algorithms. In (pp. 591-618). https://doi.org/10.1007/978-3-031-17808-5_36
Nones, M. (2017). Flood Hazard Maps in the European context. *Water International*, *42*, 324-332. https://doi.org/10.1080/02508060.2016.1269282
Norman, L., Huth, H., Levick, L., Burns, I., Guertin, D., Lara-Valencia, F., & Semmens, D. (2010). Flood hazard awareness and hydrologic modelling at Ambos Nogales, United States–Mexico border. *Journal of Flood Risk Management*, *3*, 151-165. https://doi.org/10.1111/j.1753-318X.2010.01066.x
Onuşluel Gül, G. (2013). Estimating flood exposure potentials in Turkish catchments through index-based flood mapping. *Natural Hazards*, *69*. https://doi.org/10.1007/s11069-013-0717-8
Pradhan, B. (2009). Flood susceptible mapping and risk area delineation using logistic regression, GIS and remote sensing. *Journal of Spatial Hydrology*, *9*, 1-18.
Prinos, P., Kortenhaus, A., Swerpel, B., & Jiménez, J. (2008). Review of Flood Hazard Mapping. 54.
Rahman, M. M., Chen, N., Islam, M. M., Dewan, Iqbal, J., Muhammad, R., Washakh, A., & Shufeng, T. (2019). Flood Susceptibility Assessment in Bangladesh Using Machine Learning and Multi-criteria Decision Analysis. *Earth Systems and Environment*, *3*, 585-601.
Rahmati, O., Pourghasemi, H., & Zeinivand, H. (2015). Flood susceptibility mapping using frequency ratio and weights-of-evidence models in the Golastan Province, Iran. *Geocarto International*.
Rentschler, J., Salhab, M., & Jafino, B. (2022). Flood exposure and poverty in 188 countries. *Nature Communications*, *13*. https://doi.org/10.1038/s41467-022-30727-4

Rosmadi, H., Ahmed, M., Mokhtar, M., & Lim, C. K. (2023). Reviewing Challenges of Flood Risk Management in Malaysia. *Water*, *15*, 2390. https://doi.org/10.3390/w15132390
Saaty, T., & Vargas, L. (1991). Prediction, projection and forecasting: applications of the analytic hierarchy process in economics, finance, politics, games and sports, Kluwer Academic Publishers. *Boston*.
Saaty, T. L. (1994). How to Make a Decision: The Analytic Hierarchy Process. *Aestimum*, *24*. https://doi.org/10.13128/Aestimum-7138
Sahana, M., & Patel, P. (2019). A comparison of frequency ratio and fuzzy logic models for flood susceptibility assessment of the lower Kosi River Basin in India. *Environmental Earth Sciences*, *78*. https://doi.org/10.1007/s12665-019-8285-1
Shokouhifar, Y., Lotfirad, M., Esmaeili-Gisavandani, H., & Adib, A. (2022). Evaluation of climate change effects on flood frequency in arid and semi-arid basins. *Water Supply*, *22*. https://doi.org/10.2166/ws.2022.271
Souissi, D., Zouhri, L., Hammami, S., Msaddek, M. H., Zghibi, A., & Dlala, M. (2019). GIS-based MCDM - AHP modeling for flood susceptibility mapping of arid areas, southeastern Tunisia. *Geocarto International*, *35*, 1-25. https://doi.org/10.1080/10106049.2019.1566405
Stillwell, W., & Seaver, D. (1981). Comparison of Weight Approximation Techniquesin MultiattributeUtility Decision-making. *Organizational Behavior and Human Performance*, *28*, 62-77. https://doi.org/10.1016/0030-5073(81)90015-5
Tariq, A., Yan, J., Ghaffar, B., Qin, S., Mousa, B. G., Sharifi, A., Huq, M. E., & Aslam, D.-M. (2022). Flash Flood Susceptibility Assessment and Zonation by Integrating Analytic Hierarchy Process and Frequency Ratio Model with Diverse Spatial Data. *Water*, *14*, 22. https://doi.org/10.3390/w14193069
Tehrany, M., Jones, S., & Shabani, F. (2018). Identifying the essential flood conditioning factors for flood prone area mapping using machine learning techniques (Acceptance date 10/12/2018). *CATENA*, *175*. https://doi.org/10.1016/j.catena.2018.12.011
Tehrany, M., Lee, M.-J., Pradhan, B., Jebur, M., & Lee, S. (2014). Flood susceptibility mapping using integrated bivariate and multivariate statistical models. *Environmental Earth Sciences*, *72*, 1-15. https://doi.org/10.1007/s12665-014-3289-3
Tehrany, M., Pradhan, B., & Jebur, M. (2015). Flood susceptibility analysis and its verification using a novel ensemble support vector machine and frequency ratio method. *Stochastic Environmental Research and Risk Assessment*, *29*. https://doi.org/10.1007/s00477-015-1021-9
Tockner, K., & Stanford, J. (2002). Riverine Flood Plains: Present State and Future Trends. *Environmental Conservation*, *29*, 308-330. https://doi.org/10.1017/S037689290200022X
Trọng, N., Pham Ngoc, Q., Le, H. A., Dieu, B., Long, N., & Cuong, N. (2023). Spatial Prediction of Fluvial Flood in High-Frequency Tropical Cyclone Area Using TensorFlow 1D-Convolution Neural Networks and Geospatial Data. *Remote Sensing*, *15*. https://doi.org/10.3390/rs15225429
Ullah, K., & Zhang, J. (2020). GIS-based flood hazard mapping using relative frequency ratio method: A case study of Panjkora River Basin, eastern Hindu Kush, Pakistan. *PLOS ONE*, *15*, e0229153. https://doi.org/10.1371/journal.pone.0229153
Vojtek, M., & Vojteková, J. (2019). Flood Susceptibility Mapping on a National Scale in Slovakia Using the Analytical Hierarchy Process. *Water*, *11*, 364. https://doi.org/10.3390/w11020364
Wang, Y., Hong, H., Chen, W., Li, S., Pamucar, D., Gigović, L., Drobnjak, S., Bui, D., & Duan, H. (2018). A Hybrid GIS Multi-Criteria Decision-Making Method for Flood Susceptibility Mapping at Shangyou, China. *Remote Sensing*, *11*, 62. https://doi.org/10.3390/rs11010062

White, I., Kingston, R., & Barker, A. (2010). Participatory geographic information systems and public engagement within flood risk management. *Journal of Flood Risk Management*, *3*, 337-346. https://doi.org/10.1111/j.1753-318X.2010.01083.x

Wu, S.-j., Lien, H.-C., & Chang, C.-H. (2010). Modeling risk analysis for forecasting peak discharge during flooding prevention and warning operation. *Stochastic Environmental Research and Risk Assessment*, *24*, 1175-1191. https://doi.org/10.1007/s00477-010-0436-6

Yaseen, A., Lu, J., & Chen, X. (2022). Flood susceptibility mapping in an arid region of Pakistan through ensemble machine learning model. *Stochastic Environmental Research and Risk Assessment*, *36*. https://doi.org/10.1007/s00477-022-02179-1

Zeng, Z., Li, Y., Jinyu, L., & Hamidi, A. R. (2021). Utilizing User-Generated Content and GIS for Flood Susceptibility Modeling in Mountainous Areas: A Case Study of Jian City in China. *Sustainability*, *13*, 6929. https://doi.org/10.3390/su13126929

Zhu, W., Zha, X., Luo, P., Wang, S., Cao, Z., Lyu, J., Zhou, M., He, B., & Nover, D. (2023). A quantitative analysis of research trends in flood hazard assessment. *Stochastic Environmental Research and Risk Assessment*, *37*(1), 413-428. https://doi.org/10.1007/s00477-022-02302-2

From internet,

NVE, A (2021). “Floods in Norway”, from https://publikasjoner.nve.no/rapport/2021/rapport2021_01.pdf

NVE, A (2000). “Living with floods”, from https://publikasjoner.nve.no/hydra/diverse/livingwithfloods2000.pdf

NVE, A (2007). “Flombergning for Bygdaråi ved Seljord”, from https://publikasjoner.nve.no/dokument/2007/dokument2007_02.pdf

Council, W. T. (2016). “Facts About Telemark and Norway.”, from http://www.vest-telemark.no/Aktoer/123/Schoolproject/Learn-about-Norway-andTelemark/Facts-about-Telemark-and-Norway.